P-11-41

Site investigation SFR

Fracture mineralogy including identification of uranium phases and hydrochemical characterisation of groundwater in borehole KFR106

Björn Sandström, WSP Sverige AB

Kersti Nilsson, Geosigma AB

Eva-Lena Tullborg, Terralogica AB

December 2011

Svensk Kärnbränslehantering AB
Swedish Nuclear Fuel
and Waste Management Co

Box 250, SE-101 24 Stockholm
Phone +46 8 459 84 00

ISSN 1651-4416
SKB P-11-41
ID 1348873

Site investigation SFR

Fracture mineralogy including identification of uranium phases and hydrochemical characterisation of groundwater in borehole KFR106

Björn Sandström, WSP Sverige AB

Kersti Nilsson, Geosigma AB

Eva-Lena Tullborg, Terralogica AB

December 2011

Keywords: SFR, Forsmark, Geology, Fracture mineralogy, Hydrochemistry, Borehole KFR106, Uranium.

Preface

This report deals with fracture mineralogy and groundwater hydrochemistry; Björn Sandström and Eva-Lena Tullborg have been responsible for the fracture mineralogy and Kersti Nilsson for the hydrochemistry.

Summary

This report presents the fracture mineralogy and hydrochemistry of borehole KFR106.

The most abundant fracture minerals in the examined drill core samples are clay minerals, calcite, quartz and adularia; chlorite is also common but is mostly altered and found interlayered with corrensite. The most common clay mineral is a mixed layer clay consisting of illite-smectite. Pyrite, galena, chalcopyrite, barite (-celestine) and hematite are also commonly found in the fractures, but usually in trace amounts. Other minerals identified in the examined fractures are U-phosphate, pitchblende, U(Ca)-silicate, asphaltite, biotite, monazite, fluorite, titanite, sericite, xenotime, rutile and (Ca, REEs)-carbonate.

Uranium has been introduced, mobilised and reprecipitated during at least four different episodes: 1) Originally, during emplacement of U-rich pegmatites, probably as uraninite. 2) At a second event, uranium was mobilised under brittle conditions during formation of breccia/cataclasite. Uraninite was altered to pitchblende and partly coffinitised. Mobilised uranium precipitated as pitchblende closely associated with hematite and chlorite in cataclasite and fracture sealings prior to 1,000 Ma. 3) During the Palaeozoic U was remobilised and precipitated as U-phosphate on open fracture surfaces. 4) An amorphous U-silicate has also been found in open fractures; the age of this precipitation is not known but it is inferred to be Palaeozoic or younger.

Groundwater was sampled in two sections in borehole KFR106 with pumping sequences of about 6 days for each section. The samples from sections KFR106:1 and KFR106:2 (260–300 m and 143–259 m borehole length, i.e. –261 and –187 m.a.s.l. mid elevation of the section, respectively) were taken in November 2009 and yielded groundwater chemistry data in accordance with SKB chemistry class 3 and 5. In section KFR106:1 and KFR106:2, the chloride contents were 850 and 1,150 mg/L and the drilling water content 6 and 4%, respectively. Although the water compositions were stable during the pumping and sampling periods, the drilling water contents were relatively high and might have affected the groundwater compositions to some extent.

In borehole KFR106, the groundwater in the deepest borehole section was found to be less saline than the water in the more shallow section which is in contrast to the usually expected increase in salinity with depth. However, at SFR the same reversed salinity distribution has been observed in several boreholes, for example, KFR101 and KFR102A.

Sammanfattning

Denna rapport presenterar sprickmineralogi och grundvattenkemi från borrhål KFR106.

De vanligaste sprickmineralen i de undersökta borrkärnssektionerna är lermineral, kalcit och adularia. Klorit förekommer också frekvent, men är till stor del inkluderad i blandskiktsmineralet korrensit som består av växelvisa lager av klorit och smektit. Det vanligaste lermineralet är ett blandskiktsmineral bestående av illit-smektit. Pyrit, blyglans, kopparkis, baryt (-celestin) och hematit är också vanligt förekommande i sprickorna, dock i mycket små mängder. Andra identifierade mineral är uranfosfat, pitchblende, U(Ca)-silikat, asfaltit, biotit, monazite, fluorit, titanit, sericit, xenotim, rutil och (Ca,REE)-karbonat.

Uran har mobiliserats och fällts ut under minst fyra olika perioder: 1) Först vid intrusionen av uranrika pegmatiter, troligtvis som uranit. 2) Vid ett andra tillfälle mobilserades uran under spröda förhållanden i samband med bildandet av breccia/kataklasit. Vid detta tillfälle omvandlades uraniniten till pechblände och viss koffinitisering ägde rum. Det mobiliserade uranet fälldes ut som pechblände samtidigt med hematit och klorit tidigare än för 1 000 Ma sedan. 3) Under Palaeozoikum mobiliserades uran återigen och fälldes ut som uranfosfat på öppna sprickytor. 4) Ett amorft uransilikat har också hittats i öppna sprickor. Åldern på detta mineral är Palaeozoiskt eller yngre.

Grundvatten provtogs i två sektioner i borrhål KFR106. Pumpperioderna varade ca 6 dagar i båda sektionerna. Proven från sektion KFR106:1 och KFR106:2 (260–300 m respektive 143–259 m borrhålslängd; elevation –187 m.ö.h. respektive –261 m.ö.h.) togs i november 2009 och gav grundvattendata enligt SKB klass 3 och 5. I sektionerna KFR106:1 och KFR106:2 var kloridhalterna 850 respektive 1 150 mg/L och spolvattenhalterna var 6 respektive 4 %. Vattensammansättningarna var stabila under pumpnings- och provtagningsperioderna. Dock var spolvattenhalterna relativt höga och kan ha påverkat sammansättningarna i någon grad.

Även i borrhål KFR106, liksom i de tidigare undersökta borrhålen KFR101 och KFR102A, var grundvattnet i den djupaste sektionen mindre salint än i den ytligare. Skillnaden är signifikant, men inte så uttalad som i borrhålet KFR101.

Contents

1 Introduction

This report comprises part of the complementary site investigations for the future expansion of the SFR and presents fracture mineralogy and hydrochemical data from borehole KFR106. These data will be used also within the forthcoming project "Uranium and redox conditions in Forsmark" concerning the elevated uranium contents described in groundwaters at the SFR and Forsmark sites (Laaksoharju et al. 2008, Nilsson et al. 2011).

Original data from the reported activities are stored in the primary database Sicada where data are traceable by the Activity Plan numbers (AP SFR-09-029 and AP SFR-11-004). Only data in these databases are accepted for further interpretation and modelling and therefore the data presented in this report represent copies of the original data. Data in the databases may be revised, if needed, albeit this will not necessarily result in a revision of the P-report, although the normal procedure is that major revisions entail a revision of the P-report. Minor revisions are normally presented as supplements available at www.skb.se.

Originally borehole KFR106 was not intended for hydrochemical sampling; the main purpose was to study the presence of possible subhorizontal zones in the area. However, during the SFR SDM investigations it was decided that the groundwater chemistry in the borehole was sufficiently important to investigate due to the following reasons:

1) To determine the oxygen state of uranium in the groundwater. Furthermore, to study potentially the *in situ* uranium state of the solid fracture phases, core samples were collected also.
2) First strike information is missing since no samples (Wire-Line) were collected during drilling.
3) Electrical Conductivity (EC) data from this borehole indicated that the groundwater is less saline in the deeper parts of the borehole (similar to conditions in boreholes KFR101 and KFR102A). Therefore, it was decided that groundwater sampling in KFR106 was important to understand the three dimensional distribution of different water types.

Table 1-1. Controlling documents for the performance of the activities.

Activity plan	**Number**	**Version**
Sprickmineralogiska undersökningar i KFR106.	AP SFR-11-004	1.0
Pumpning för hydrologisk provtagning i två sektioner av borrhål KFR106.	AP SFR-09-029	1.0
Method descriptions	**Number**	**Version**
Metodbeskrivning för sprickmineralanalys.	SKB MD 144.001	1.0
Metodbeskrivning för vattenprovtagning och analys i instrumenterade borrhål (under framtagning).	SKB MD 425.001	In prep.
Mätsystembeskrivning – Handhavandedel; System för hydrologisk och meterologisk datainsamling. Vattenprovtagning och utspädningsmätning i observationshål.	SKB MD 368.010	1.0

1.1 Borehole KFR106

KFR106 is an approximately 300 m long conventional type core-drilled borehole, and not of the telescopic type; the technical description and design of the borehole is presented in Nilsson (2009). Borehole KFR106 was drilled from the small islet Kobben located 225 m SE of the pier at the Forsmark harbour (Figure 1-1). No sedimentary overburden is present on the islet and drilling was performed directly on the bedrock surface. The borehole is 300.13 m long, inclined 69.89° from the horizontal towards the SSE (195.11°) and reaches a depth of about 290 m below the surface. The upper 9.13 m of the borehole was percussion drilled and then cased, followed by core drilling using the triple tube technique (Nilsson 2009). The geology of borehole KFR106 is described in Petersson et al. (2010) and Curtis et al. (2011) and a summary is presented in Figure 1-2.

The drilling of the borehole was completed on September 3, 2009 and the borehole was drilled using Baltic Sea water as drilling water; information on the drilling water composition is found in Appendix 1.

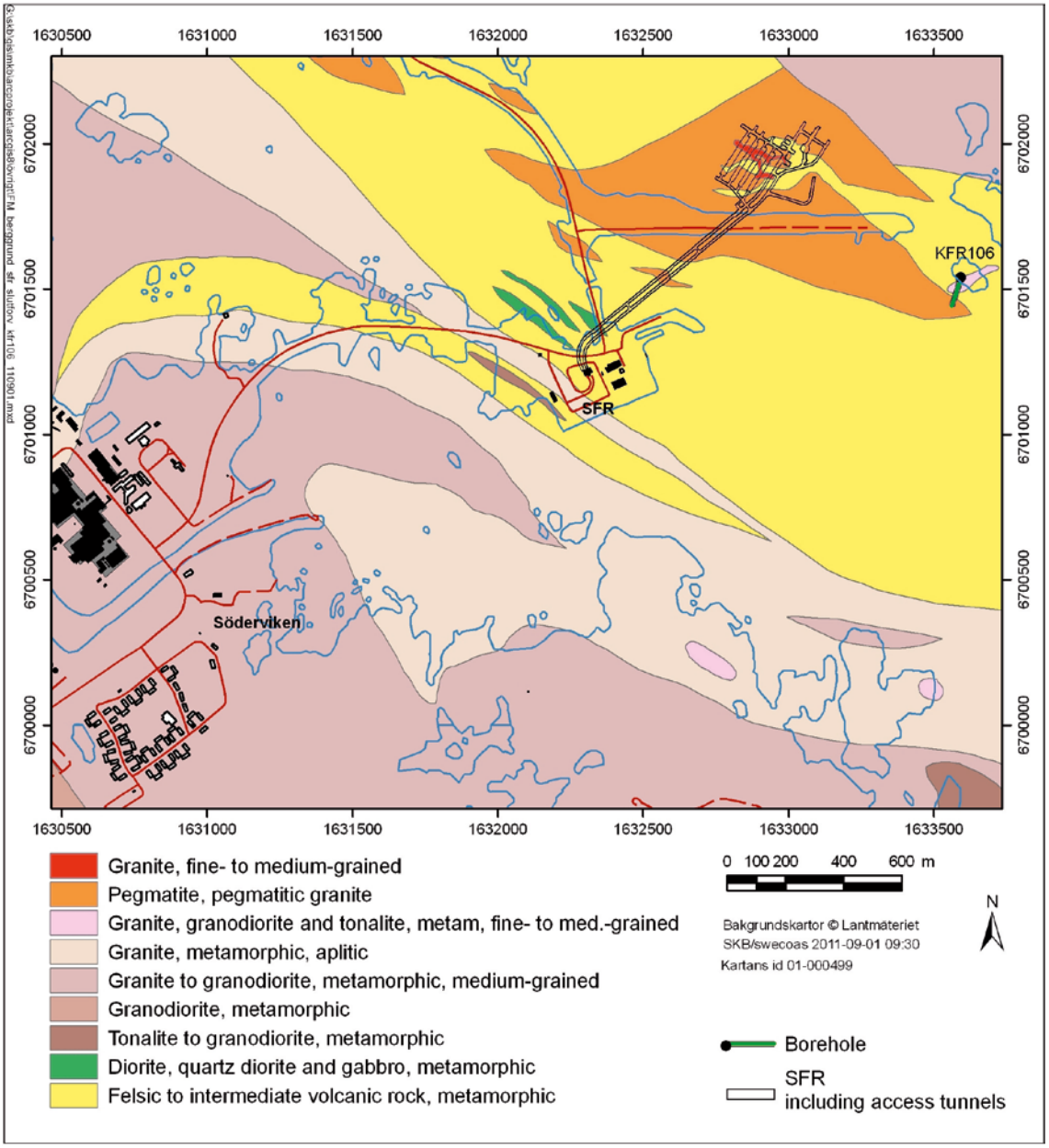

Figure 1-1. *Bedrock geology of the SFR area together with the surface projection of borehole KFR106.*

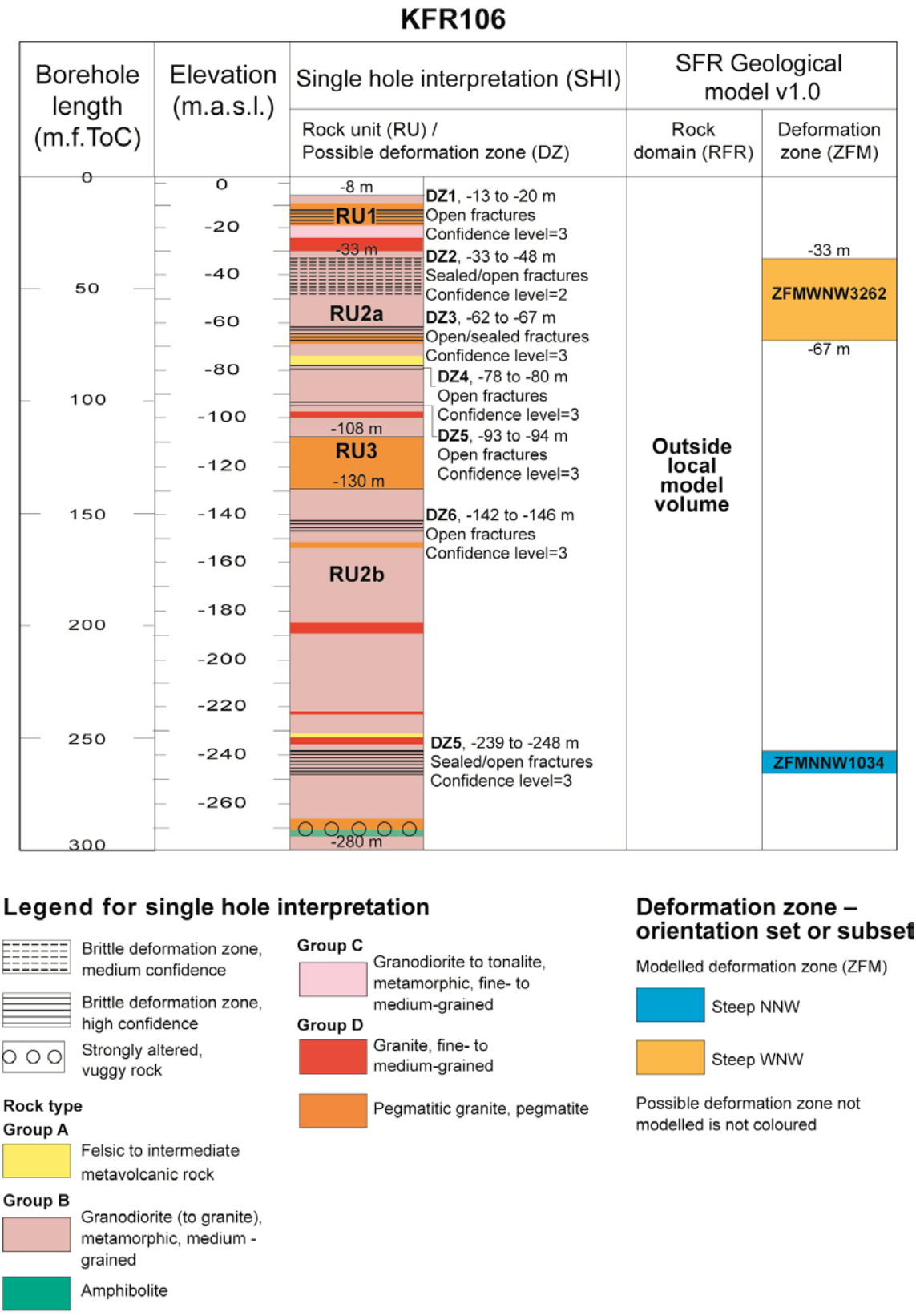

Figure 1-2. *Geology of borehole KFR106 adopted from Curtis et al. (2011).*

2 Background

2.1 Fracture mineralogy

During the Forsmark site investigation a number of groundwater samples with elevated uranium contents (>10 µm/L) were identified (Laaksoharju et al. 2008), and at the SFR site elevated uranium contents were identified in most of the bedrock groundwater samples (Nilsson et al. 2011). It has been suggested that the source of the uranium in the groundwater at Forsmark is an easily dissolvable uranium phase present in fractures and/or in the rock (Sandström et al. 2008, Smellie et al. 2008). However, only a single, small uranium mineral grain was identified (KFM03A 644.17 m) consisting of pitchblende associated with hematite and Fe-rich chlorite (Sandström et al. 2008). Later, during the complementary investigations for the future expansion of the SFR, uranium minerals were identified in several of the investigated fractures from boreholes KFR01, KFR08, KFR10, KFR19, KFR7A and KFR105. The uranium phases identified in these drill cores were uranium phosphate and uranium silicate (Sandström and Tullborg 2011).

In order to further explain the elevated groundwater uranium contents and to obtain an understanding of the uranium systems in the Forsmark and SFR groundwaters, it was decided to initiate a project with special focus on analysing the oxidation state of uranium in the groundwaters and measuring the uranium decay series in the solid phases. The fracture mineralogy presented in this report represents the first phase of this project which will provide background information for the interpretation of the data obtained during future studies.

Since mishandling of the drill cores after drilling could affect the oxidation state of uranium, the drill core samples were removed immediately on recovery, gently dried and then quickly wrapped into two heavy-duty PVC bags and finally sealed in plastic coated aluminium foil; all three layers were repeatedly flushed with nitrogen, evacuated and heat sealed (Waber et al. 2009).

2.2 Hydrochemistry

The three packed-off borehole sections in KFR106 comprise 40, 116 and 142 m long sections, i.e. KFR106:1, KFR106:2 and KFR106:3, respectively. Such long sections usually mean that several water conducting fractures contribute to the groundwater sampled, and therefore careful attention must be paid to the hydraulics of the borehole sections (e.g. variations in transmissivities) to insure that each groundwater sample collected is representative for the water-bearing fracture in question.

In the upper section of KFR106:3, there are several relatively large flow anomalies spread along the entire section. This implies that extensive pumping must be performed initially in order to minimise admixing/contamination of the water already present in the borehole section before starting pumping to collect representative groundwaters from selected water-bearing fractures. However, because of the absence of a dominant hydraulic fracture system in this borehole section, no groundwater sampling was performed.

In the central section of KFR106:2 there is one dominating anomaly in the upper part of the borehole section; however, another flow anomaly, contributing about 10% of the total flow is located some 40 m below. This is not an ideal situation for removal of the initial section water, i.e. water present in the borehole section before sampling. However, plug flow calculations (Figure 2-1) have shown that pumping for at least 8 days would be enough to ensure that most of the water from the borehole section comprises formation groundwater from the dominant hydraulic fracture system of interest.

In the lowest section of KFR106:1, there is only one anomaly situated just below the packer. This is most favourable for obtaining a groundwater sample where the composition is dominated by formation water representing only one hydraulic structure. Therefore, sampling was carried out accordingly.

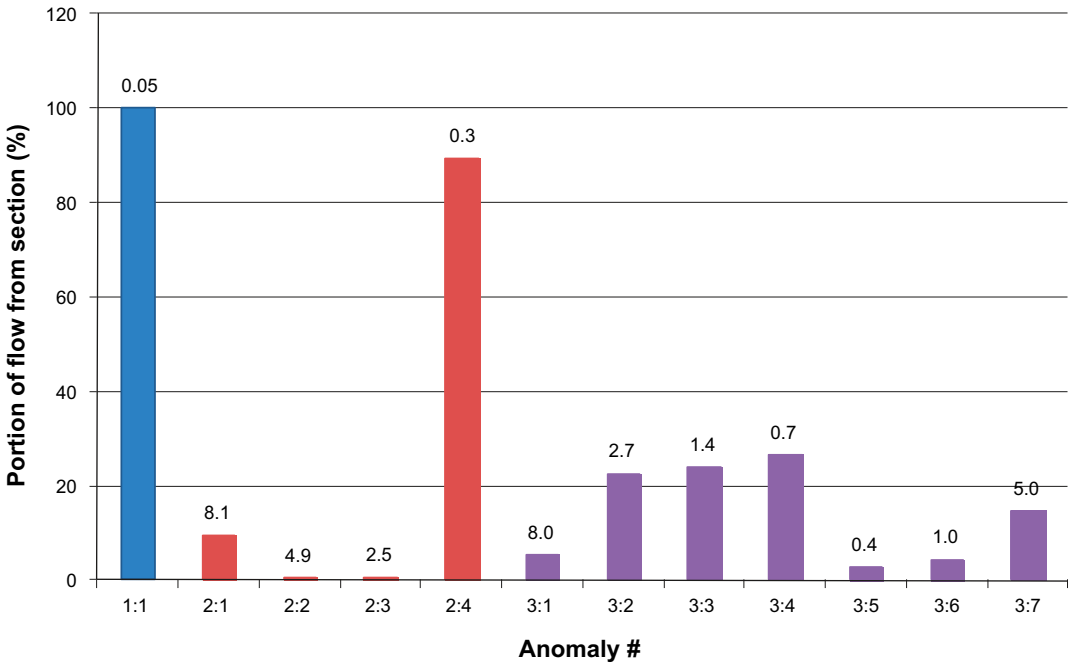

Figure 2-1. *The anomalies in the figure refer to those presented in Appendix 2 (PFL-logging). The figure shows the ratio of the total flow from a specific anomaly. The labels above the bars show the time (days) for the flow (plug flow) from the respective anomaly to reach the aperture of the tube connected to the borehole section, assuming a pump flow of 8 L/hour.*

Conventional boreholes do not allow effective pumping during drilling, which implies risks of high drilling water contents in groundwater samples. During the drilling of KFR106, Baltic Sea water was used.

Only those borehole activities that are necessary in order to select borehole sections were carried out prior to the groundwater sampling. The more downhole equipment used in the borehole, the greater is the risk of disturbance and contamination. The activities/investigations performed in KFR106 prior to the groundwater sampling are listed in Table 2-1.

Table 2-1. Activities performed in KFR106 prior to the groundwater sampling.

Activities performed *	Date of completion*	Borehole length (m)*
Percussion drilling	2009-06-23	0.00–9.13
Core drilling	2009-09-03	9.13–300.13
Fracture mineral sampling; uranium	2009-09-07	16.62–300.00
Geophysical logging	2009-09-10	3.00–299.50
BIPS logging	2009-09-23	9.00–297.30
Radar logging	2009-09-22	0.00–290.00
Flow logging (PFL)	2009-10-07	2.32–300.13
Packer installation	2009-10-21	

*From Sicada.

3 Objective and scope

In this report, characterisations of the mineralogy of the drill core sections sampled for the uranium project are presented. The emphasis has been to relate the fractures in the sampled drill core sections with the previously identified and characterised fracture mineral generations in the Forsmark area (Sandström et al. 2008, 2009) and to identify the uranium phases present in the fractures. The samples selected for this present study and reported here are listed in Table 3-1.

The hydrochemical results from analysis of groundwaters sampled in two sections in borehole KFR106 are also presented in this report. Borehole section lengths for the investigated sections are given in Table 3-2 and borehole sections, sampling dates, collected samples and analyses performed are presented in Table 3-3. Due to space restrictions, only three delimited borehole sections for continuous pressure measurements (Hydro Monitoring System; HMS) have been installed. None of the sections represent a so-called circulation section and therefore air-lift pumping had to be used to retrieve the groundwater samples.

Evaluation of the interrelationship between the fracture mineralogy and hydrochemistry is outside the scope of this report and will be carried out within the forthcoming "Uranium and redox conditions in Forsmark" project.

Table 3-1. Samples selected for fracture mineralogical characterisation. Elevation data have been extracted from Sicada (data delivery Sicada_11_082 (2011-08-16), Sicada_11_082_1 (2011-09-12) and Sicada_11_082_2 (2011-09-15).

Idcode Borehole	Secup m	Seclow m	Elevation_Secup m.a.s.l.	Elevation_Seclow m.a.s.l.
KFR106	16.97	17.42	–14.90	–15.32
KFR106	19.00	19.30	–16.81	–17.09
KFR106	68.38	68.51	–63.15	–63.28
KFR106	85.13	85.52	–78.87	–79.23
KFR106	86.88	87.33	–80.51	–80.93
KFR106	100.56	101.08	–93.33	–93.82
KFR106	112.91	113.35	–104.90	–105.31
KFR106	131.42	131.71	–122.22	–122.49
KFR106	154.22	154.99	–143.54	–144.26
KFR106	156.11	156.20	–145.31	–145.39
KFR106	175.25	175.58	–163.20	–163.50
KFR106	188.14	188.56	–175.24	–175.63
KFR106	229.59	230.11	–213.96	–214.45
KFR106	244.83	245.35	–228.19	–228.68
KFR106	262.48	262.97	–244.67	–245.13
KFR106	292.03	292.07	–272.26	–272.29
KFR106	295.79	296.19	–275.76	–276.14

Table 3-2. Borehole section lengths for the sections included in the hydrochemical sampling in KFR106, November 2009.

Borehole	Section (m borehole length)	Mid section elevation (m.a.s.l.)
KFR106:1	260–300	–187
KFR106:2	143–259	–261

Table 3-3. Sampling data and analytical protocol for groundwater sampling in KFR106.

Idcode	Section (m)	Sampling date	Sample no.	Analyses	Comments
KFR106:1	260–300	2009-11-04	16599	Class 3	pH (field), EC (field), Temp (field), U and Th (ICP)
KFR106:1	260–300	2009-11-04	16600	Class 3	pH (field), EC (field), Temp (field), U and Th (ICP)
KFR106:1	260–300	2009-11-05	16601	Class 5	pH (field), EC (field), Temp (field), U and Th (ICP), δ^2H, ^3H, $\delta^{18}O$ and U- and Th isotopes
KFR106:2	143–259	2009-11-04	16602	Class 3	pH (field), EC (field), Temp (field), U and Th (ICP)
KFR106:2	143–259	2009-11-04	16603	Class 3	pH (field), EC (field), Temp (field), U and Th (ICP)
KFR106:2	143–259	2009-11-05	16604	Class 5	pH (field), EC (field), Temp (field), U and Th (ICP), δ^2H, ^3H, $\delta^{18}O$ and U- and Th isotopes

4 Execution

4.1 Fracture mineralogy

4.1.1 Sampling

Sampling of the drill core was carried out between 2009-08-25 and 2009-09-07 in connection with the drilling of the borehole. To minimise potential oxidation effects induced by exposure of the rock samples to air, samples were collected and preserved following the methodology of Waber et al. (2008). Following drilling, the drill core samples were immediately removed, gently cleaned using a dry towel following drilling and selection, and then wrapped into two heavy duty PVC bags and finally sealed in plastic coated aluminium foil. All three layers were repeatedly flushed with nitrogen, evacuated and heat sealed. The time for the sample selection and packing was minimised to less than 10–15 minutes after core recovery. The packed samples were then air freighted to the laboratory in Helsinki where they were stored in a glove box under oxygen-free conditions.

Additional sampling of the borehole was carried out in 2009-12-02 using a gamma-spectrometer for identifying radioactive parts of the drill core that may reveal U-bearing minerals.

The samples were subsequently investigated in Helsinki (2011-04-14) when it was decided which analyses were suitable/possible for each sample. From each drill core sample, a minor part from suitable samples was removed from the glow box for the mineralogical characterisation presented in this report.

4.1.2 Preparation

To fit the sample into the SEM-EDS sample chamber a rock saw was used if required; subsequently all samples were each mounted on a sample stub for the SEM-EDS analyses. Thin sections were prepared by Minoprep AB, Hunnebostrand, Sweden.

4.1.3 Analytical work

SEM-EDS

A Hitachi S-3400N scanning electron microscope (SEM) equipped with an INCADryCool energy dispersive X-Ray spectrometer (EDS) and operated using low-vacuum mode (15 Pa), was used to examine the fracture surfaces at the University of Gothenburg, Sweden. Mineral identification was carried out using EDS-spectrums and quantitative mineral analyses.

The quantitative analyses were carried out on carbon coated thin sections under high vacuum conditions with a working distance of 9.9 mm, an accelerating voltage of 20 kV, a specimen current of ~3.5 nA and a counting time of 40 s. The instrument is calibrated with natural minerals and simple oxide standards; cobalt was used as a reference standard. Raw counts were reduced using ZAF correction on an online Oxford INCA X-ray microanalysis system. The accuracy for the major element analyses is generally better than 5% with detection limits of 0.2 wt%.

XRD

XRD analyses were carried out by Erik Jonsson at the Geological Survey of Sweden (SGU), Uppsala, Sweden. The samples were first examined by microscopy and subsamples were then selected and milled in acetone in an agate mortar and dried. The major part of the sample powders were taken out by ethanol and after drying mounted in the sample holder. XRD analyses were carried out with a Siemens D5000 Bragg-Brentan type teta-teta diffractometer with cupper radiation (CuK α) at 40 kV and 40 mA. The X-rays were focussed with a graphite monochromator. Scans were run from 2°–65° (2-theta) and analyses were performed with a fixed 2° divergence, a 2 mm receiving slit and a 0.6 mm receiving slit. From the microscopy examination, it was suspected that the minerals were at least partially metamict and therefore the analytical time was doubled (2 h) to obtain better resolution.

The XRD raw files were stored in the Bruker AXS software DIFFRAC^{plus} 2.2, and evaluated using the EVA software together with the PDF database (ver. 1994).

4.2 Hydrochemistry

4.2.1 Sampling equipment

The sampled borehole KFR106 was sealed off by inflated packers so that three different borehole sections were created; general details of the instrumentation in a cored borehole are presented in Figure 4-1.

Due to the small diameter of the standpipes in a core-drilled borehole, an air-lift pump was used to retrieve the water samples from the sampled sections instead of a conventional pump. An outline of the sampling set-up showing the pump equipment is presented in Figure 4-2 and Figure 4-3. The pump operates with the aid of two tubes which are lowered almost to the bottom of the standpipe. The two tubes are connected to each other via a unit with non-return valves at the bottom. By applying a gas pressure to one of the tubes it will be emptied via the other tube and the water can be collected at the surface. When the first tube is emptied, a pump control unit releases the gas pressure and the tube will be filled with water from the standpipe. Again, the gas pressure is applied by the control unit and the procedure is repeated. By using a multiple connection to the control unit and a number of pairs of tubes, more than one borehole section may be pumped at the same time.

The sampling conditions caused by air-lift pumping are different from the conventional pumping used, for instance, in the hydrogeochemical monitoring programme. The more effective (intermittent) pump action might affect the borehole walls, and thus have an impact on the water composition. Especially, constituents such as hydrogen sulphide, TOC, DOC and trace metals may be affected.

No pressure registrations have been made during the pumping and sampling period as no equipment was installed at that time.

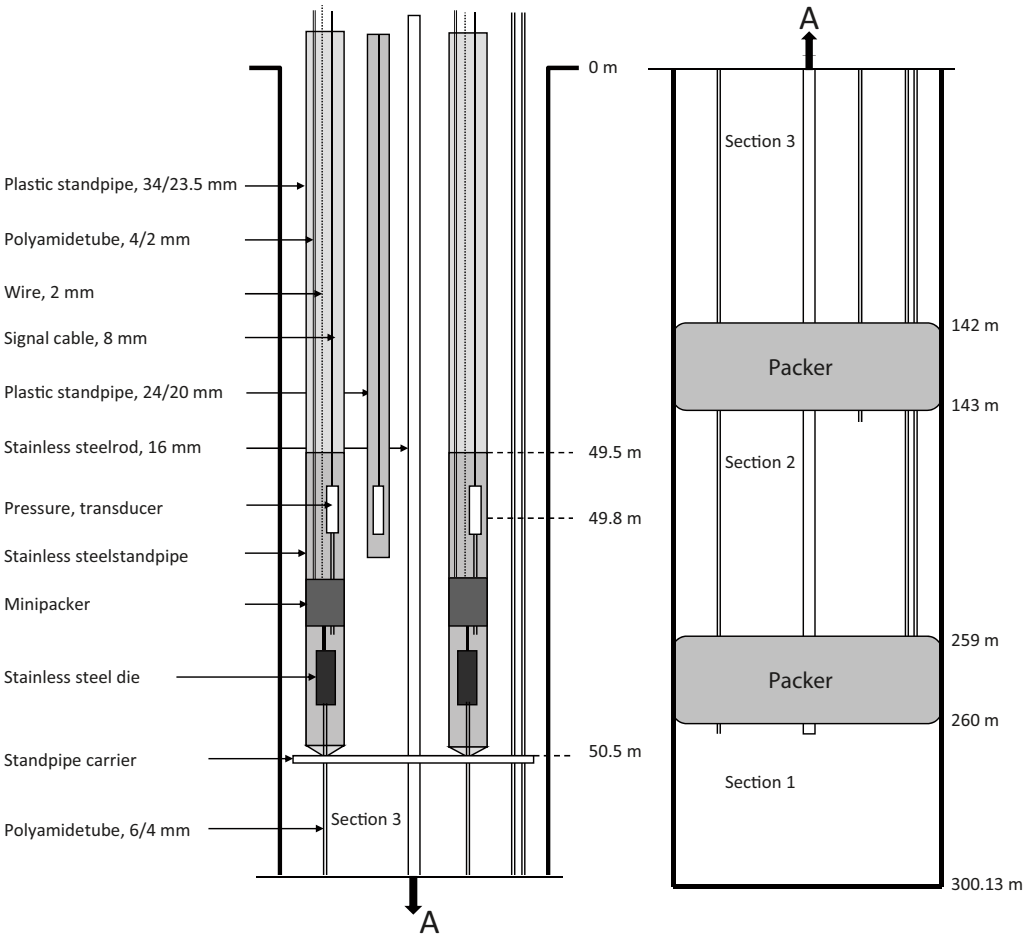

Figure 4-1. *Schematic picture of the instrumentation in a conventional core drilled borehole. The positions given are valid for borehole KFR106.*

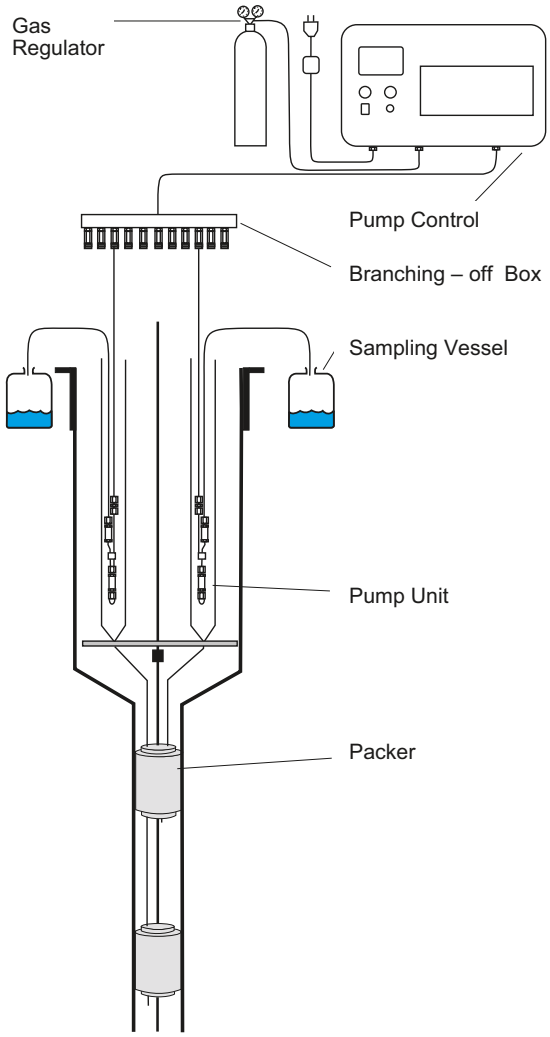

Figure 4-2. *Schematic picture of the sampling set-up and equipment used to perform air-lift pumping.*

Figure 4-3. *Air-lift pump equipment used in small diameter standpipes.*

4.2.2 Performance

Groundwater sampling and field measurements

The water volume in section KFR106:1 was exchanged 2.9 (first sample) to 3.4 times (third sample) during the pumping and sampling period, and 1.2 (first sample) to 1.4 times (third sample) in section KFR106:2. The total volumes pumped prior to the groundwater sampling are given in Appendix 3. Existing hydraulic connections during the pumping period in November 2009 are unknown, as no pressure registrations were performed at the time of pumping and sampling.

In addition to sampling groundwater, field measurements of temperature, electric conductivity (EC) and pH were conducted during the sampling period. The water pumped from the borehole was led through a measurement cell with probes and electrodes as well as a temperature sensor for measurements of field pH (pH_F), field electrical conductivity (EC_F) and groundwater temperature. The results are given in Appendix 1.

Sample portions intended for analysis of major constituents were filtered using a syringe equipped with disposable 0.4 µm membrane filters. During the entire sampling, laboratory gloves were used to minimise the risk of contaminating the samples.

Groundwater sample treatment and analyses

An overview of sample treatment and analysis routines for major constituents, minor anions, trace metals and isotopes is given in Appendix 4; the routines are applicable independently of sampling method or sampling object.

5 Results

5.1 Fracture mineralogy

5.1.1 Identified fracture minerals

A summary of the fracture mineralogy in the analysed drill core samples is presented in Table 5-1; the samples are described in more detail in Appendix 5. BIPS images of the sampled sections are presented in Appendix 6.

Description of identified fracture minerals

Idealised mineral formulas according to Deer et al. (1992).

Adularia ($KAlSi_3O_8$) is a low-temperature form of K-feldspar. The colour can be brick-red due to hematite staining, but also greenish varieties occur in fine-grained mixtures with quartz.

Albite ($NaAlSi_3O_8$) is commonly found in fracture fillings together with hydrothermal K-feldspar (adularia). The mineral occurs both as white and red varieties, the latter due to hematite staining.

Allanite ($(Ca,Mn,Ce,La,Y,Th)_2(Fe^{2+},Fe^{3+},Ti)(Al,Fe^{3+})O.OH[Si_2O_7][SiO_4]$) is found as small grains on one fracture surface.

Asphaltite ("bergbeck" in Swedish). The term is used in a broad sense, meaning black, highly viscous to solid hydrocarbons.

Barite ($BaSO_4$) occurs as small, often euhedral crystals on the fracture surfaces. $(Ba,Sr)SO_4$, probably as a solid solution between barite and celestine, has also been identified.

Biotite ($K_2(Mg,Fe^{2+})_{6-4}(Fe^{3+},Al,Ti)_{0-2}Si_{6-5}Al_{2-3}O_{20}(OH,F)_4$) occurs in the fractures but originates from the wall rock.

Calcite ($CaCO_3$) occurs abundantly and as several generations.

Chalcopyrite ($CuFeS_2$) occurs as small grains and is generally found together with pyrite and galena.

Chlorite ($(Mg,Fe,Al)_3(Si,Al)_4O_{10}(OH)_2$) occurs abundantly and is a dark-green mineral found in several associations. XRD identifies the chlorite as clinochlore but large variations in FeO/MgO ratios are indicated from SEM-EDS analyses (Sandström and Tullborg 2011).

Fluorite (CaF_2). Only one small crystal of fluorite has been identified.

Galena (PbS) occurs in small amounts and is generally found together with pyrite.

Hematite (Fe_2O_3) generally occurs as micro-grains of hematite causing red staining of clay minerals and chlorite in many fracture coatings.

Illite ($K,H_2O)Al_2[(Al,Si)Si_3O_{10}](OH)_2$) occurs as micro- to cryptocrystalline, micaceous flakes (Sandström and Tullborg 2010), and is usually light grey in colour.

Laumontite ($CaAl_2Si_4O_{12} \cdot 4H_2O$) is a zeolite mineral. It is brittle and the crystals show prismatic shapes. The mineral itself is white, but, at Forsmark, it is stained red due to micro-grains of hematite, although white varieties are also present.

Table 5-1. Fracture mineralogy of the analysed samples as determined by binocular microscope, SEM-EDS and XRD analysis.

Drill core	Adj Secup (m)	Clay mineral	Chlorite	Quartz	Adularia	Albite	Calcite	Pyrite	Galena	Barite	U-mineral	Fe-oxide	(Ca,REE)-carbonate	Other
KFR106	16.97	x(i-s[1])			x	x	x	x	x	x(c[2])		x(Hm[3])	x	asphaltite, galena
KFR106	19.00	x(i-s[1])					x	x	x	x			x	
KFR106	68.38	x(corr[4])		x			x	x		x				allanite
KFR106	85.13	x(corr[4])	x	x	x			x	x	x	x(p[5])			biotite, drilling debris
KFR106	86.88	x(i-s[1])		x	x		x	x	x	x(c[2])	x(p[5])			ChPy[6], monazite, fluorite
KFR106	100.56	x(i-s[2]), (corr[4])		x	x			x	x	x(c[2])		x(Hm[3])		ChPy[6]
KFR106	112.91	x(illite)							x	x		x(Hm[3])		biotite, ChPy[6], monazite, (Cu,Fe,W)-sulphide
KFR106	131.42	x(i-s[2]), (corr[4])						x						laumontite
KFR106	154.22	x(i-s[1])		x	x		x	x						
KFR106	154.61	x(i-s[1])	x	x		x	x	x		x(c[2])				titanite, monazite
KFR106	156.11	x(i-s[1])			x			x		x		x(Hm[3])		metallic iron
KFR106*	175.25			x		x					x(oxide)	x(Hm[3])		zircon, Th-silicate, muscovite, (Mn,Ca)-silicate
KFR106	188.14	x(i-s[1])		x	x					x				sericite, ChPy[6]
KFR106	229.59	x(i-s[1]), (corr[4])						x		x				
KFR106	244.83	x(i-s[1]), (corr[4])					x	x	x					
KFR106	262.48	x(i-s[1]), (illite)		x	x		x	x						metallic iron
KFR106	295.79	x(i-s[1])	x	x			x	x	x					xenotime, monazite, ChPy[6]
KFR106	292.03	x(corr[4])		x	x	x	x		x		x(Pitchb[7])	x(Hm[3])		titanite, apatite, rutile

* = pegmatite sample.

[1](i-s) = smectite-illite.

[2](c) = barite-celestine.

[3](Hm) = hematite.

[4](corr) = corrensite.

[5](p) = phosphate.

[6]ChPy = Chalcopyrite.

[7](Pitchb) = Pitchblende.

Mixed layer clays

Corrensite is a chlorite-like mixed layer clay with layers of chlorite and smectite/vermiculite, usually with a ratio of 1:1. XRD analyses indicate a poorly ordered crystalline structure (Sandström and Tullborg 2011).

Smectite-illite is a mixed layer clay consisting of layers of smectite and illite. XRD analyses indicate a poorly ordered crystalline structure (Sandström and Tullborg 2011). *Smectites* are a group of swelling clay minerals containing different proportions of Ca and/or Na together with Mg and Fe.

Monazite ($(Ca,La,Th)PO_4$) is found as a few small, poorly crystallised grains on the fracture surfaces.

Pitchblende (UO_2) has been identified in one sample; it is poorly crystallised and partly coffinitised.

Pyrite (FeS_2) is found in many fractures, generally as small euhedral, cubic crystals.

Quartz (SiO_2) generally occurs as small and occasionally hematite stained euhedral crystals covering the fracture walls. They often have a greyish sugary appearance but can also be transparent and then appear to have the colour of the wall rock.

REE-carbonate ($(Ca,REE,)CO_3$) occurs sparsely as small, poorly crystallised crystals on fracture surfaces.

Sericite ($K_2Al_4[Si_6Al_2O_{20}(OH,F)_4$) is a fine-grained muscovite.

Titanite ($Ca,Ti[SiO_4](O,OH,F)$)

Uranium silicate. An unknown U(Ca)-silicate was identified in one sample.

Uranium phosphate was identified in two fractures.

Xenotime ($Y(PO_4)$) has been identified in one sample.

5.1.2 Uranium minerals

Uranium oxide mineral in KFR106: 292.03–292.07 m

The sample at 292.03–292.07 m consists of a cataclasite at the contact between pegmatite and amphibolite. XRD analysis shows that the uranium mineral in general is x-ray amorphous (Figure 5-1). However, a few relatively strong peaks suggest that also uraninite is present (Figure 5-2). In addition, the rock sample contains calcite and hematite.

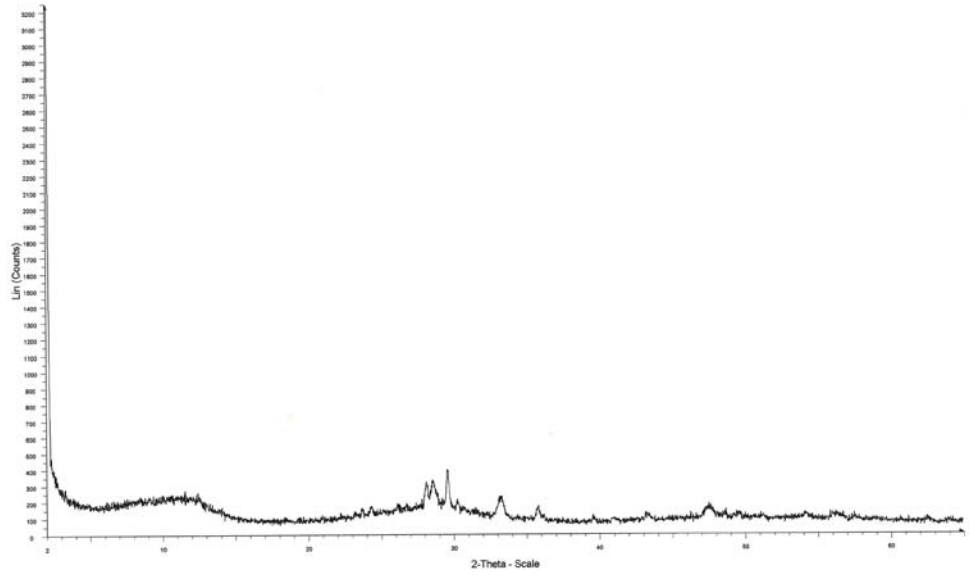

Figure 5-1. *XRD-diffractogram showing the large proportion of x-ray amorphous material. From uranium-rich phase in sample KFR106: 292.10-292.13 m.*

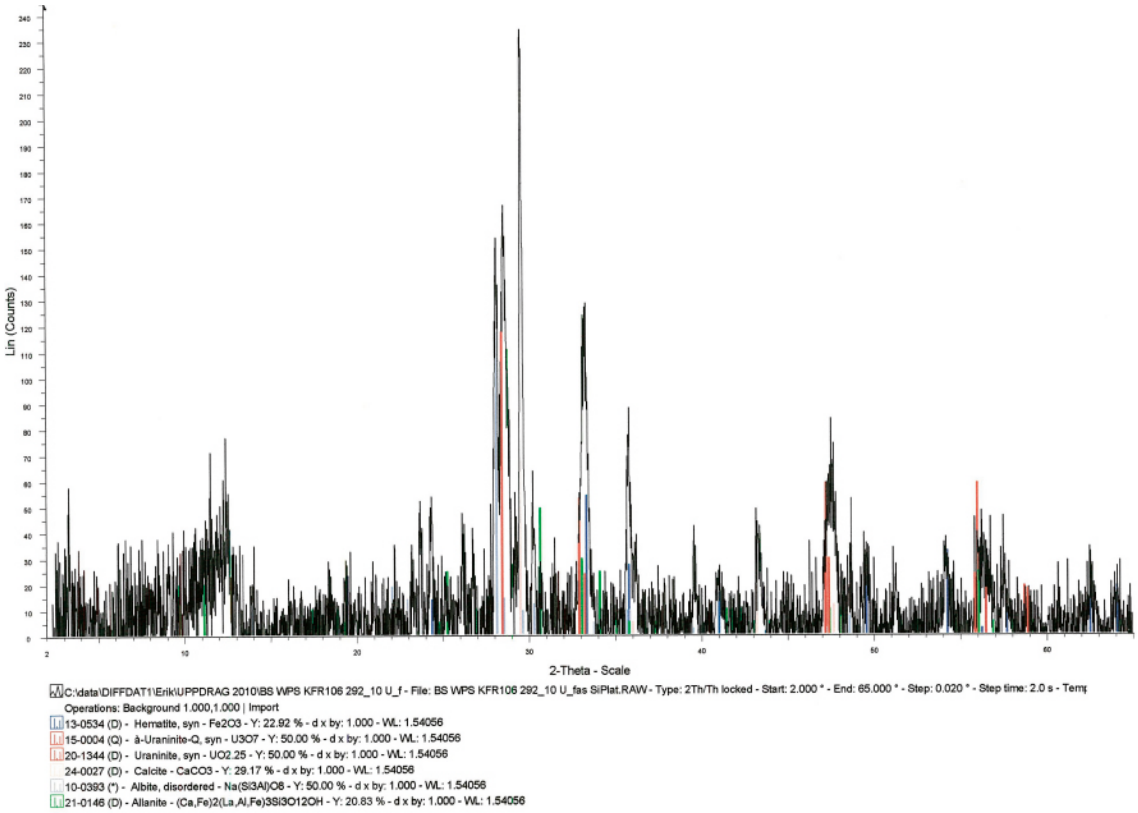

Figure 5-2. *X-ray diffractogram of sample KFR106: 292.03-292.07 m with exaggerated y-scale and broad amorphous peaks removed.*

Two thin sections were prepared from the sample (Figure 5-3). Subsample A is partly pegmatitic and is cut by fine-grained parts of mylonite/cataclasite consisting mainly of albite, quartz and chlorite. The mylonite/cataclasite is cut by sealed microfractures. Subsample B is dominated by fine-grained cataclasite consisting mainly of albite, quartz and chlorite cut by sealed microfractures. Based on the SEM-EDS, three different U-phases were identified in KFR106: 292.03–292.07 m; these phases are described below.

Phase 1 – Pitchblende grains

In general, pitchblende is somewhat lighter than uraninite, having a specific gravity of between 6 and 9, but its other properties, with the exception of crystal form, are the same. It occurs as irregular masses often with a rounded, layered, botryoidal structure.

In the sampled drill cores, pitchblende occurs as botryoidal grains and shows concentric banding (Figure 5-4). The mineral contains mainly U, Pb, Ca and Si but minor amounts of Mg, Mn, Fe and Al are also present; the UO_2 content is around 63–70 wt% (Table 5-2). The concentric bands are characterised by alternating Pb-concentrations (Figure 5-4B).

The XRD analysis also suggests the presence of uraninite with the theoretical formula UO_2. However, natural uraninite also contains radiogenic lead due to decay of U, and Ca can occur in the mineral due to solid solution. Other elements, including Si, are often present in low concentrations due to admixture or coffinitisation (e.g. Janeczek and Ewing 1992). The low totals (88–94 wt%) for the uranium phases (Table 5-2) obtained by EDS-analyses are probably due to hydration in combination with the presence of U(VI) in the U-mineral. The composition of the analysed mineral is in agreement with published data of the pitchblende variety of uraninite and the the XRD results, based mainly x-ray amorphous material and the botryoidal form, are also in agreement with that of the micro-crystalline pitchblende (cf. Frondel 1958).

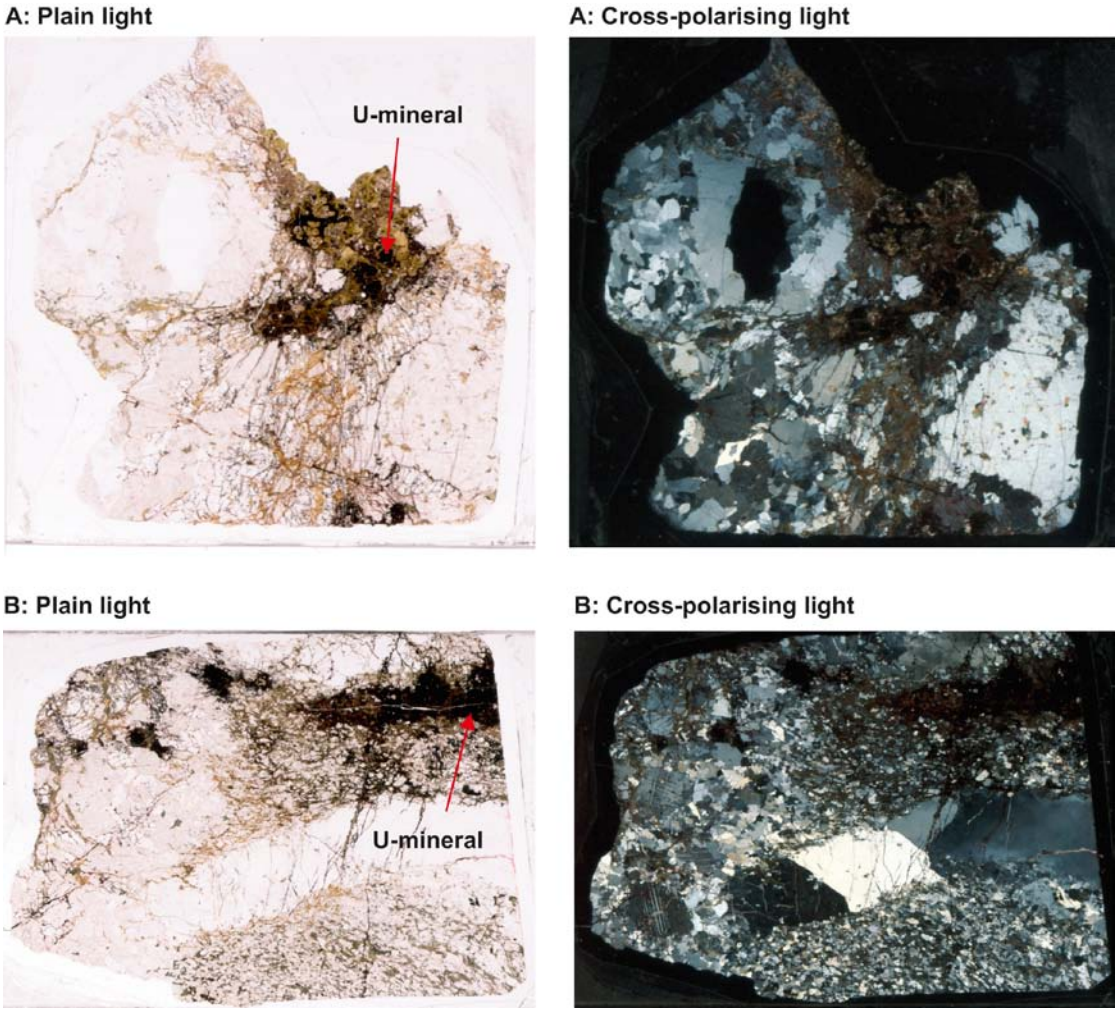

Figure 5-3. *Scanned thin sections from KRF106: 292.03-292.07 m. The vertical scale of the microphotographs is 2.6 cm.*

Uraninite is easily altered and may oxidise with partial conversion of U(IV) to U(VI) and the alteration is accompanied by a change in colour from black to dark brown. The alteration is also associated with hydration and U may be leached from the crystal, leaving an excess of daughter nuclides (e.g. lead, Frondel 1958). This is in agreement with the mineralogical and geochemical observation of the uranium mineral in sample KFR106: 292.03–292.07 m. The Si content indicates partial coffinitisation of the pitchblende (cf. Janeczek and Ewing 1992).

Altogether, it is inferred that the uranium mineral is coffinitised pitchblende that formed as a secondary product of uraninite alteration.

Phase 2 – Pitchblende in micro-fractures

Micro-fractures are observed sealed with a uranium mineral radiating out from the pitchblende grains; these fractures may have formed initially due to radiation damage (Figure 5-5A) and later infilled with this mineral. The uranium mineral is associated with calcite, hematite and galena (Figure 5-5B). The only significant geochemical difference between the uranium mineral in these micro-fractures and the pitchblende described above is that it contains no detectable Pb (<0.2 wt% PbO), more Fe (1.2–1.8 wt% FeO), and is more hydrated as evidenced by the low totals (Table 5-2). The low totals are probably explained by a combination of hydration and the presence of U(VI).

It is inferred that the uranium mineral in question is pitchblende and represents precipitation of U that was mobilised and leached from the uraninite during the same event that altered the uraninite to pitchblende as described above. During this event, U was leached from the crystal relative to lead, however, some Pb was also mobilised and precipitated as galena. The low concentration of radiogenic lead in this pitchblende suggests that it is significantly younger than the Phase 1 pitchblende.

Phase 3 – Pitchblende in cataclasite matrix

A U-rich phase occurs also in the matrix of the cataclasite associated with chlorite, calcite, galena, hematite, rutile and titanite (Figure 5-6). After precipitation of these minerals, a second event with precipitation of mainly calcite and clay mineral in a thin fracture cutting the cataclasite has occurred (Figure 5-6A). Geochemically, it has a composition intermediate to the two pitchblende phases described above with a lead content between <0.2 and 2.5 wt% PbO and a FeO-content between 1.4–1.5 wt% in the analysed samples (Table 5-2).

This phase is also pitchblende in type and it is inferred that is represents the geochemical and physical alteration of uraninite during the formation of the cataclasite during the same event as proposed for the alteration of the uraninite (Phase 1 pitchblende) and precipitation of pitchblende in the micro-fractures (Phase 2) as described above.

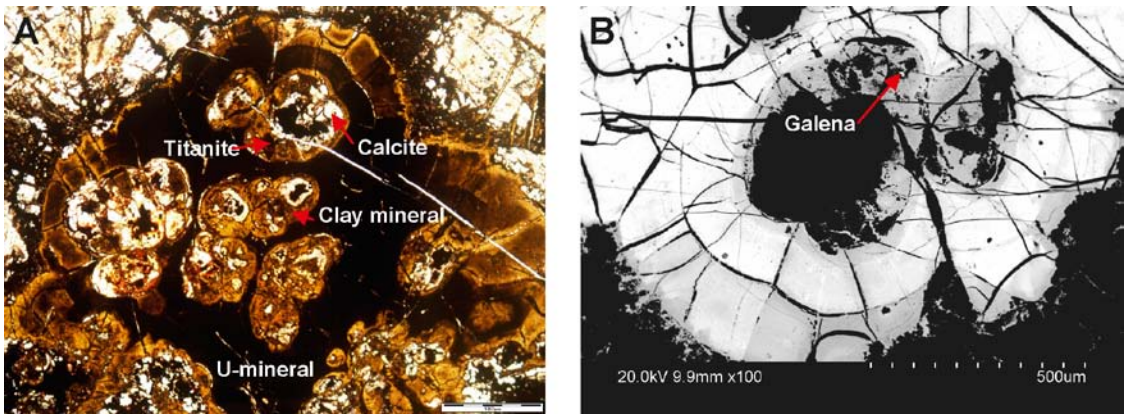

Figure 5-4. *A) Microphotograph of botryoidal U-mineral (Phase 1 pitchblende) with inclusions filled with mainly Mg-rich clay minerals, calcite, titanite and galena. The scale bar is 1,000 µm. B) Backscattered electron image (BSE) of a Phase 1 pitchblende with concentric banding. The density variation within the concentric bands seen in the BSE image is due to variations in the Pb-content (cf. Table 5-2). The micro-fractures within the U-mineral are sealed with calcite.*

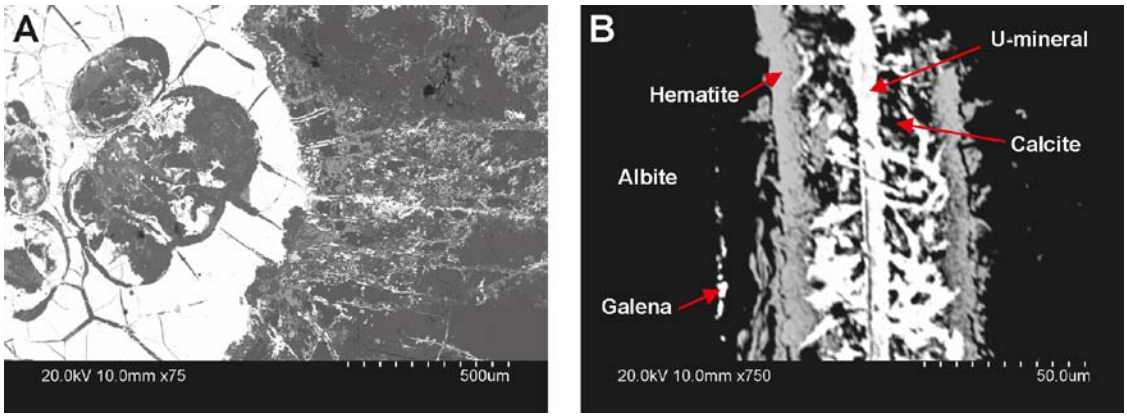

Figure 5-5. *A) Backscattered electron image (BSE) of micro-fractures sealed with a U-mineral (Phase 2 pitchblende) radiating out from the larger (Phase 1) pitchblende grain. B) BSE-image of micro-fracture cutting an albite grain sealed with a U-mineral associated with hematite, calcite and galena.*

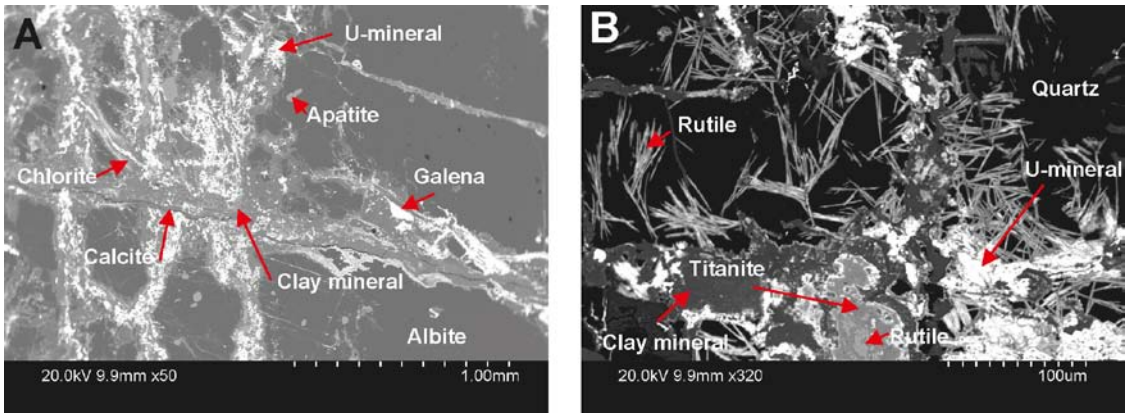

Figure 5-6. *A) Backscattered electron image (BSE) of cataclasite with matrix consisting mainly of chlorite and U-minerals. B) BSE image of rutile, titanite, clay mineral and U-minerals in the cataclasite matrix.*

Table 5-2. SEM-EDS data of uranium phases in sample KFR106: 292.03–292.07 m

Sample	A1	A2	A3	A4	A5	A6	A7	A8	A9	A10	B1	B2	B3
	BSE bright zone			BSE dark zone			Micro fracture				In cataclasite		
Na_2O	<0.2	<0.2	<0.2	<0.2	<0.2	0.2	<0.2	<0.2	<0.2	<0.2	<0.2	0.4	<0.2
MgO	0.2	0.5	0.5	<0.2	<0.2	0.2	0.2	0.2	<0.2	<0.2	<0.2	<0.2	<0.2
Al_2O_3	0.3	0.3	<0.2	0.4	<0.2	0.5	0.3	0.3	0.3	0.4	0.8	0.7	1.0
SiO_2	4.3	4.2	3.3	5.7	5.7	6.0	5.7	5.5	5.6	6.3	6.4	7.9	6.6
CaO	7.8	8.2	6.7	9.8	10.3	11.2	10.0	9.3	10.3	3.6	8.0	7.9	8.7
MnO	0.8	0.8	0.6	0.8	0.8	0.7	0.6	0.7	0.7	<0.2	0.6	0.5	0.6
FeO	<0.2	<0.2	<0.2	0.2	0.3	0.8	1.2	1.3	1.3	1.8	1.4	1.5	1.4
PbO	11.7	11.7	13.8	7.2	6.3	3.9	<0.2	<0.2	<0.2	<0.2	1.7	<0.2	2.5
UO_2	64.1	65.6	64.2	63.5	64.6	70.2	66.6	61.7	64.6	63.9	66.6	64.9	65.5
TiO_2	<0.2	<0.2	<0.2	<0.2	<0.2	<0.2	<0.2	<0.2	<0.2	<0.2	<0.2	0.42	0.4
ZnO	<0.2	<0.2	<0.2	<0.2	<0.2	<0.2	<0.2	0.2	<0.2	<0.2	<0.2	<0.2	<0.2
BaO	<0.2	<0.2	<0.2	<0.2	<0.2	<0.2	<0.2	<0.2	<0.2	2.7	<0.2	<0.2	<0.2
Total	89.2	91.2	89.0	87.5	88.0	93.7	84.6	79.2	84.5	78.7	85.5	84.2	86.6

Uranium oxide in KFR106: 175.25–175.58 m

Uranium oxide occurs between grains and in micro-fractures within grains in a pegmatite sample (Figure 5-7). No quantitative data were obtained due to the uneven surface of the sample but it contains significant amounts of Si and may be coffinitised uraninite.

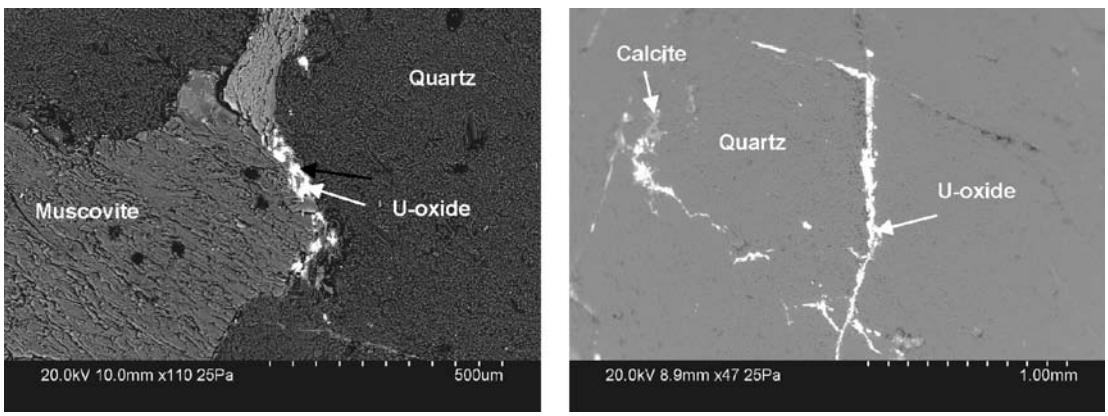

Figure 5-7. *Left: U-oxide between two grains of muscovite and quartz in pegmatite. Sample KFR106: 175.25-175.58 m. Right: U-oxide and calcite in micro-fractures within a quartz grain.*

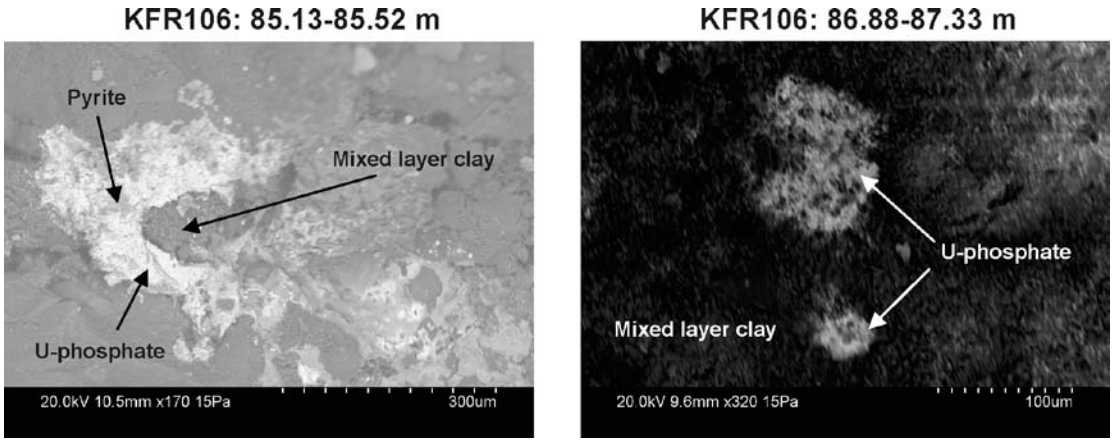

Figure 5-8. *Backscattered electron images of U-phosphate. Observe the intergrown pyrite and uranium phosphate in KFR106: 85.13-85.52 m (left-hand image).*

Uranium phosphate in KFR106: 85.13–85.52 and KFR106: 86.88–87.33 m

Uranium phosphate occurs as small (<0.3 mm) poorly crystallised mineral grains on the fracture surface (Figure 5-8). Due to the small size and uneven surface, no quantitative data were obtained from the EDS-analyses, but the Si, Mg, Al and Fe energy peaks in the EDS-spectra are inferred to come from clay minerals which were difficult to avoid due to the disseminated character of the U-mineral. Excluding these elements, the main constitutes are U, P and Ca (Table 5-2). Based on the good correlation between U and P in the analysed bulk fracture filling material at SFR (Sandström and Tullborg 2011), it is inferred that the U-mineral is an U-phosphate. One possibility is that this secondary mineral is autonite, a hydrated phosphate of Ca and U ($Ca(UO_2)_2(PO_4)\cdot 10–12\ H_2O$) (Frondel 1958).

The U-phosphate is cogenetic with pyrite (Figure 5-8); a similar U-phosphate was found cogenetic with asphaltite in borehole KFR01 (Sandström and Tullborg 2011). It is therefore suggested that that the U-phosphate belongs to generation 3 in the relative sequence of fracture minerals in the Forsmark area, i.e. of Palaeozoic origin (cf. Sandström et al. 2009).

5.2 Groundwater analyses

5.2.1 Basic analyses

Basic analyses included the major constituents Na, K, Ca, Mg, Fe, Li, Mn, S, Sr, SO_4^{2-}, Cl^-, Si, HCO_3^-, Br^-, F^- and I^-. Furthermore, both laboratory data and field measurement data on pH and electrical conductivity (EC) were obtained during the KRF106 sampling and the groundwater temperature was recorded in the field.

The charge balance errors provide an indication of the quality and uncertainty of the analyses of major constituents; the errors did not exceed the acceptable limit of ± 5% in any case. The basic water analysis data and relative charge balance errors are compiled in Appendix 1, Table A1-1.

5.2.2 Trace elements

Analyses of trace elements included only U and Th and are compiled in Appendix 1, Table A1-2.

5.2.3 Stable and radioactive isotopes

Isotope determinations included the stable isotopes δ^2H and $\delta^{18}O$ as well as the radioactive isotopes ^3H (TU), ^{234}U, ^{235}U, ^{238}U, ^{230}Th and ^{232}Th. Available isotope data are compiled in Appendix 1, Tables A1-3 and A1-4.

6 Summary and discussion

6.1 Fracture mineralogy

The most abundant fracture minerals in the examined drill core samples are clay minerals, calcite, quartz and adularia. Chlorite is also common but is mostly altered and found interlayered with clay minerals to form the mixed layer clay corrensite. The most common clay mineral is a mixed layer clay consisting of illite-smectite, often poorly crystallised. Pyrite, galena, chalcopyrite, barite (-celestine) and hematite are also commonly found in the fractures, but usually only in trace amounts. Other minerals identified are U-phosphate, pitchblende, U(Ca)-silicate, asphaltite, biotite, monazite, fluorite, titanite, sericite, xenotime and rutile and (Ca,REE)-carbonate. The general fracture mineralogy of drill core KFR106 is similar to other examined drill cores from the SFR area (Sandström and Tullborg 2011).

Three different U-minerals were found in the examined drill cores. The inferred oldest mineral of these was found in the contact between a pegmatite and a cataclasite. The mineral is a partly coffinitised pitchblende and it is suggested that it represents altered higher temperature crystalline uraninite originally found within the pegmatite. The U was mobilised during a hydrothermal event associated with the formation of the cataclasite and occurred under oxidising conditions as indicated by the presence of cogenetic hematite. It is inferred that the uraninite alteration and precipitation of pitchblende in the cataclasite is related to (or older) than precipitation of generation 2 minerals, i.e. precipitation occurred prior to 1,000 Ma (cf. Sandström et al. 2009). Pitchblende associated with hematite has previously been found in a sample from borehole KFM03A from the Forsmark site investigation (Sandström et al. 2008). In addition, an unidentified U(Ca)-silicate was found in a pegmatite sample from KFR106: 175.25–175.58 m. High U-content in the pegmatites is indicated by high natural gamma radiation (Curtis et al. 2011) and the same observations were made within the Forsmark site investigation area (Stephens et al. 2007).

Uraninite disseminations in skarn and pitchblende in veins associated with hematite, chlorite and quartz in old mines near Forsmark were described by Welin (1964). He suggested that precipitation of the disseminated uraninite occurred as the result of tectonic deformation in close connection with emplacement of pegmatites in the area. The pitchblende was inferred to have resulted from later circulation of U-bearing fluids during tectonic deformation; these observations concur with the present study. The age of the uraninite- and pitchblende-bearing veins in the area were dated to 1,585 Ma by U-Pb chronology (Welin 1964) although it is difficult to evaluate the accuracy of these ages, which were carried out on bulk uranium-ore samples. However, the ages are in agreement with the inferred age of >1,000 Ma of the pitchblende made in this study based on the genetic relation between pitchblende and the well-defined sequence of fracture mineral generations in Forsmark (cf. Sandström et al. 2009).

On the surface of two open fractures from KFR106, U-phosphate was found cogenetic with pyrite and mixed layer clays. In KFR01, the same kind of U-phosphate has precipitated cogenetically with generation 3 asphaltite and pyrite (Sandström and Tullborg 2011). Thus, it is concluded that precipitation of the U-phosphate is associated with precipitation of generation 3 minerals, i.e. it is of Palaeozoic age (cf. Sandström et al. 2006, 2009). It is plausible that the source of the U precipitated as phosphates was the uranium already present in the fracture system. It is also possible that additional U was added to the system by fluids emanating in the organic-rich sediments covering the area during the Palaeozoic (cf. Andersson et al. 1985, Larson et al. 1999, Sandström et al. 2006).

Based on the different U-minerals and their paragenetic associations, it is suggested that uranium has been mobilised and reprecipitated at several episodes:

1. Originally, U was introduced to the system during emplacement of U-rich pegmatites, probably as high temperature crystalline uraninite. Granite dykes in the Forsmark area interpreted to be of the same age as the pegmatites have been dated to ca. 1.85 Ga (Hermansson et al. 2007).
2. At a second event, U was mobilised under brittle and oxidising conditions during formation of breccia/cataclasite. The uraninite was altered to more amorphous, lower temperature pitchblende and partly coffinitised. Mobilised uranium precipitated as pitchblende closely associated with hematite and chlorite in cataclasite and fracture sealings. This event occurred prior to 1,000 Ma.

3. During the Palaeozoic, U was remobilised and precipitated as U-phosphate on open fracture surfaces; the U-phase is poorly crystallised or amorphous. The prevailing conditions in the fracture system during the Palaeozoic were reducing and the U-phosphate is associated with pyrite. Input of U emanating from the overlying, often uranium-rich alum shale that covered the Forsmark area during the Palaeozoic, is also possible.
4. An amorphous U-silicate has also been found on open fractures; the age of this precipitation is not known but it is inferred to be Palaeozoic or younger.

6.2 Hydrochemistry

The hydrogeochemical investigations in KFR106:1 and KFR106:2 included sampling of three consecutive samples in each borehole section in November 2009; some observations regarding the performance and the results are listed below:

- The observed EC in the deepest borehole section, KFR106:1 (850 mS/m), was indeed lower than the observed EC in section KFR106:2 (1,150 mS/m) at intermediate borehole depth. The value is slightly higher than the one in KFR101 at about the same depth.
- The collected samples from the borehole section in KFR106:1 and KFR106:2 showed rather high drilling water contents (6 and 4%, respectively). The water composition was generally stable in both sections through the sampling periods.
- The oxygen-18 signature in KFR106:1 is low and indicates a large contribution from glacial meltwater, although smaller in contribution than in borehole KFR101 at the same depth. In KFR106:2, the oxygen-18 signature suggests a mixed transition type groundwater. Tritium is 4.0 TU in the upper section and 2.1 TU in the lower section. The brackish-glacial water is in general expected to be tritium free and 2 TU cannot be explained by the drilling water content of 6%. However, the Mg content and other marine indicators point towards a component of marine water also in this sample which may explain the presence of tritium.
- The uranium concentration was relatively high in both sections (12 µg/L in KFR106:1 and 21 µg/L in KFR106:2) and the thorium concentrations were below the detection limit in all samples. The $^{234}U/^{238}U$ activity ratios were 2.17 and 2.5 respectively, which is within the range for other samples from Forsmark and SFR with elevated uranium concentrations.

References

SKB's (Svensk Kärnbränslehantering AB) publications can be found at www.skb.se/publications.

Andersson A, Dahlman B, Gee D G, Snäll S, 1985. The Scandinavian alum shales. Uppsala: Sveriges Geologiska Undersökning. (Serie Ca 56)

Curtis P, Markström I, Petersson J, Triumf C-A, Isaksson H, Mattsson H, 2011. Site investigation SFR. Bedrock geology. SKB R-10-49, Svensk Kärnbränslehantering AB.

Deer W A, Howie R A, Zussman J, 1992. An introduction to the rock-forming minerals. 2nd ed. Harlow: Longman.

Frondel C, 1958. Systematic mineralogy of uranium and thorium. Washington: U.S. Government Printing Office. (Geological Survey Bulletin 1064)

Hermansson T, Stephens M B, Corfu F, Andersson J, Page L, 2007. Penetrative ductile deformation and amphibolite-facies metamorphism prior to 1851 Ma in the western part of the Svecofennian orogen, Fennoscandian Shield. Precambrian Research 153, 29–45.

Janeczek J, Ewing R C, 1992. Dissolution and alteration of uraninite under reducing conditions. Journal of Nuclear Materials 190, 157–173.

Laaksoharju M, Smellie J, Tullborg E-L, Gimeno M, Hallbeck L, Molinero J, Waber N, 2008. Bedrock hydrogeochemistry Forsmark. Site descriptive modelling, SDM-Site Forsmark. SKB R-08-47, Svensk Kärnbränslehantering AB.

Larson S Å, Tullborg E-L, Cederbom C, Stiberg J-P, 1999. Sveconorwegian and Caledonian foreland basins in the Baltic shield revealed by fission-track thermochronology. Terra Nova 11, 210–215.

Nilsson A-C, Tullborg E-L, Smellie J, Gimeno M J, Gómez J B, Auqué L F, Sandström B, Pedersen K, 2011. Site investigation SFR. Bedrock hydrogeochemistry. SKB R-11-06, Svensk Kärnbränslehantering AB.

Nilsson G, 2009. Forsmark site investigation. Drilling of the cored borehole KFR106. SKB P-09-55, Svensk Kärnbränslehantering AB.

Petersson J, Nissen J, Curtis P, Bockgård N, Mattsson H, Stråhle A, Winell S, 2010. Site investigation SFR. Geological single-hole interpretation of KFR106 and HFR106. SKB P-10-08, Svensk Kärnbränslehantering AB.

Sandström B, Tullborg E-L, 2011. Site investigation SFR. Fracture mineralogy and geochemistry of borehole sections sampled for groundwater chemistry and Eh. Results from boreholes KFR01, KFR08, KFR10, KFR19, KFR7A and KFR105. SKB P-11-01, Svensk Kärnbränslehantering AB.

Sandström B, Tullborg E-L, de Torres T, Ortiz J E, 2006. The occurrence and potential origin of asphaltite in bedrock fractures, Forsmark, central Sweden. GFF 128, 233–242.

Sandström B, Tullborg E-L, Smellie J, MacKenzie A B, Suksi J, 2008. Fracture mineralogy of the Forsmark site. SDM-Site Forsmark. SKB R-08-102, Svensk Kärnbränslehantering AB.

Sandström B, Tullborg E-L, Larson S Å, Page L, 2009. Brittle tectonothermal evolution in the Forsmark area, central Fennoscandian Shield, recorded by paragenesis, orientation and $^{40}Ar/^{39}Ar$ geochronology of fracture minerals. Tectonophysics 478, 158–174.

Smellie J, Tullborg E-L, Nilsson A-C, Sandström B, Waber N, Gimeno M, Gascoyne M, 2008. Explorative analysis of major components and isotopes. SDM-Site Forsmark. SKB R-08-84, Svensk Kärnbränslehantering AB.

Stephens M B, Fox A, La Pointe P, Simeonov A, Isaksson H, Hermanson J, Öhman J, 2007. Geology Forsmark. Site descriptive modelling Forsmark stage 2.2. SKB R-07-45, Svensk Kärnbränslehantering AB.

Waber H N, Gimmi T, Smellie J A T, 2009. Porewater in the rock matrix. Site descriptive modelling, SDM-Site Forsmark. SKB R-08-105, Svensk Kärnbränslehantering AB.

Welin E, 1964. Uranium disseminations and vein fillings in iron ores of northern Uppland, central Sweden. Geologiska föreningens i Stockholm förhandlingar 86, 51–82.

Appendix 1

KFR106 drilling water composition

Idcode	Secup m	Seclow m	Sample no	Sampling date	$\delta^{2}H$ dev SMOW*	^{3}H TU*	$\delta^{18}O$ dev SMOW
KFR106	143.0	259.0	16601	2009-11-05	–81.1	4.0	–11.6
KFR106	260.0	300.1	16604	2009-11-05	–100.9	2.1	–14.2
Baltic sea water			16375	2009-08-24	–61.6	11.9	–8.2
Baltic sea water			16376	2009-08-31	–61.2	12.3	–8.0
Baltic sea water			16377	2009-09-02	–59.4	12.3	–8.4

*Units are defined in Appendix 4 SICADA: isotopes_1_T.

Results of differential flow logging in KFR106

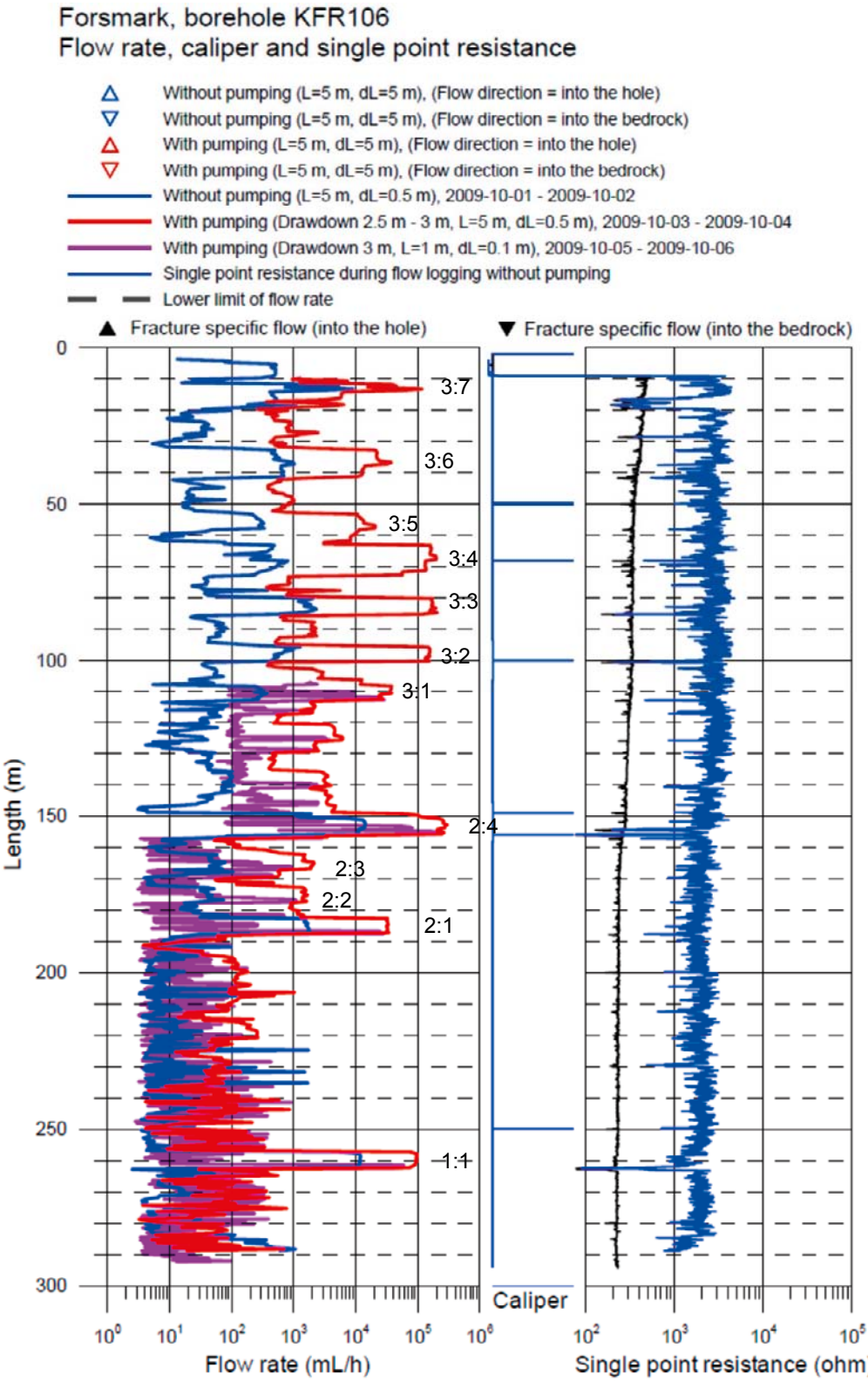

Figure A2-1. *Borehole KFR106: Differential flow measurements. The numbering refers to the flow anomalies considered in the plug flow calculations performed for section KFR106:1, KFR106:2 and KFR106:3.*

Appendix 3

Sampling information

Idcode:section	Tube volume [dm^3]	Section volume [dm^3]	Total volume [dm^3]	Pumping time	Flow rate [mL/min]	Pumped volume [dm^3]	Turnover section volumes	Sampling date	Sample no.
KFR106:1	25.7	173.3	198.9	109 h 10 min	120	570	2.87	2009/11/04	16599
“	“	“	“	5 h 35 min	120	605	3.04	2009/11/04	16600
“	“	“	“	18 h 50 min	120	685	3.44	2009/11/05	16601
KFR106:2	22.4	489.1	511.5	109 h 10 min	120	615	1.20	2009/11/04	16602
“	“	“	“	5 h 35 min	120	655	1.28	2009/11/04	16603
“	“	“	“	18 h 50 min	120	740	1.45	2009/11/05	16604

Appendix 4

Sampling and analytical methods

Table A4-1. Sample handling routines and analytical methods.

Component/group	Component/element	Sample container (material)	Volume (mL)	Filtration	Preparation/Conservation*	Analysis method	Time before analysis on site/ delivery time to lab.
Anions 1	HCO_3 pH(lab) cond. (lab)	Plastic	250	Yes (not in the field)	No	Titration Potentiometric measurement Conductivity measurement	The same day – maximum 24 hours
Anions 2	Cl, SO_4, Br^-, F^-, I^-	Plastic	100	Yes (not in the field)	No	Titration (Cl^-) IC (Cl^-, SO_4, Br^-, F^-) ISE (F^-)	Not critical (month)
	Br, I	Plastic	100	Yes (not in the field)	No	ICP MS	Not critical (month)
Cations, Si and S according to SKB chemistry class 3	Na, K, Ca, Mg, S(tot), Si(tot), Li, Sr	Plastic (at low conc. acid washed bottles)	100	Yes (not in the field)	Yes (not in the field, 1 mL HNO_3)	ICP-AES ICP-MS	Not critical (month)
Cations, Si and S according to SKB chemistry class 4 and 5	Na, K, Ca, Mg, S(tot), Si(tot), Fe, Mn, Li, Sr	Plastic (Acid washed)	100	Yes (immediately in the field)	Yes (1 mL HNO_3)	ICP-AES ICP-MS	Not critical (month)
Fe(II), Fe(tot)	Fe(II), Fe(tot)	Plastic (Acid washed)	500	Yes	Yes (5 mL HCl))	Spectrophotometry Ferrozine method	As soon as possible the same day
Hydrogen sulphide	HS–	Glass (Winkler)	About 120×2	No	Ev 1 mL 1 M NaOH+ 1 mL 1 M ZnAc	Spectrophotometry	Immediately, or if conserved a few days
Environmental metals	Al, As, Ba, B, Cd, Co, Cr, Cu, Hg, Mo, Ni, P, Pb, V, Zn	Plastic (Acid washed)	100	Yes	Yes (1 mL HNO_3)	ICP-AES ICP-MS	Not critical (month)
Lantanoids, U, Th etc.	Sc, Rb, Y, Zr, I, Sb, Cs, La, Hf, Tl, Ce, Pr, Nd, Sm, Eu, Gd, Tb, Dy, Ho, Er, Tm, Yb, Lu, U, Th	Plastic (Acid washed)	100	Yes	Yes (1 mL HNO_3)	ICP-AES ICP-MS	Not critical (month)
Dissolved organic Carbon, dissolved inorganic Carbon	DOC, DIC	Plastic	250 25	Yes	Frozen and transported in isolated bag	UV oxidation, IR detection Carbon analysator Shimadzu TOC5000	Short transportation time

Component/group	Component/element	Sample container (material)	Volume (mL)	Filtration	Preparation/Conservation*	Analysis method	Time before analysis on site/ delivery time to lab.
Total organic Carbon	TOC	Plastic	250 25	No	Frozen and transported in isolated bag	UV oxidation, IR detection Carbon analysator Shimadzu TOC5000	Short transportation time
Environmental isotopes	^{2}H, ^{18}O	Plastic	100	No	– –	MS	Not critical (month)
Tritium Chlorine-37	^{3}H (enhanced.) Chlorine-37	Plastic (dry bottle) Plastic	500 100	No No	– –	LSC MS	Not critical (month)
Carbon isotopes	^{13}C, ^{14}C	Glass (brown)	100×2	No	–	(A)MS	A few days
Sulphur isotopes	^{34}S	Plastic	500–1,000	Yes	–	Combustion, MS	No limit
Strontium-isotopes	$^{87}Sr/^{86}Sr$	Plastic	100	Yes	–	TIMS	Days or Week
Uranium and Thorium isotopes	^{234}U, ^{235}U, ^{238}U, ^{232}Th, ^{230}Th,	Plastic	50	No	–	Alfa spectroscopy	No limit
Boron isotopes	^{10}B	Plastic	100	Yes	Yes (1 mL HNO_3)	ICP – MS	No limit
Radon and Radium isotopes	^{222}Rn, ^{226}Ra	Plastic	500	No	No	LSS	Immediate transport
Dissolved gas (content and composition)	Ar, N_2, CO_2, O_2, CH_4, H_2, CO, C_2H_2, C_2H_4, C_2H_6, C_3H_8	Cylinder of stainless steel	200	No	No	GC	Immediate transport
Colloids	Filter series and fractionation (see below)	Polycarbonate filter	0.45, 0.2 and 0.05 µm	–	N_2 atmosphere	ICP-AES ICP-MS	Immediate transport
Humic and fulvic acids	Fractionation	Fractions are collected in plastic bottles	250	–	N_2 atmosphere	UV oxidation, IR detection (DOC)	Immediate transport
Archive samples acidified	–	Plastic (washed in acid)	100×2 **	Yes	Yes (1 mL HNO_3)	–	Storage in freezer container
Archive samples not acidified	–	Plastic	250×2 **	Yes	No	–	Storage in freezer container
Carbon isotopes in humic and fulvic acids	^{13}C, ^{14}C (pmc)	DEAE cellulose (anion exchanger)	–	–	–	(A)MS	A few days
Nutrient salt + silicate	NO_2, NO_3, NO_2+NO_3, NH_4, PO_4, SiO_4	Sample tubes, plastic	25×2	Yes (in the field)	No, frozen immediately***	Spectrophotometry	Short transportation time
Component group	Component/ element	Sample container (material)	Volume (mL)	Filtration	Preparation/ Conservation*	Analysis method	Time before analysis on site/ delivery time to lab.
Total concentra-tions of Nitrogen and Phosphorous	N-tot, P-tot	Plastic	100	No	No, frozen immediately***	Spectrophotometry	Short transportation time

Component/group	Component/element	Sample container (material)	Volume (mL)	Filtration	Preparation/Conservation*	Analysis method	Time before analysis on site/ delivery time to lab.
Particulate Carbon, Nitrogen and Phosphorous	POC, PON, POP	Plastic	1,000	Yes (within 4 h) using prepared filters and blank filters	Filtration; the filters are frozen immediately 2 filters/sample	Elementar-analysator (N, C) own method 990121 (P)	Short transportation time
Chlorophyll	Chlorophyll a, c and pheopigment	Plastic	1,000–2,000	Yes (within 4 h)	Filtration; the filters are frozen immediately	Spectrophotometry Fluorometry	Short transportation time
Oxygen	Dissolved O_2	Winkler, glass	2´ ~120	No	Mn (II) reagent Iodide reagent	Spectrophotometry SIS SS-EN 25813	Within 3 days
Archive samples for supplementary radionuclides		Plastic	5,000	No	50 mL HNO_3	–	Storage in freezer container

* Suprapur acid is used for conservation of samples.

** Minimum number. The number of archive samples can vary depending on the number of similar samples collected at the same occasion.

*** The sample is frozen before transport to the laboratory. For this reason it is possible that the silicate concentration can change due to polymerisation.

Abbreviations and definitions:

IC	Ion chromatograph
ISE	Ion selective electrode
ICP-AES	Inductively Coupled Plasma Atomic Emission Spectrometry
ICP-MS	Inductively Coupled Plasma Mass Spectrometry
INAA	Instrumental Neutron Activation Analysis
IR	Infra Red
MS	Mass Spectrometry
TIMS	Thermal Ionization Mass Spectrometer
LSC	Liquid Scintillation Counting
(A)MS	(Accelerator) Mass Spectrometry
GC	Gas Chromatography
LSS	Liquid Scintillation Spectroscopy

Table A4-2. Reporting limits and measurement uncertainties – updated 2008.

Component	Method[1]	Reporting limits (RL), detection limits (DL) or range[2]	Unit	Measurement uncertainty[3]
pH	Potentiometric	3–10	pH unit	±0.1
EC	Electrical Conductivity measurement	1–150 150–10,000	mS/m	5% 3%
HCO_3	Alkalinity titration	1	mg/L	4%
Cl^- Cl^-	Mohr-titration IC	≥ 70 0.5–70	mg/L	5% 8%
SO_4	IC	0.5	mg/L	12%
Br^-	IC	DL 0.2, RL 0.5	mg/L	15%
Br	ICP SFMS	0.001, 0.004, 0.010[4]	mg/L	25%[5]
F^- F^-	IC Potentiometric	DL 0.2, RL 0.5 DL 0.1, RL 0.2	mg/L	13% 12%
I^-	ICP SFMS	0.001, 0.004, 0.010[4]	mg/L	25%[5]
Na	ICP AES	0.1	mg/L	13%
K	ICP AES	0.4	mg/L	12%
Ca	ICP AES	0.1	mg/L	12%
Mg	ICP AES	0.09	mg/L	12%
S(tot)	ICP AES	0.16	mg/L	12%
Si(tot)	ICP AES	0.03	mg/L	14%
Sr	ICP AES	0.002	mg/L	12%
Li	ICP AES	0.004	mg/L	12.2%
Fe	ICP AES	0.02	mg/L	13.3%[6]
Fe	ICP SFMS	0.0004, 0.002, 0.004[4]	mg/L	20%[6]
Mn	ICP AES	0.003	mg/L	12.1%[5]
Mn	ICP SFMS	0.00003, 0.00004, 0.0001[4]	mg/L	53%[6]
Fe(II), Fe(tot)	Spectrophotometry	DL 0.006, RL 0.02	mg/L	0.005 (0.02–0.05 mg/L) 9% (0.05–1 mg/L) 7% (1–3 mg/L)
HS^-	Spectrophotometry, SKB	SKB DL 0.006, RL 0.02	mg/L	25%
HS^-	Spectrophotometry, external laboratory	0.01	mg/L	0.02 (0.01–0.2 mg/L) 12% (>0.2 mg/L)
NO_2 as N	Spectrophotometry	0.1	µg/L	2%
Component	Method[1]	Reporting limits (RL), detection limits (DL) or range[2]	Unit	Measurement uncertainty[3]
NO_3 as N	Spectrophotometry	0.2	µg/L	5%
NO_2+NO_3 as N	Spectrophotometry	0.2	µg/L	0.2 (0.2–20 µg/L) 2% (> 20 µg/L)
NH_4 as N	Spectrophotometry, SKB	11	µg/L	30% (11–20 µg/L) 25% (20–50 µg/L) 12% (50–1,200 µg/L)
NH_4 as N	Spectrophotometry external laboratory	0.8	µg/L	0.8 (0.8–20 µg/L) 5% (> 20 µg/L)
PO_4 as P	Spectrophotometry	0.7	µg/L	0.7 (0.7–20 µg/L) 3% (> 20 µg/L)
SiO_4	Spectrophotometry	1	µg/L	2.5% (>100 µg/L)
O_2	Iodometric titration	0.2–20	mg/L	5%
Chlorophyll a, c pheopigment[7]	/1/	0.5	µg/L	5%

Component	Method[1]	Reporting limits (RL), detection limits (DL) or range[2]	Unit	Measurement uncertainty[3]
PON[7]	/1/	0.5	µg/L	5%
POP[7]	/1/	0.1	µg/L	5%
POC[7]	/1/	1	µg/L	4%
Tot-N[7]	/1/	10	µg/L	4%
Tot-P[7]	/1/	0.5	µg/L	6%
Al,	ICP SFMS	0.2, 0.3, 0.7[4]	µg/L	17.6%[6]
Zn	ICP SFMS	0.2, 0.8, 2[4]	µg/L	15.5, 17.7, 25.5%[6]
Ba, Cr, Mo,	ICP SFMS	0.01, 0.04, 0.1[4]	µg/L	Ba 15%[4], Cr 22%[5] Mo 39%[6]
Pb	ICP SFMS	0.01, 0.1, 0.3[4]	µg/L	15%[6]
Cd	ICP SFMS	0.002, 0.02, 0.5[4]	µg/L	15.5%[6]
Hg	ICP AFS	0.002	µg/L	10.7%[6]
Co	ICP SFMS	0.005, 0.02, 0.05[4]	µg/L	25.9%[6]
V	ICP SFMS	0.005, 0.03, 0.05[4]	µg/L	18.1%[6]
Cu	ICP SFMS	0.1, 0.2, 0.5[4]	µg/L	14.4%[6]
Ni	ICP SFMS	0.05, 0.2, 0.5[4]	µg/L	15.8%[6]
P	ICP SFMS	1, 5, 40[4]	µg/L	16.3%[6]
As	ICP SFMS	0.01 (520 mS/m)	µg/L	59.2%[6]
La, Ce, Pr, Nd, Sm, Eu, Gd, Tb, Dy, Ho, Er, Tm, Yb, Lu	ICP SFMS	0.005, 0.02, 0.05[4]	µg/L	20%, 20%, 25%[6]
Sc, In, Th	ICP SFMS	0.05, 0.2, 0.5[4]	µg/L	25%[6]
Rb, Zr, Sb, Cs	ICP SFMS	0.025, 0.1, 0.25[4]	µg/L	15%, 20%, 20%[5] 25%[6]
Tl	ICP SFMS	0.025, 0.1, 0.25[4]	µg/L	14.3%[5 and 6]
Y, Hf	ICP SFMS	0.005, 0.02, 0.05[4]	µg/L	15%, 20%, 20%[5] 25%[6]
U	ICP SFMS	0.001, 0.005, 0.01[4]	µg/L	13.5%, 14.3%, 15.9%[5] 19.1%, 17.9%, 20.9%[6]
DOC	UV oxidation, IR detection Carbon analysator	0.5	mg/L	8%
TOC	UV oxidation, IR detection Carbon analysator	0.5	mg/L	10%
δ^2H	MS	2	‰ SMOW[8]	0.9 (one standard deviation)
$\delta^{18}O$	MS	0.1	‰ SMOW[8]	0.1 (one standard dev.)
^3H	LSC	0.8	TU[9]	0.8
$\delta^{37}Cl$	A (MS)	0.2	‰ SMOC[10]	0.2[17]
$\delta^{13}C$	A (MS)	–	‰ PDB[11]	0.3[17]
^{14}C pmc	A (MS)	–	PMC[12]	0.4[17]
$\delta^{34}S$	MS	0.2	‰ CDT[13]	0.4 (one standard dev.)
$^{87}Sr/^{86}Sr$	TIMS	–	No unit (ratio)[14]	0.00002
$^{10}B/^{11}B$	ICP SFMS	–	No unit (ratio)[14]	–
^{234}U, ^{235}U, ^{238}U, ^{232}Th, ^{230}Th	Alfa spectr.	0.0001	Bq/L[15]	≤5% (Counting statistics uncertainty)
^{222}Rn, ^{226}Ra	LSS	0.015	Bq/L	≤5% (Counting statistics uncertainty)

[1] Many elements may be determined by more than one ICP technique depending on concentration range. The most relevant technique and measurement uncertainty for the concentrations normally encountered in groundwater are presented. In cases where two techniques were frequently used, both are displayed.

[2] Reporting limits (RL) are generally 10×standard deviation if nothing else is stated. Measured values below RL or DL are stored as negative values in SICADA (i.e. –RL value and –DL value).

[3] Measurement uncertainty reported by the laboratory is generally as ± percent of measured value in question at 95% confidence interval.

[4] Reporting limits at electrical conductivity 520 mS/m, 1,440 mS/m and 3,810 mS/m respectively.

[5] Measurement uncertainty at concentrations 100×RL

[6] Measurement uncertainty at concentrations 10×RL

[7] Determined only in surface waters. PON, POP and POC refers to Particulate Organic Nitrogen, Phosphorous and Carbon, respectively

[8] Per mille deviation[16] from SMOW (Standard Mean Oceanic Water).

[9] TU=Tritium Units, where one TU corresponds to a tritium/hydrogen ratio of 10^{-18} (1 Bq/L Tritium = 8.45 TU).

[10] Per mille deviation[16] from SMOC (Standard Mean Oceanic Chloride).

[11] Per mille deviation[16] from PDB (the standard PeeDee Belemnite).

[12] The following relation is valid between pmC (percent modern carbon) and Carbon-14 age: $pmC = 100 \cdot e^{((1950-y-1.03t)/8274)}$ where y = the year of the C-14 measurement and t = C-14 age.

[13] Per mille deviation[16] from CDT (the standard Canyon Diablo Troilite).

[14] Isotope ratio without unit.

[15] The following expressions are applicable to convert activity to concentration; for uranium-238 and thorium-232: 1 ppm U = 12.4 Bq/kg^{238}U, 1 ppm Th = 3.93 Bq/kg^{232}Th.

[16] Isotopes are often reported as per mill deviation from a standard. The deviation is calculated as: $\delta yI = 1{,}000 \times (K_{sample} - K_{standard})/K_{standard}$, where K= the isotope ratio and yI =2H, 18O, 37Cl, 13C or 34S etc.

[17] SKB estimation from duplicate analyses by the contracted laboratory.

Appendix 5

Fracture sample descriptions

The fracture mineral generations referred to in the descriptions are described in /Sandström et al. 2008, 2009/ and Chapter 2.

Borehole: KFR106
Secup: 16.97 m
Seclow: 17.42 m

Identified minerals: Reactivated generation 2 fracture (red-stained adularia and albite, calcite) with generation 3 mineralisation along the open fracture surface consisting of adularia, clay mineral, pyrite, (Ca,LREE)-carbonate, calcite, asphaltite, galena and barite-celestine (enrichment of LREEs in the barite).

Fracture mineral generation: Fracture sealed with generation 2 minerals reactivated and coated with generation 2 minerals.

Figure A5-1. *Photograph of drillcore sample.*

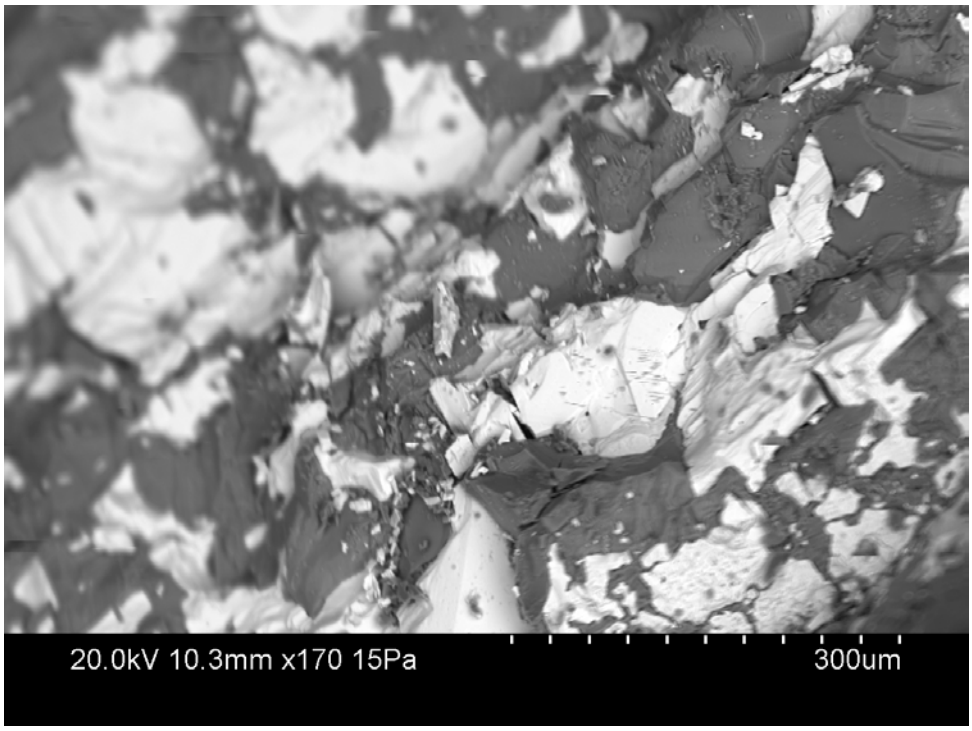

Figure A5-2. *Backscattered electron image showing barite on calcite.*

Borehole: KFR106
Secup: 19.00 m
Seclow: 19.30 m

Identified minerals: Calcite (sharp platy crystals), pyrite (cubic crystals together with FeS_2 needles), mixed layer clay (illite/smectite), (Ca,LREE)-carbonate, barite and galena.

Fracture mineral generation: Cataclasite, possibly belonging to generation 2 cut by fracture coated with generation 3 minerals.

Figure A5-3. *Photograph of drillcore sample.*

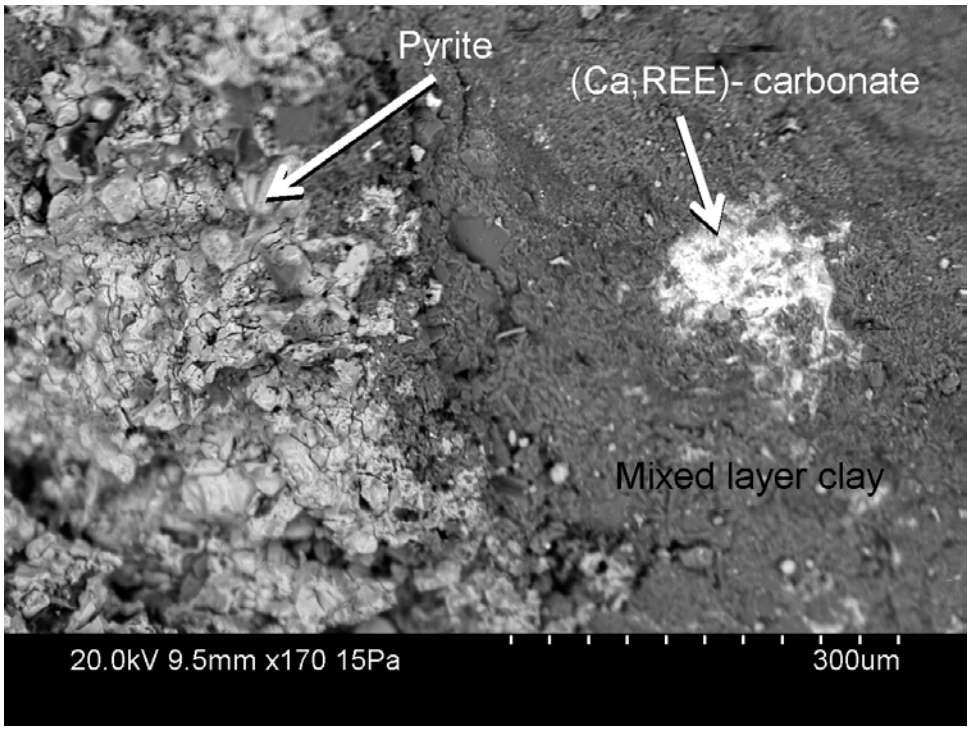

Figure A5-4. *Backscattered electron image of pyrite and (Ca,LREE)-carbonate on mixed layer clay coating.*

Figure A5-5. *Backscattered electron image of cubic- and needle-shaped pyrite crystals on mixed layer clay.*

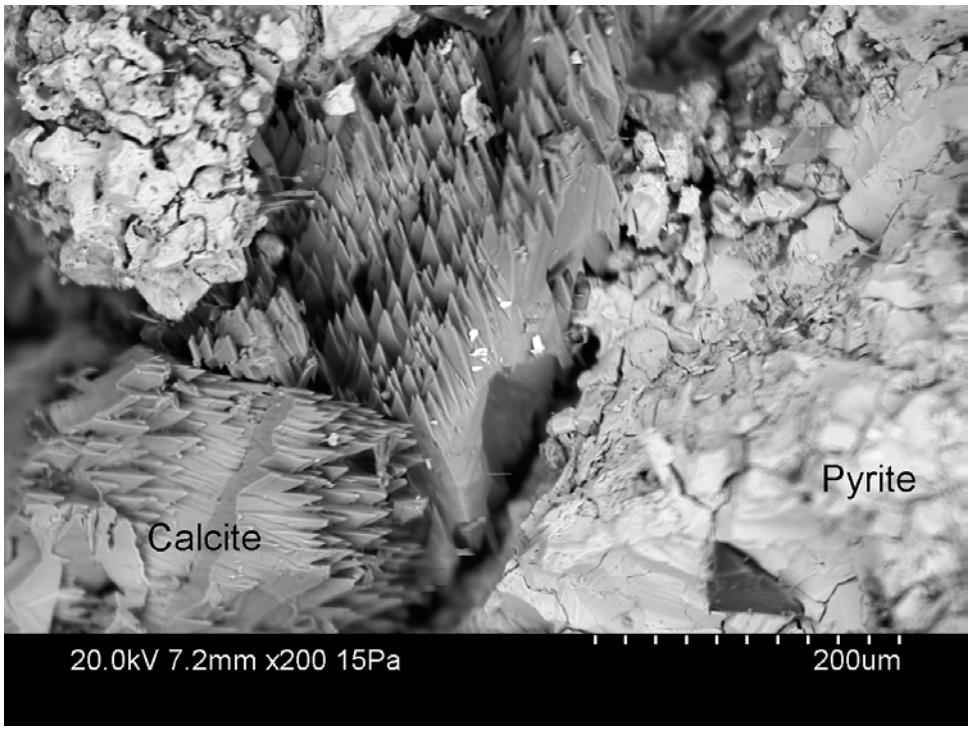

Figure A5-6. *Backscattered electron image of calcite and pyrite crystals.*

Borehole: KFR106
Secup: 68.38 m
Seclow: 68.51 m

Deformation zone: ZFMWNW3262

Identified minerals: Fracture perpendicular to core axis: Thin patchy coatings of calcite (mostly fresh but small corroded crystals also occur), clay minerals, pyrite and allanite as several small grains (may be part of the wall rock, but the allanite seems to be more frequent than in the wall rock).

Fracture parallel with core axis: Euhedral quartz, calcite, barite.

Fracture mineral generation: Generation 3**.**

Figure A5-7. *Photograph of drillcore sample.*

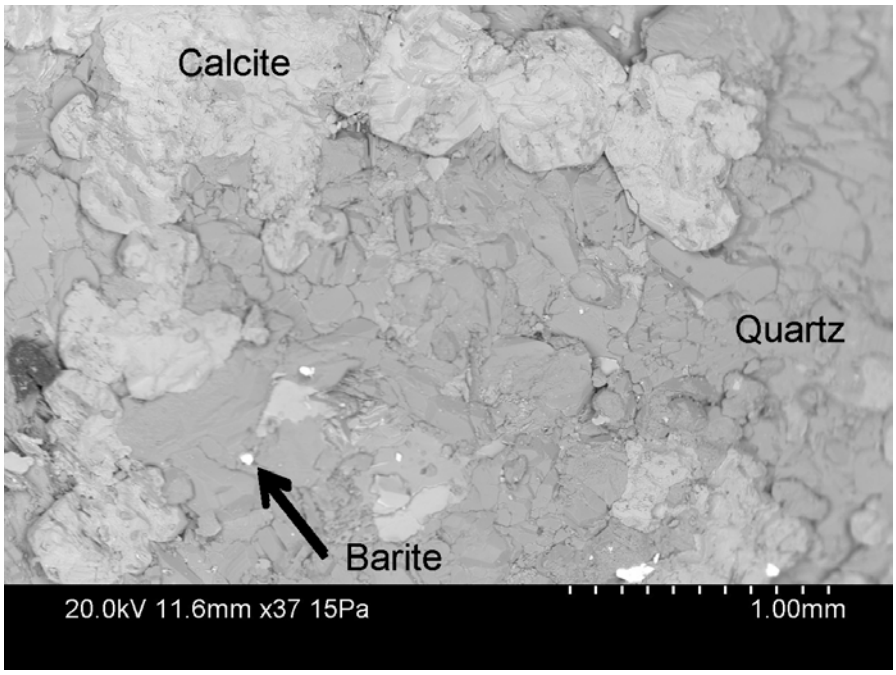

Figure A5-8. *Backscattered electron image of calcite and barite on quartz coating.*

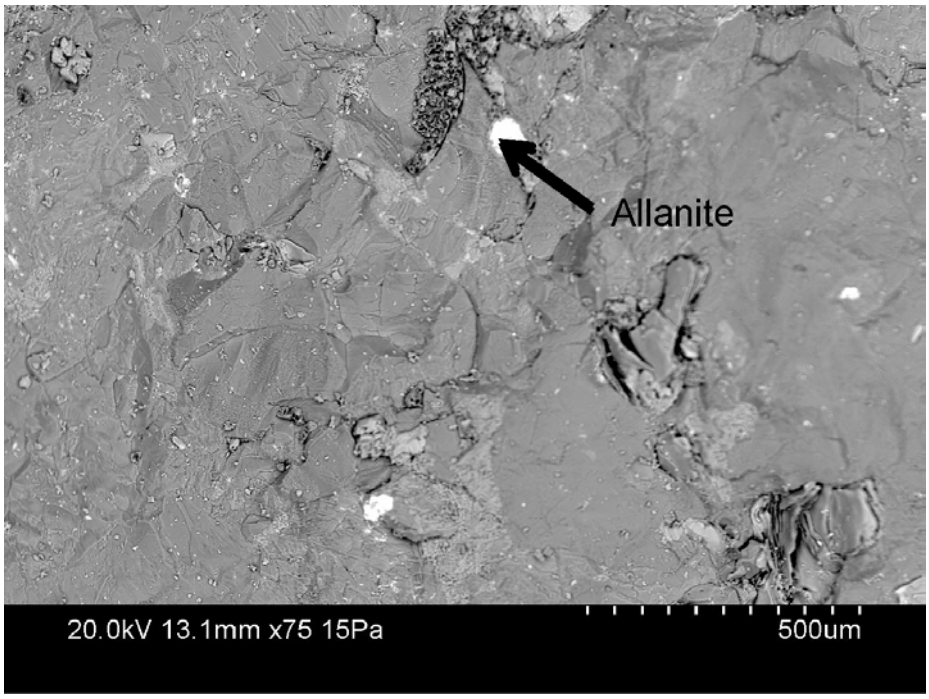

Figure A5-9. *Backscattered electron image of allanite on quartz coating.*

Borehole: KFR106
Secup: 85.13 m
Seclow: 85.52 m

Identified minerals: Quartz, biotite, chlorite, corrensite, adularia, pyrite, galena, barite, U-phase ~ 10 µm long (probably oxide) with some Ca and possibly Pb. Small flakes of unknown (Fe,Zn)-oxide(Cl), (W,Cu)S and Fe,Zn,Cl,O, probably debris from drilling, and monazite from the wall rock.

Side 1: Corrensite, quartz, U(Y?)-phosphate (300–400 µm in size), pyrite and chalcopyrite. Close association between pyrite and the U-phase; contamination by metallic W and Zn.

Side 2 (perpendicular to core axis): Quartz, pyrite, Fe-rich mixed layer clay and contamination by metallic Zn and Cu.

Fracture mineral generation: No obvious generation affiliation but probably older fracture with subsequent precipitation of generation 4 minerals.

Figure A5-10. *Photograph of drillcore sample.*

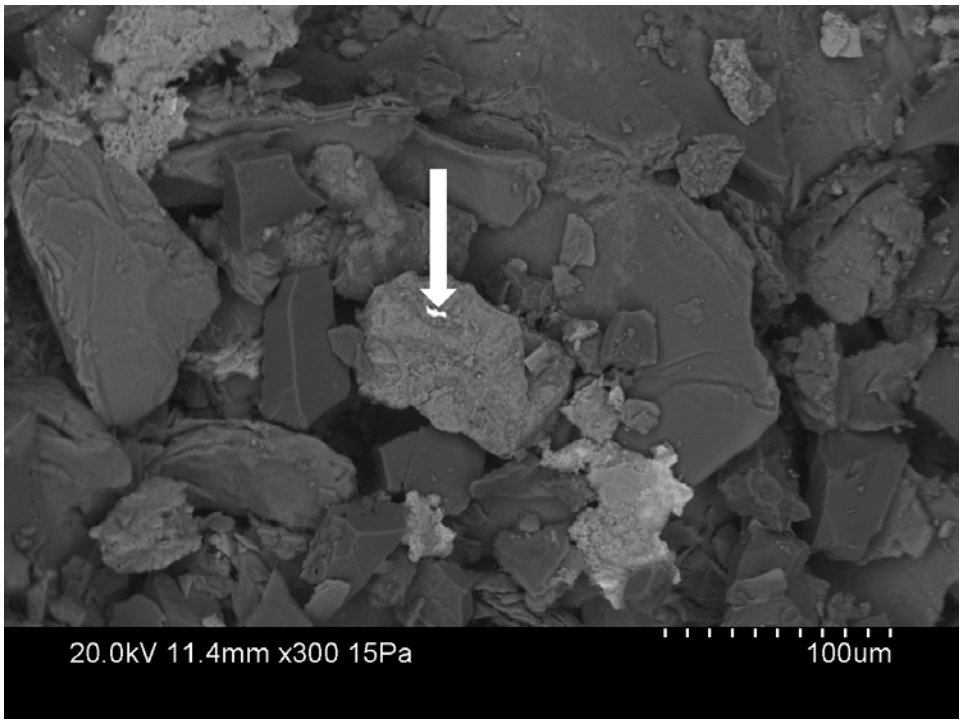

Figure A5-11. *Backscattered electron image of a small uranium-phase flake, about 10 µm long on a grain of an unidentified (Fe,Zn)-oxide.*

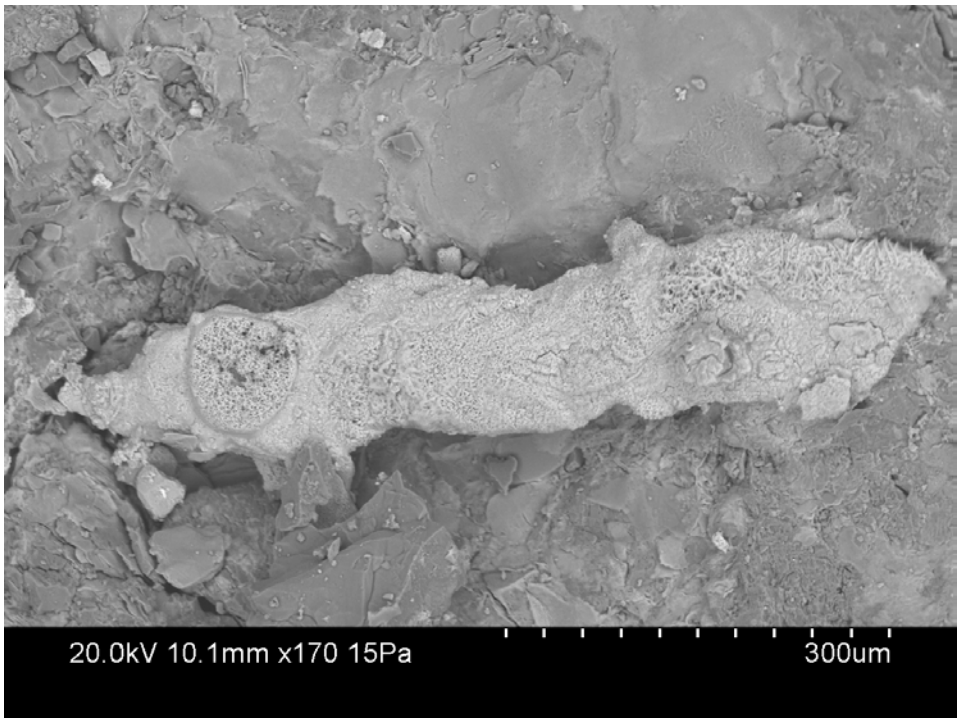

Figure A5-12. *Backscattered electron image of an unknown oxide* ***associated*** *with Fe, Zn and Cl; probably debris from the drilling.*

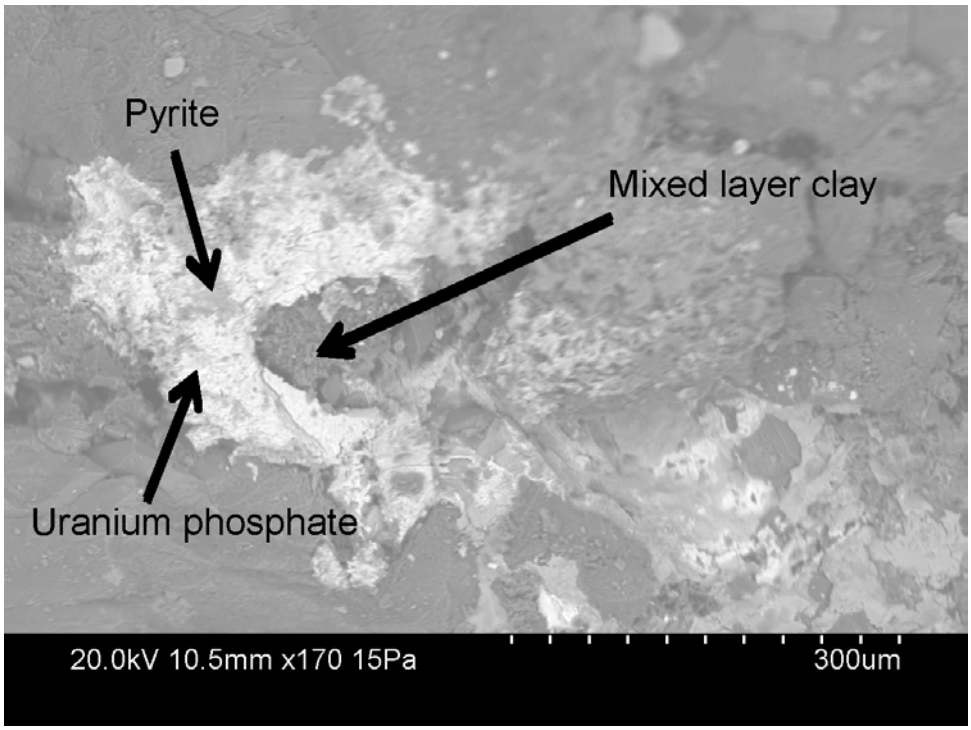

Figure A5-13. *Backscattered electron image of uranium phosphate and pyrite on mixed layer clay.*

Borehole: KFR106
Secup: 86.88 m
Seclow: 87.33 m

Identified minerals: Open fracture parallel with core axis. Calcite, pyrite, quartz and adularia, Mixed layer clay (illite-smectite Mg-rich), barite/celestine, U(Y)-phosphate, chalcopyrite, galena, "monazite" (LREE-phosphate with Ca) and fluorite.

Fracture mineral generation: Generation 3 and 4.

Figure A5-14. *Photograph of drillcore sample.*

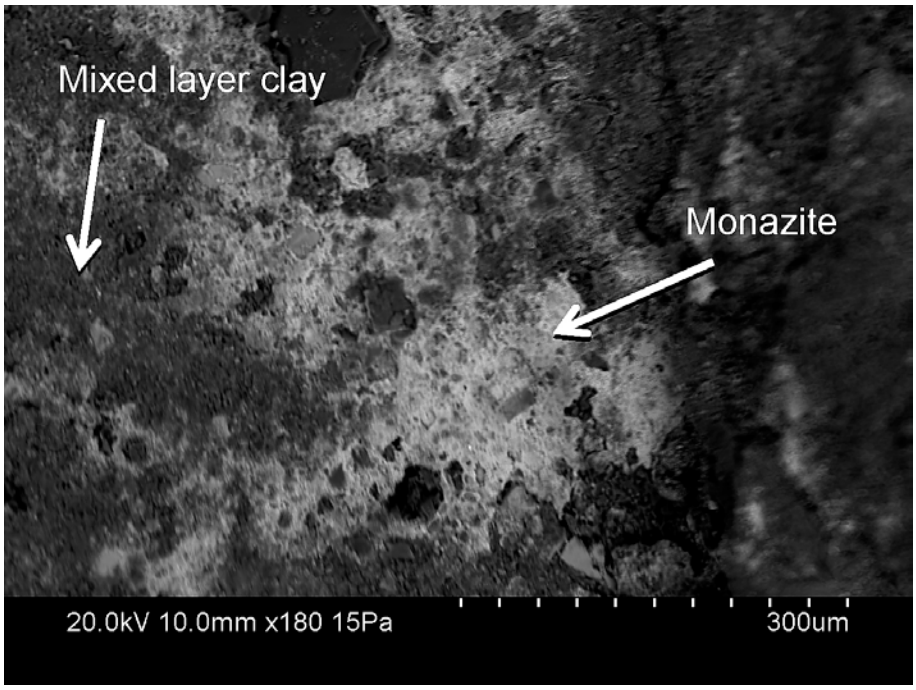

Figure A5-15. *Backscattered electron image of monazite crust together with mixed layer clay.*

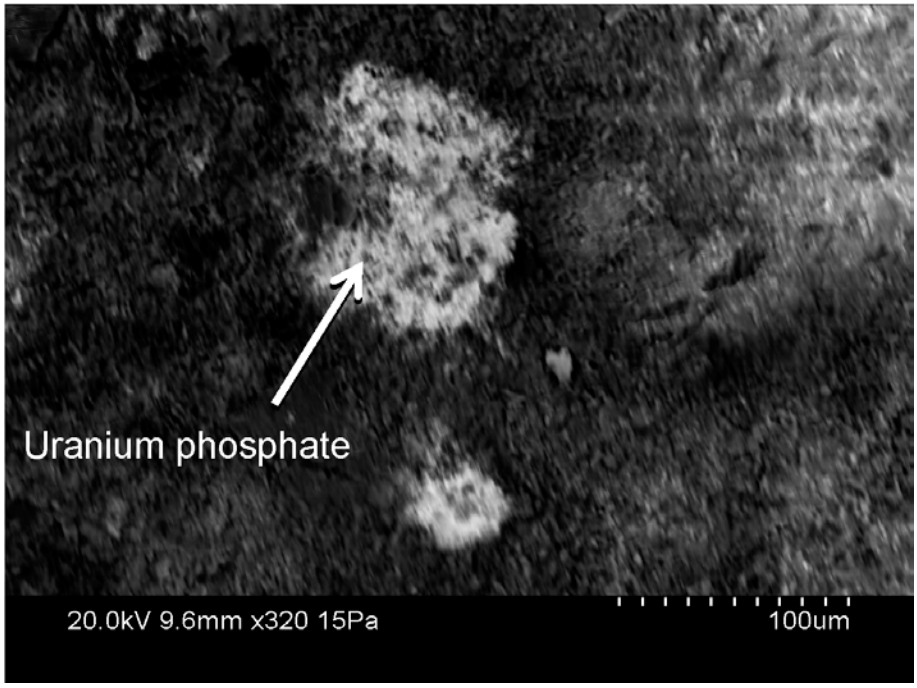

Figure A5-16. *Backscattered electron image of uranium phosphate on mixed layer clay.*

Borehole: KFR106
Secup: 100.56 m
Seclow: 101.08 m

Identified minerals: Subsample 1 (reddish brown): Mixed layer clay (probably smectite/illite), quartz, adularia, corrensite, barite/celestine, chalcopyrite, galena, micro-grains of hematite and albite.

Subsample 1: Mixed layer clay (green), pyrite, chalcopyrite and quartz.

Fracture mineral generation: Generation 3 and 4.

Figure A5-17. *Photograph of drillcore sample.*

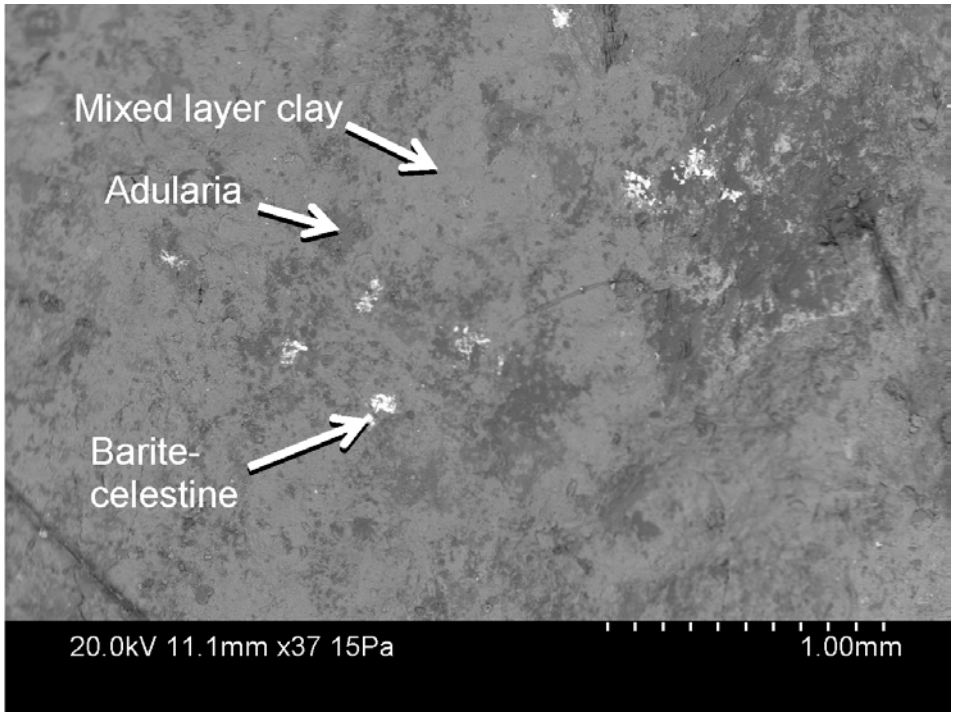

Figure A5-18. *Backscattered electron image of barite on surface coated with mixed layer clay and adularia.*

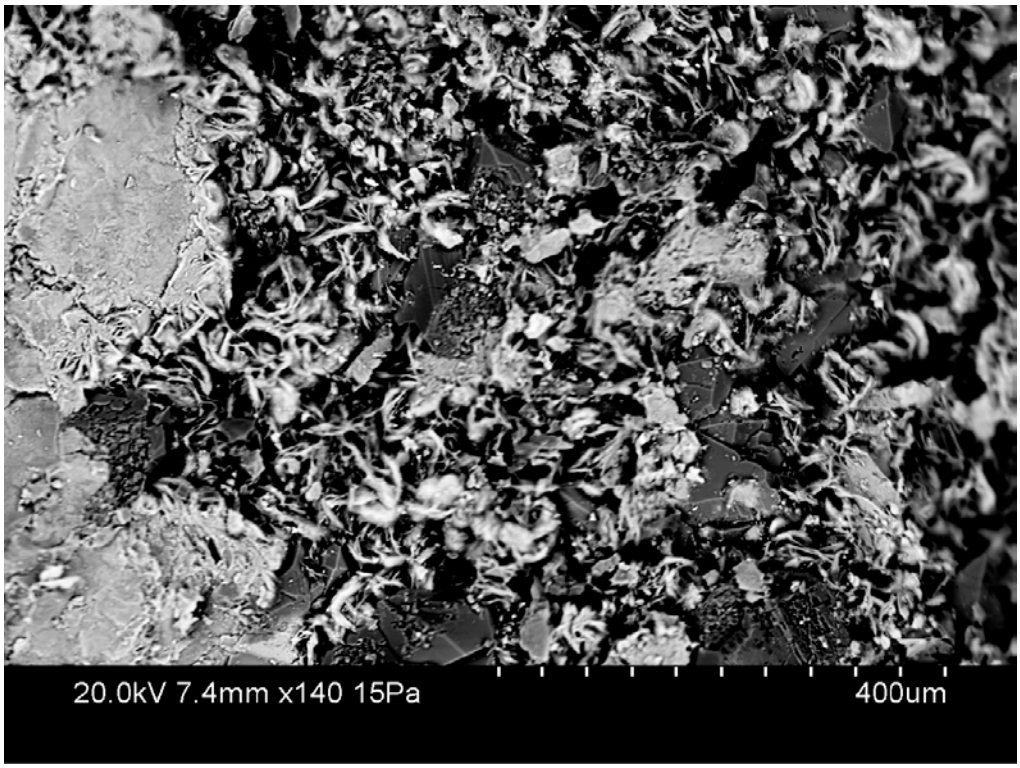

Figure A5-19. *Backscattered electron image of mixed layer clay.*

Borehole: KFR106
Secup: 112.91 m
Seclow: 113.35 m

Identified minerals: Biotite, apatite (wall rock), illite, monazite, Cu,Fe,W-sulphide, galena, chalcopyrite and barite. Hematite pigmentation occurs in altered biotite.

Fracture mineral generation: Generation 2 or older with later precipitation of generation 3 and/or 4.

Figure A5-20. *Photograph of drillcore sample.*

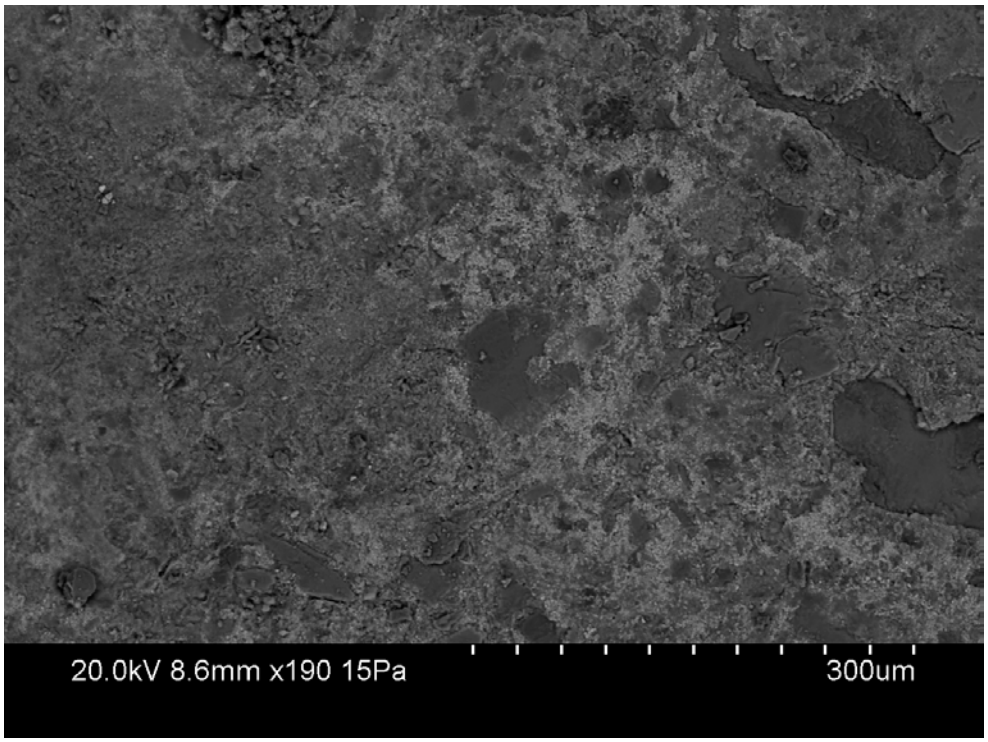

Figure A5-21. *Backscattered electron image of hematite-stained biotite.*

Borehole: KFR106
Secup: 131.42 m
Seclow: 131.72 m

Identified minerals: Laumontite, mixed layer clay (illite-smectite), corrensite and pyrite**.**

Fracture mineral generation: Generation 2 with later precipitation of generation 3.

Figure A5-22. *Photograph of drillcore sample.*

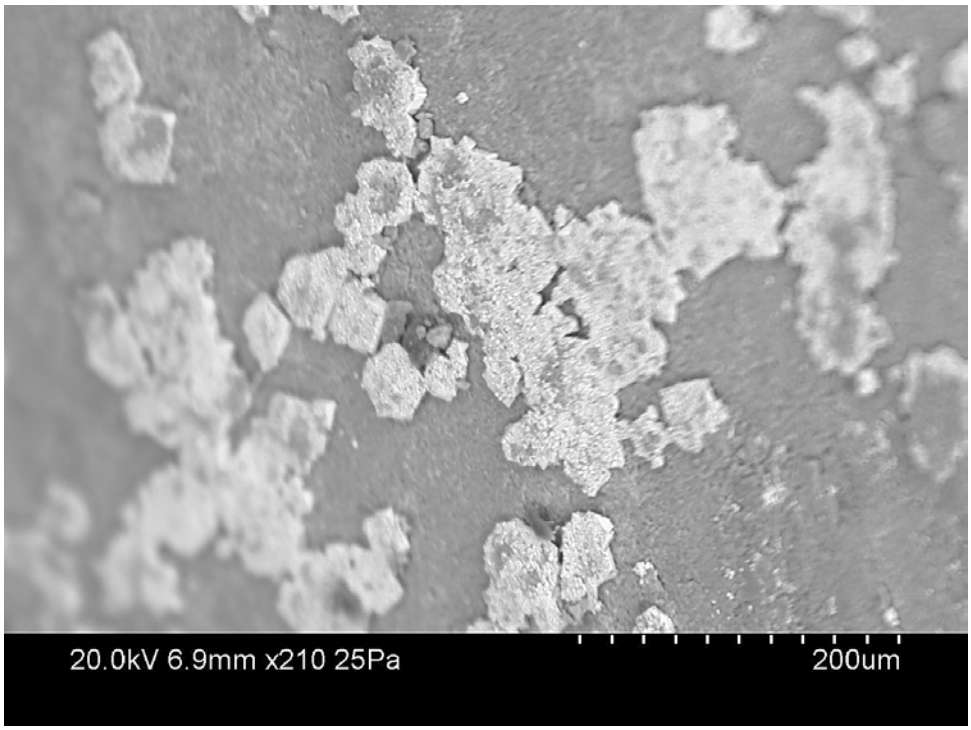

Figure A5-23. *Backscattered electron image of flaky pyrite on mixed layer clay coating.*

Borehole: KFR106
Secup: 154.22 m
Seclow: 154.99 m

Identified minerals: Chlorite, calcite, pyrite, mixed layer clay, quartz, adularia, pyrite, barite-celestine, titanite, albite and monazite (wall rock). Two fracture surfaces; one shows less variability in minerals (quartz, adularia > pyrite and calcite), and the other contains the long list of minerals above.

Fracture mineral generation: Both surfaces contain a mineral paragenesis typical for generation 3.

Figure A5-24. *Photograph of drillcore sample.*

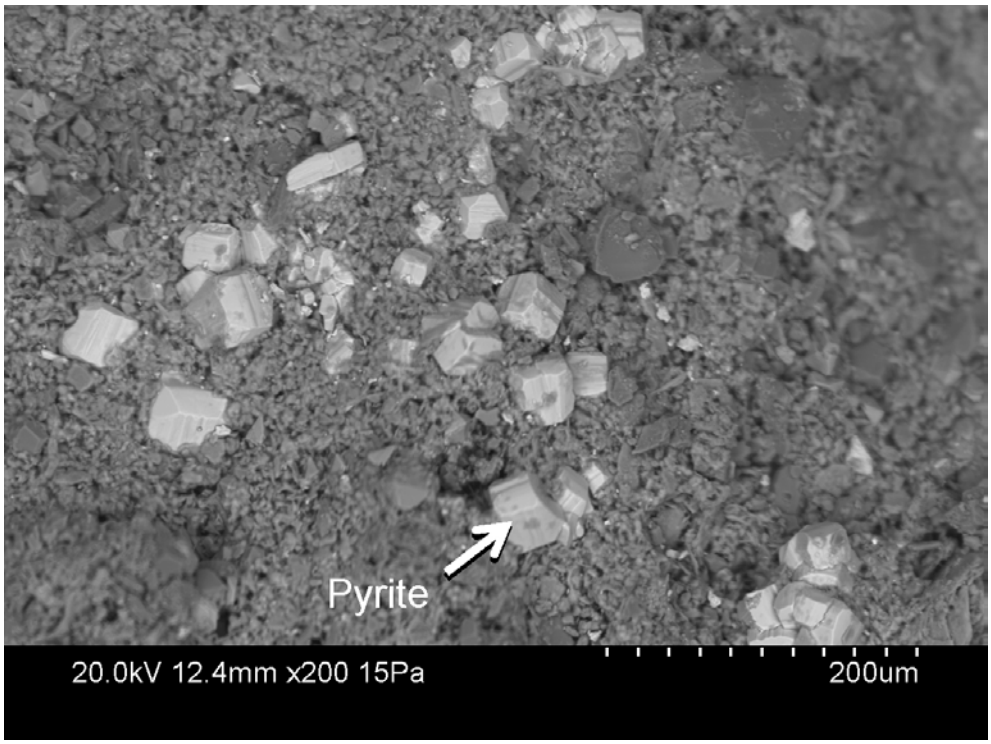

Figure A5-25. *Backscattered electron image of pyrite crystals together with adularia (gray).*

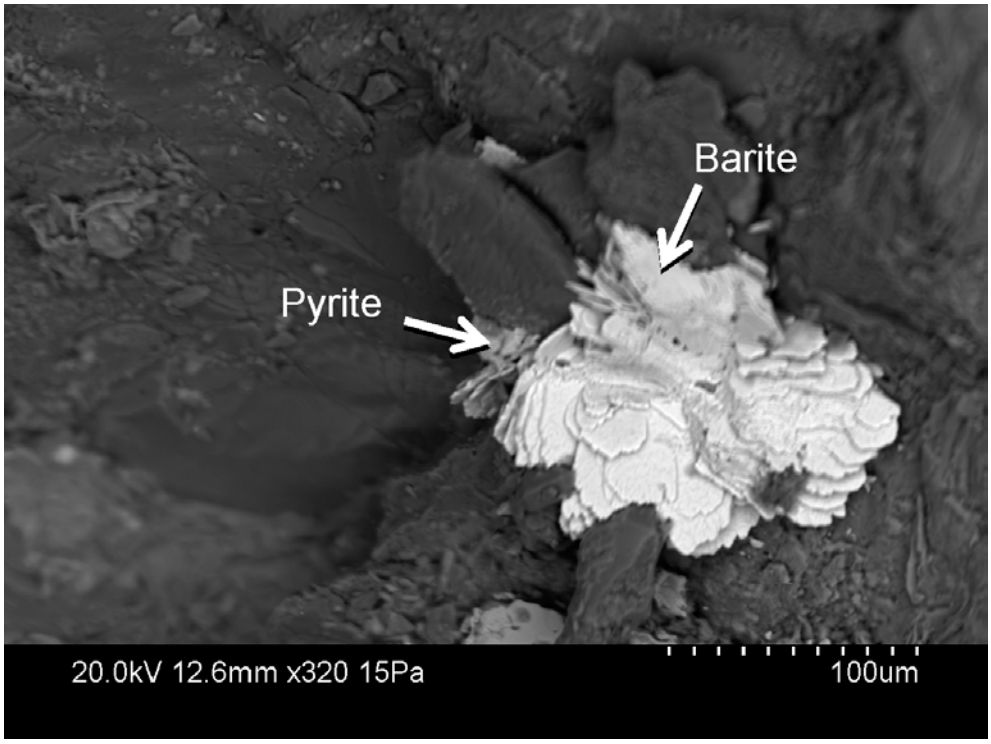

Figure A5-26. *Backscattered electron image of barite and pyrite crystals.*

Borehole: KFR106
Secup: 156.11 m
Seclow: 156.20 m

Identified minerals: Fracture parallel with core axis: Mixed layer clay, hematite, metallic iron (with Cr), barite, pyrite and adularia.

Fracture parallel with the core axis: Biotite surface (part of wall rock) with barite (crystals up to 1 mm in size) and chalcopyrite.

Fracture mineral generation: Generation 2 or older; later precipitation of generation 4 minerals.

Figure A5-27. *Photograph of drillcore sample.*

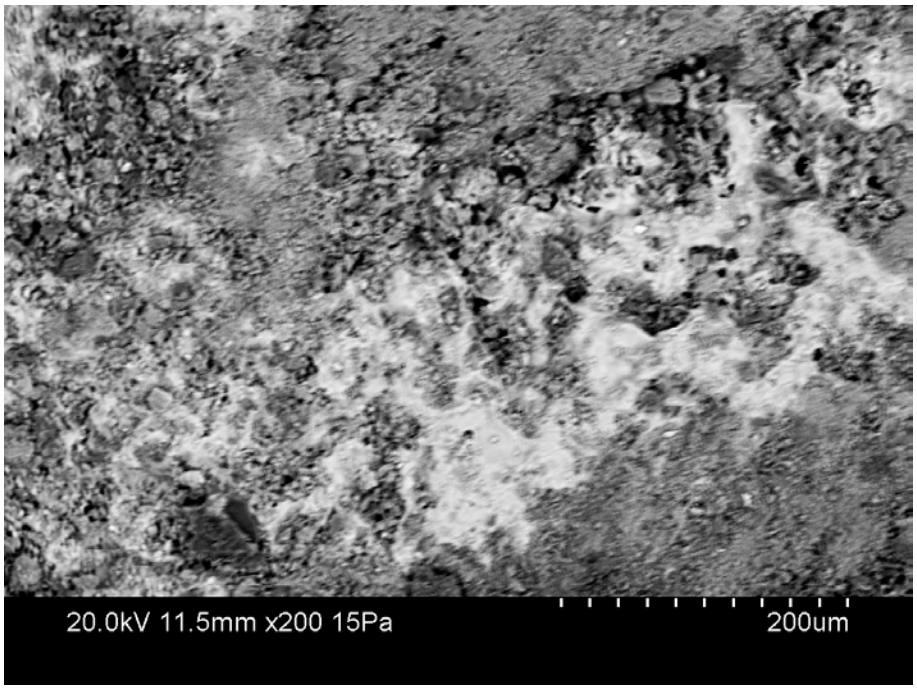

Figure A5-28. *Backscattered electron image of Fe-oxide (bright) together with mixed layer clay.*

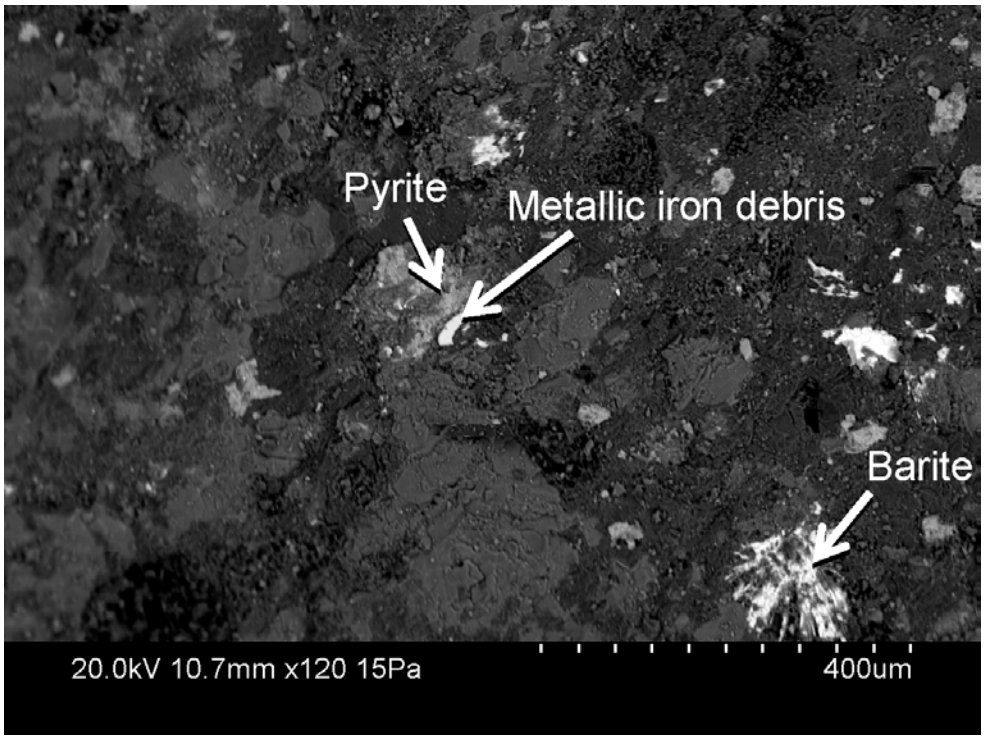

Figure A5-29. *Backscattered electron image of barite and pyrite on surface coated with mixed layer clay. A small shard of metallic iron is also present on the surface, probably contamination from the drilling.*

Borehole: KFR106
Secup: 175.25 m
Seclow: 175.58 m

Identified minerals: Pegmatite sample: quartz, albite, K-feldspar, muscovite, Mn(Ca)-oxide and U (Ca)-silicate in thin sealed fracture and voids. Y-(HREE)-rich zircon, Th-silicate (several small crystals and one large with a length of 300 µm), apatite, zircon and hematite.

Figure A5-30. *Photograph of drillcore sample.*

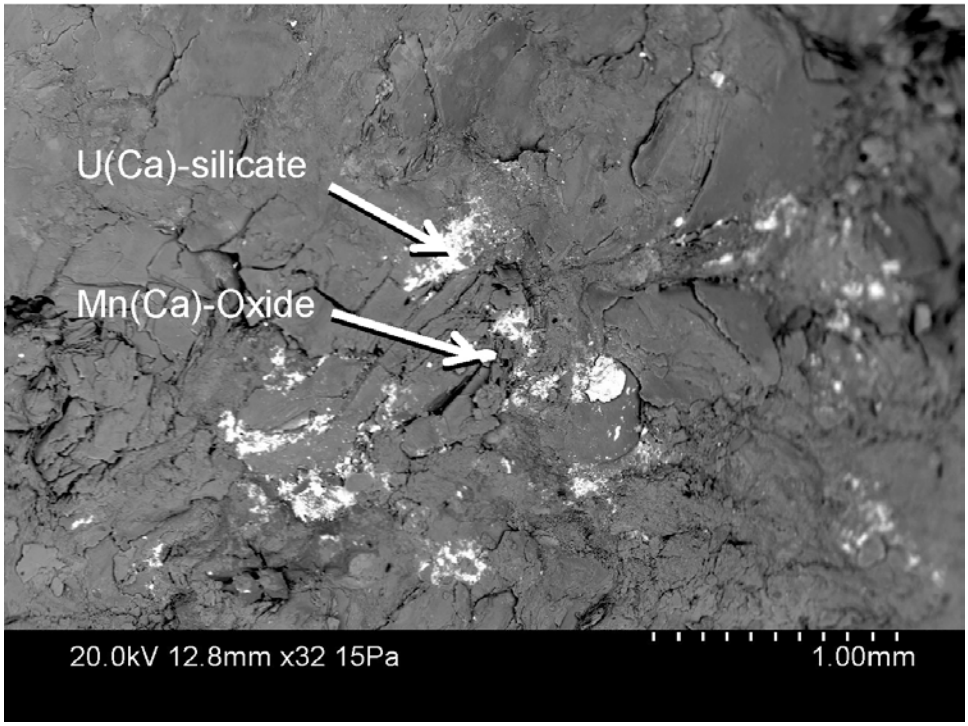

Figure A5-31. *Backscattered electron image of U(Ca)-silicate and Mn(Ca)-oxide on calcite.*

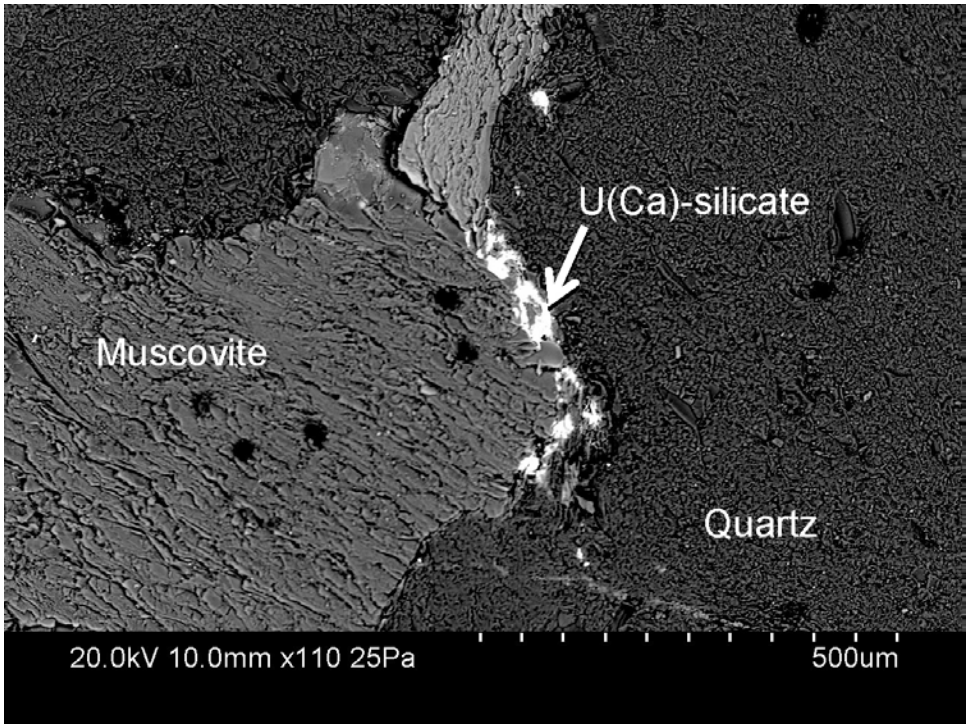

Figure A5-32. *Backscattered electron image of U(Ca)-silicate along grain boundary between muscovite and quartz.*

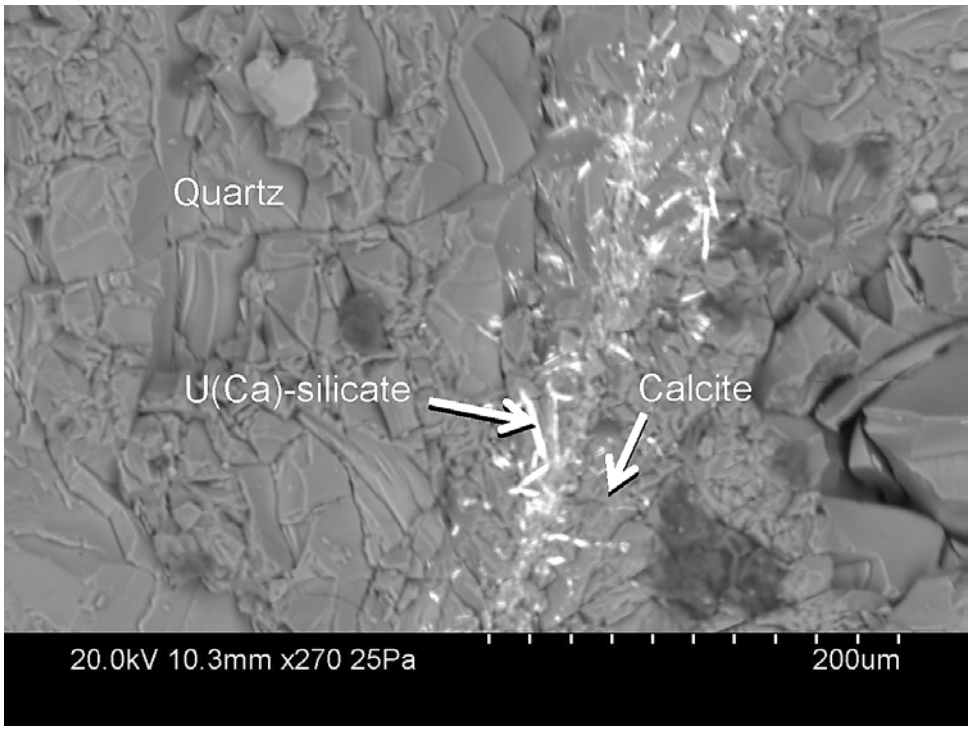

Figure A5-33. *Backscattered electron image of U(Ca)-silicate and calcite in a microfracture in quartz.*

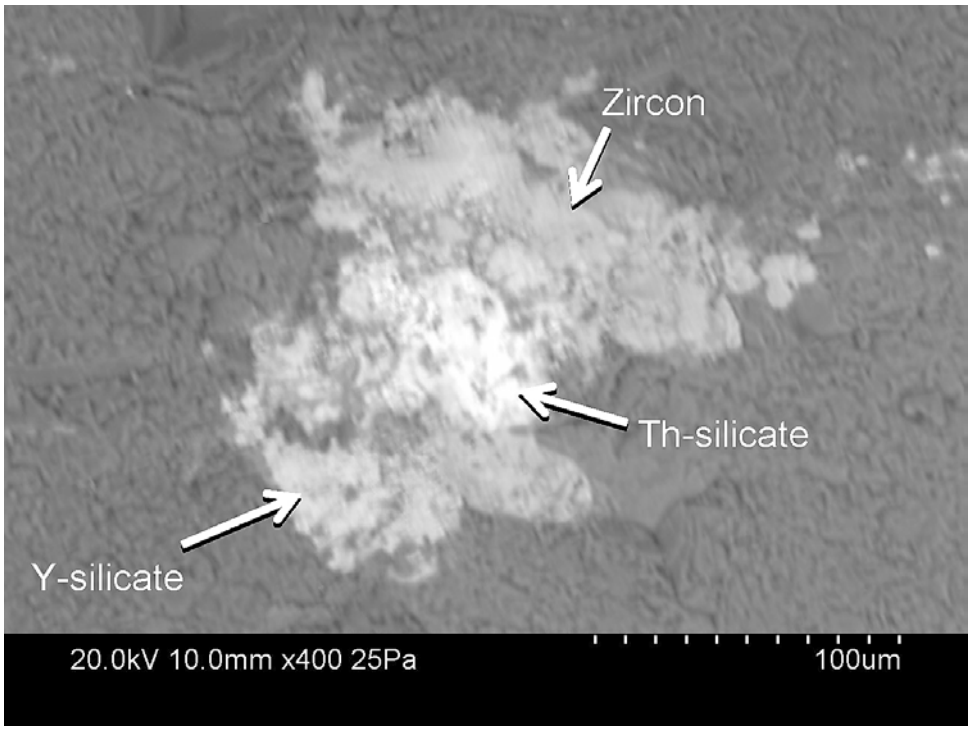

Figure A5-34. *Backscattered electron image of zircon, Th-silicate and Y-silicate in K-feldspar.*

Borehole: KFR106
Secup: 188.14 m
Seclow: 188.56 m

Identified minerals: Quartz, several types of mixed layer clay (one Mg-rich), sericite, barite, adularia and chalcopyrite.

Fracture mineral generation: Generation 4.

Figure A5-35. *Photograph of drillcore sample.*

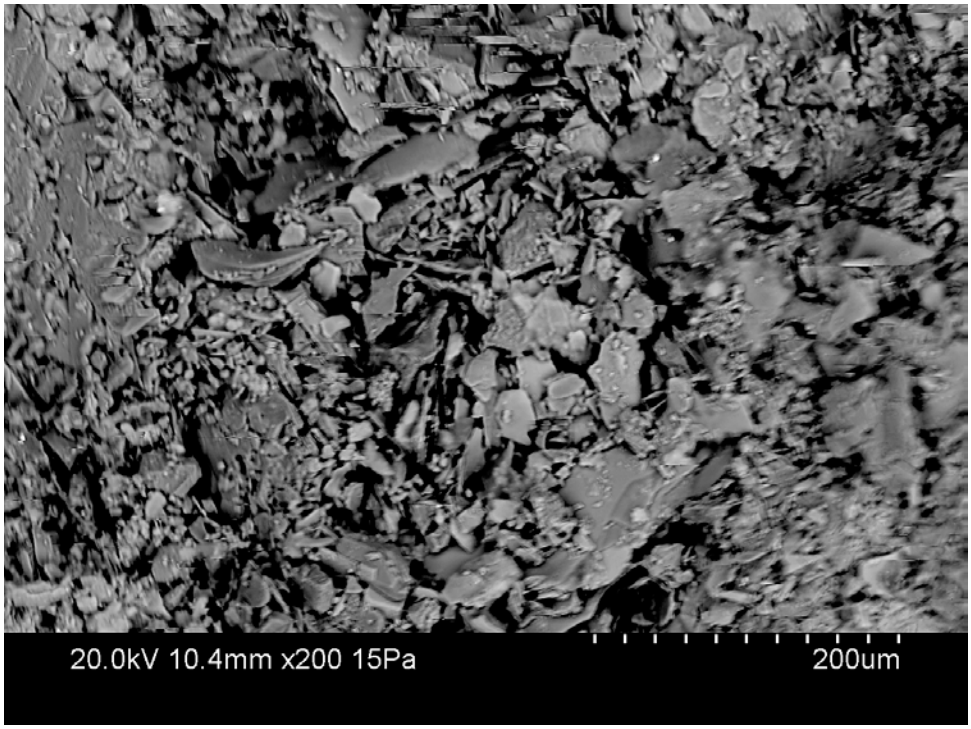

Figure A5-36. *Backscattered electron image of fracture coated with mixed layer clay.*

Borehole: KFR106
Secup: 229.59 m
Seclow: 230.11 m

Identified minerals: Corrensite, pyrite, small grains of barite and mixed layer clay.

Fracture mineral generation: Generation 3.

Figure A5-37. *Photograph of drillcore sample.*

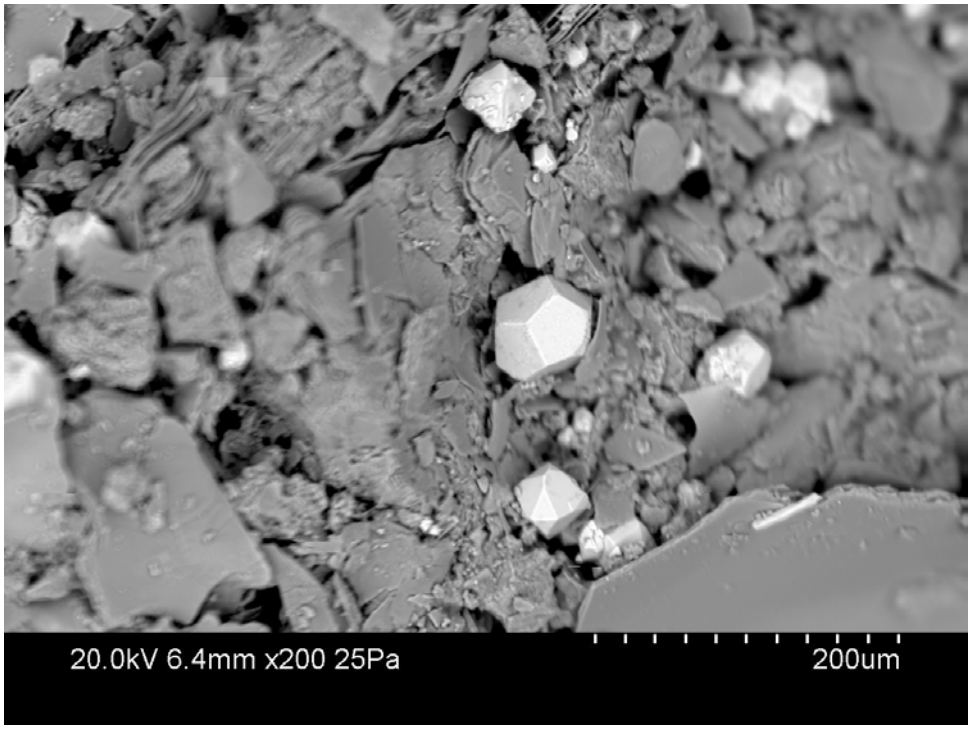

Figure A5-38. *Backscattered electron image of pyrite crystals together with mixed layer clay.*

Borehole: KFR106
Secup: 244.83 m
Seclow: 245.35 m

Deformation zone: ZFMNW1034

Identified minerals: Mixed layer clay (illite-smectite), corrensite, calcite, quartz, pyrite (crystals up to about.2 mm) and galena.

Fracture mineral generation: Generation 4 (and possibly 3).

Figure A5-39. *Photograph of drillcore sample.*

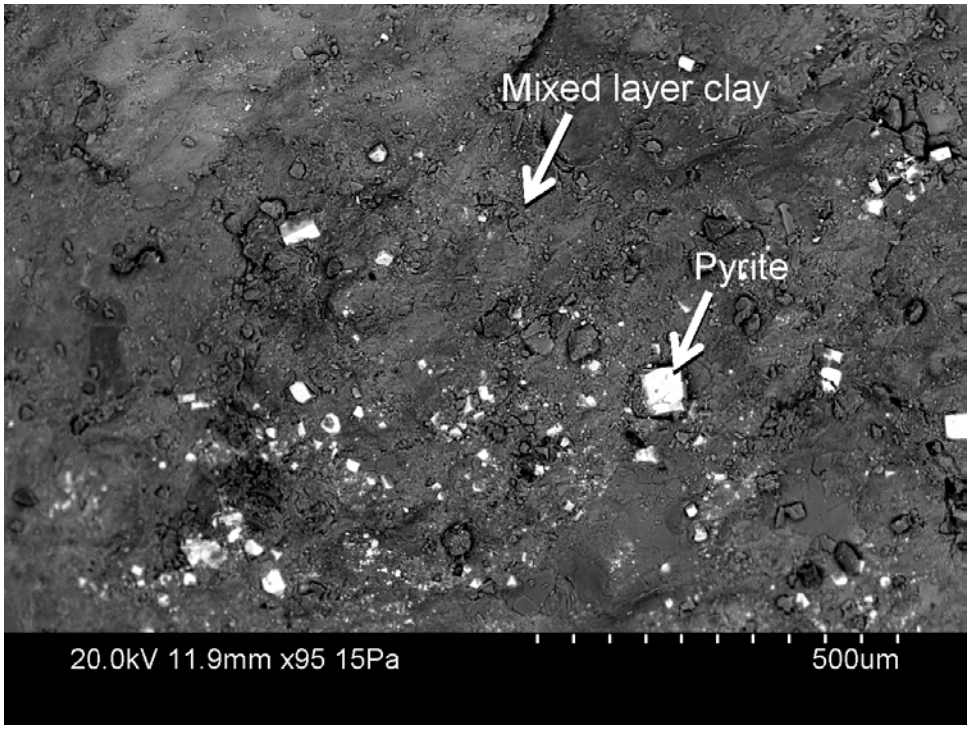

Figure A5-40. *Backscattered electron image of crystals of pyrite and mixed layer clay.*

Borehole: KFR106
Secup: 262.48 m
Seclow: 262.97 m

Deformation zone: ZFMNW1034

Identified minerals: Mixed layer clay, illite, quartz, calcite, adularia, pyrite and fragments of metallic iron (with Cr).

Fracture mineral generation: Fracture reactivated several times and dominated by generation 4 minerals.

Figure A5-41. *Photograph of drillcore sample.*

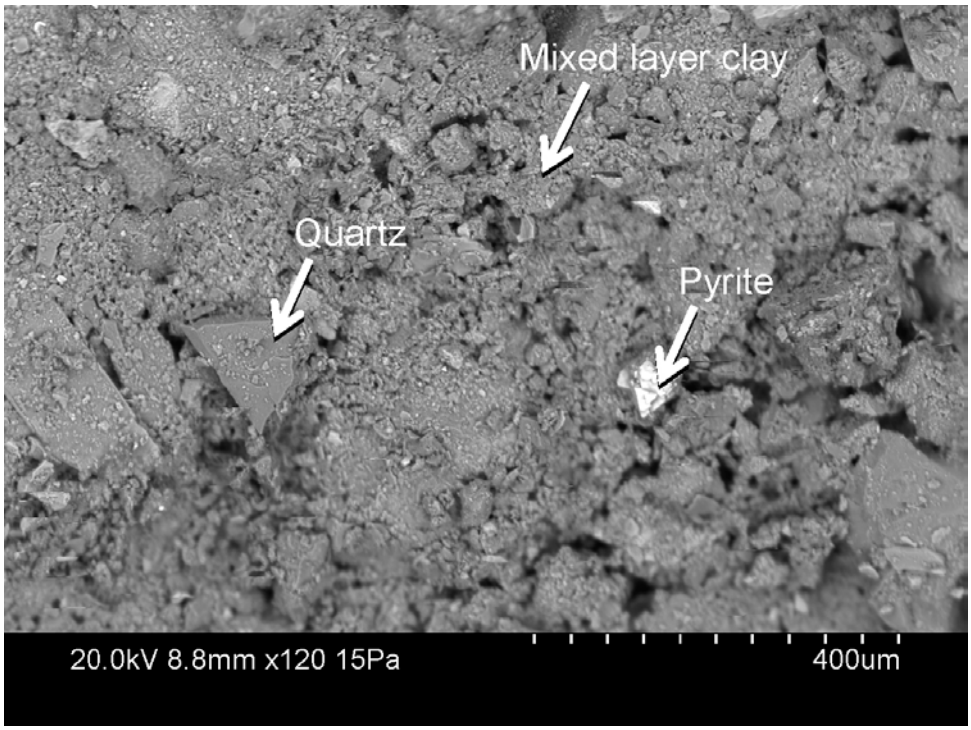

Figure A5-42. *Backscattered electron image of mixed layer clay,quartz and pyrite.*

Borehole: KFR106
Secup: 295.79 m
Seclow: 296.19 m

Identified minerals: Subsample 2: Chlorite, mixed layer clay (illite-smectite), calcite, quartz, pyrite, galena and xenotime. Subsample 2 (parallel to core axis): Mixed layer clay (illite-smectite), monazite, pyrite, galena, quartz and chalcopyrite.

Fracture mineral generation: Generation 3 and 4.

Figure A5-43. *Photograph of drillcore sample.*

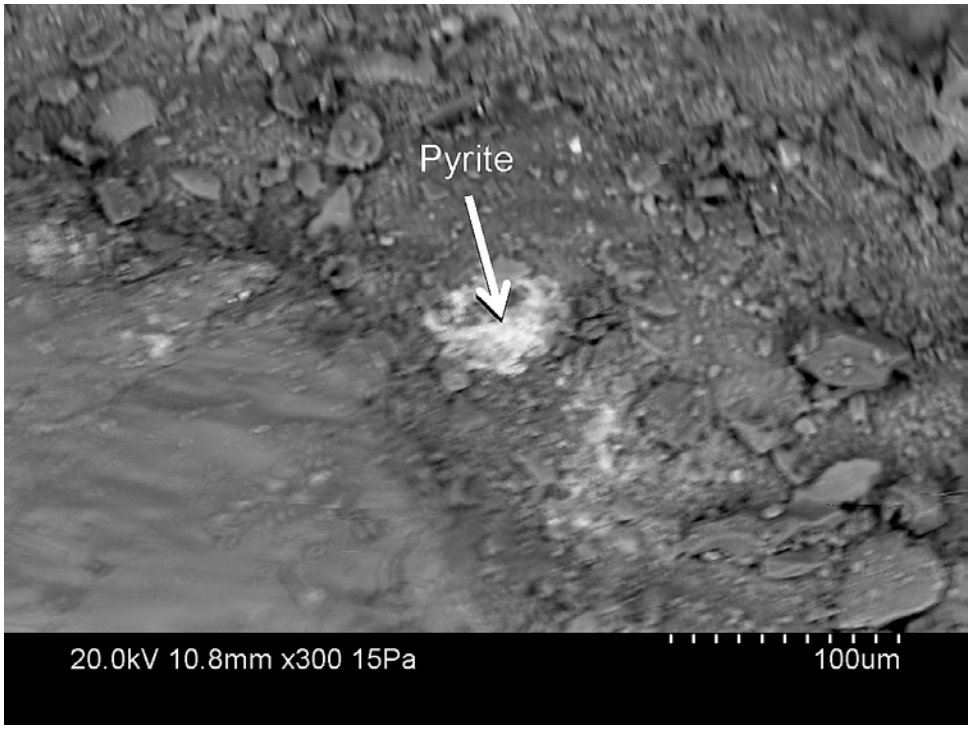

Figure A5-44. *Backscattered electron image of pyrite on albite and mixed layer clay (Fracture 1).*

Borehole: KFR106
Secup: 292.03 m
Seclow: 292.07 m

Identified minerals: Albite, K-feldspar, quartz, hematite, calcite, pitchblende, galena, apatite, chlorite clay mineral, titanite and rutile.

Fracture mineral generation: The sample is partly pegmatitic and cut by fine-grained portions of mylonite/cataclasite belonging to generation 2 or older.

Figure A5-45. *Photograph of drillcore sample.*

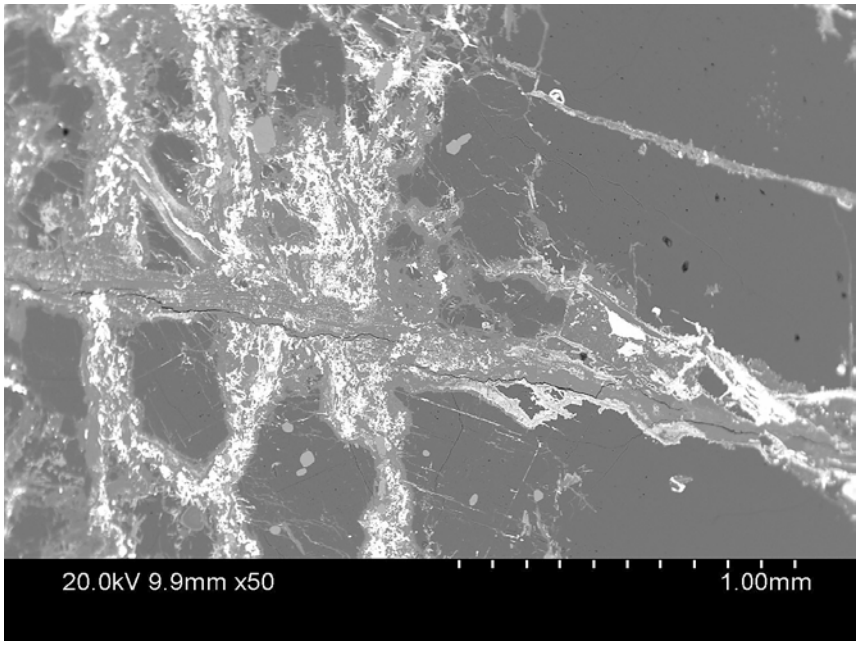

Figure A5-46. *Backscattered electron image of cataclasite with a matrix consisting mainly of chlorite and uranium minerals*

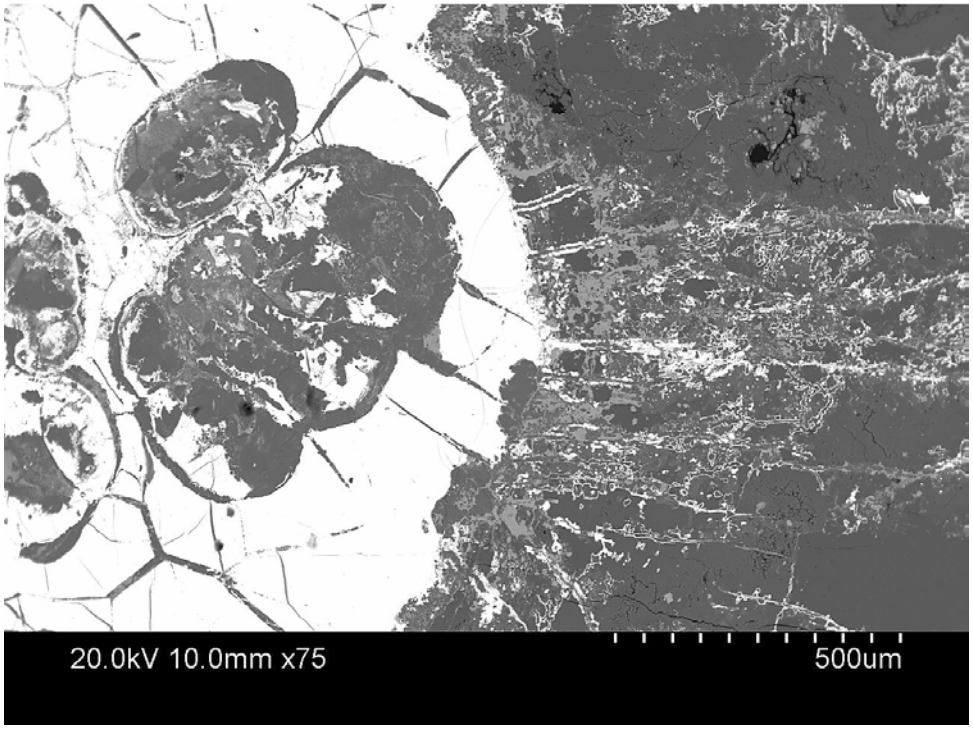

Figure A5-47. *Backscattered electron image of micro-fractures sealed with a uranium mineral radiating out from the larger pitchblende grain.*

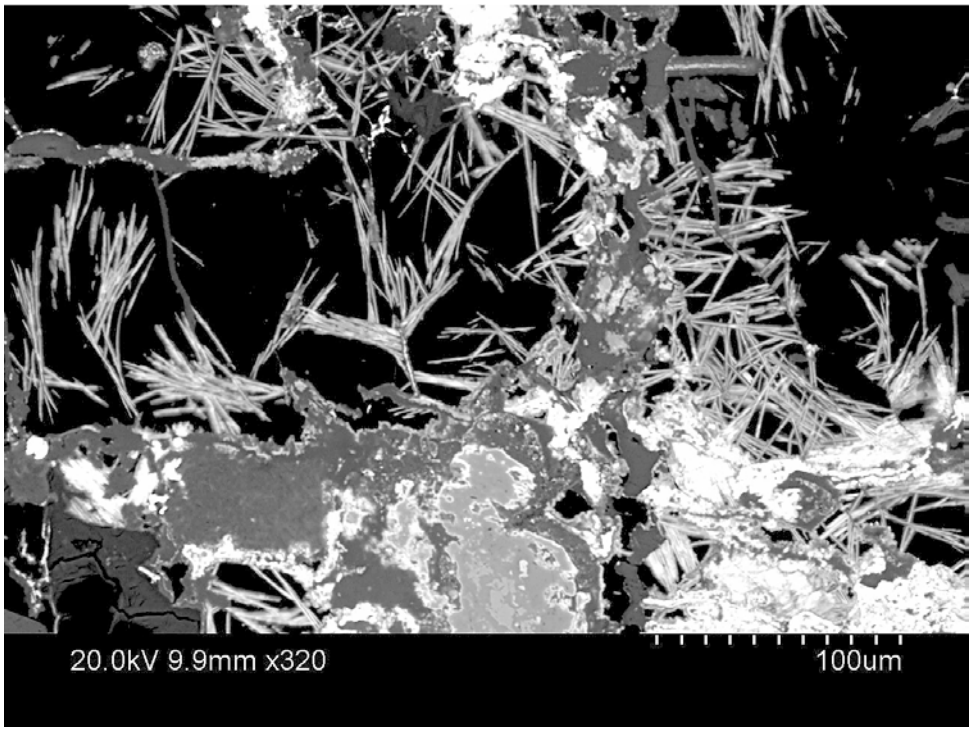

Figure A5-48. *Backscattered electron image of rutile, titanite, clay mineral and uranium minerals in the cataclasite matrix.*

Appendix 6

BIPS images of borehole sections sampled for fracture mineralogy

Black numbers: Borehole length.
Red numbers: Adjusted borehole length (the SecUp and SecLow used in the report).

Arrows represent the SecUp and SecLow of the sampled drill-core section.

Borehole: KFR106
Mapping:

Depth range: 16.000 - 18.000 m
Azimuth: 196.0
Inclination: -69.0

KFR106 16.97-17.42 m

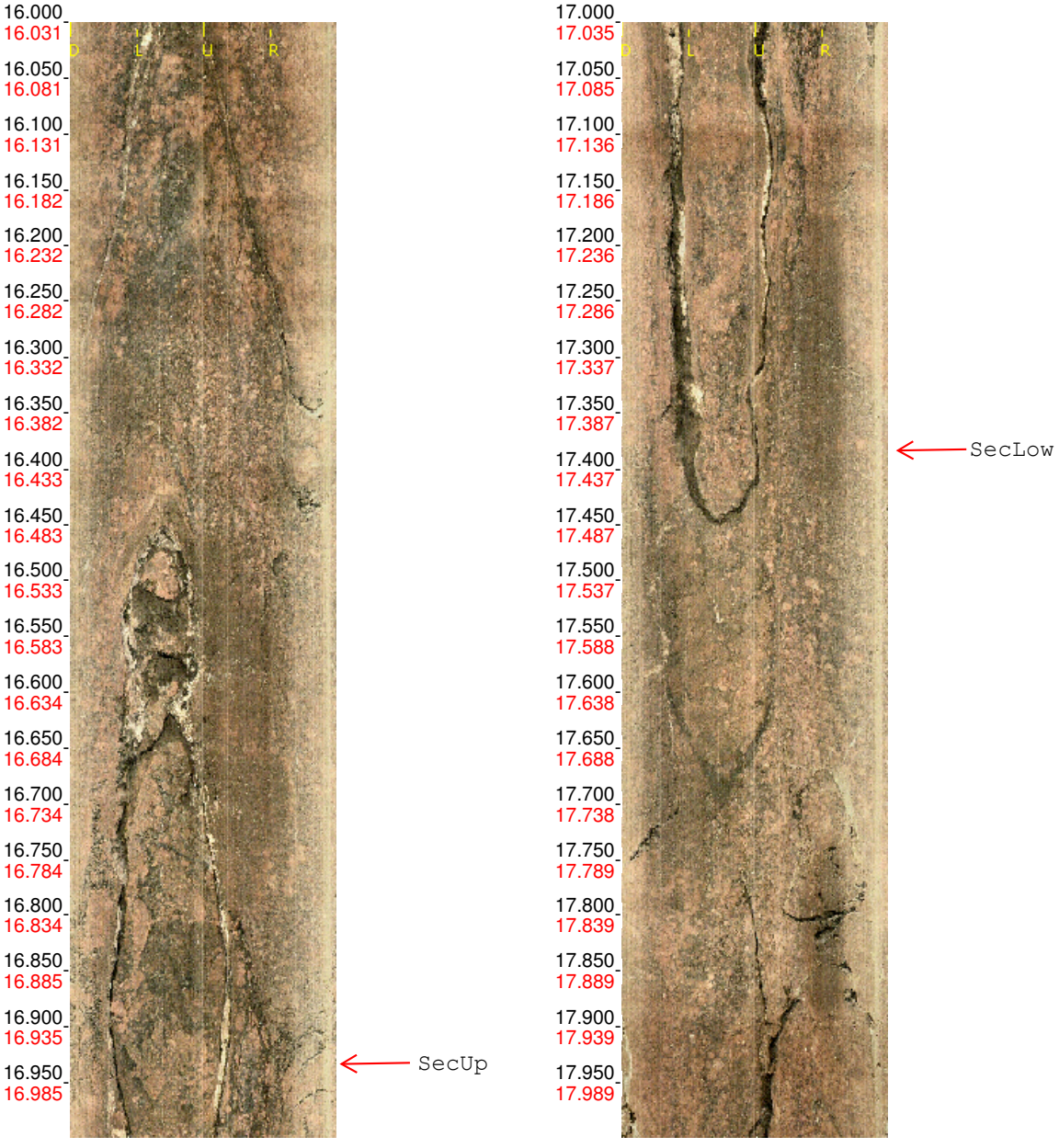

Borehole: KFR106
Mapping:

Depth range: 18.000 - 20.000 m
Azimuth: 196.0
Inclination: -69.0

KFR106 19.00-19.30 m

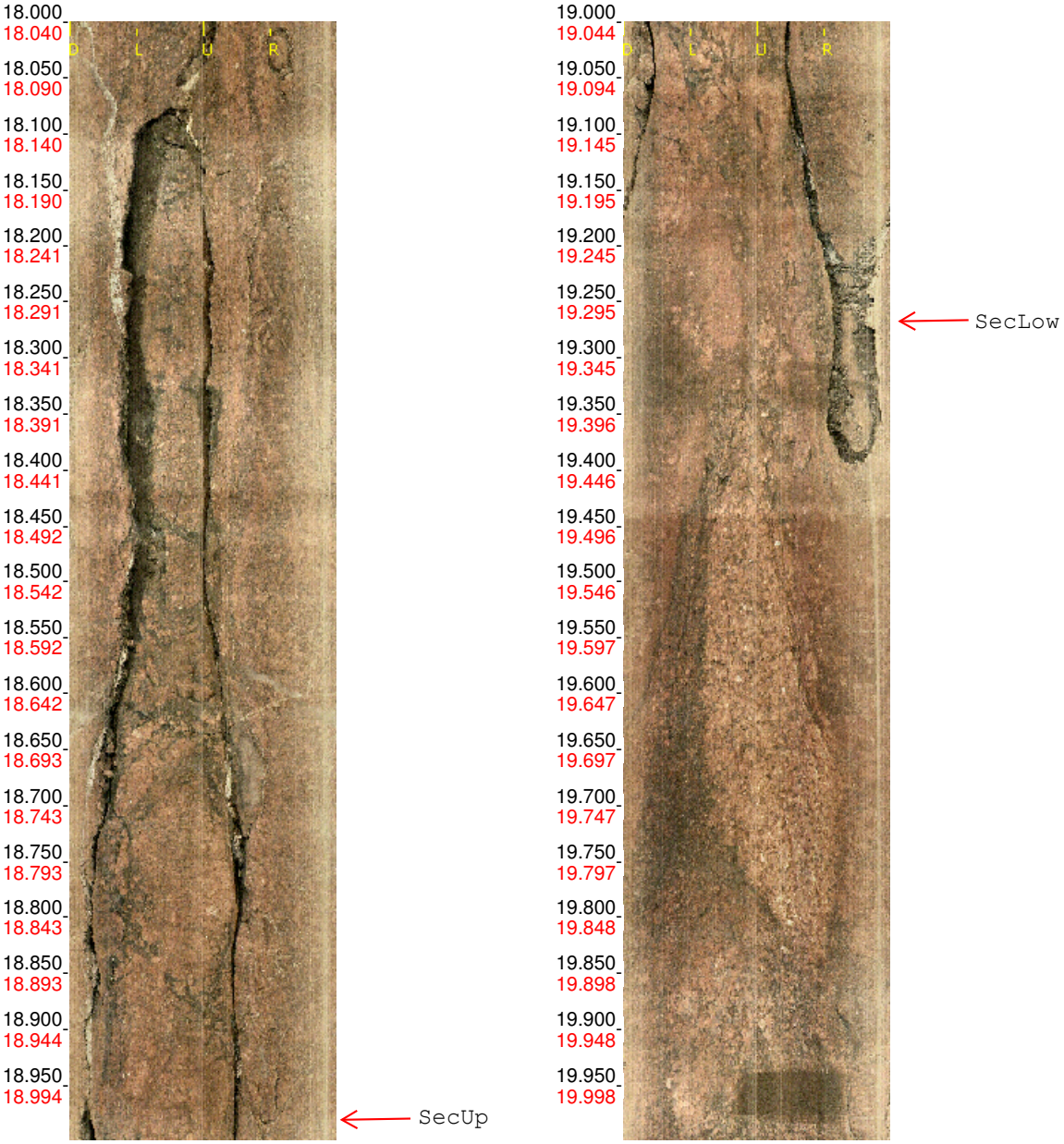

Borehole: KFR106
Mapping:

Depth range: 67.500 - 69.500 m
Azimuth: 196.0
Inclination: -69.0

KFR106 68.38-68.51 m

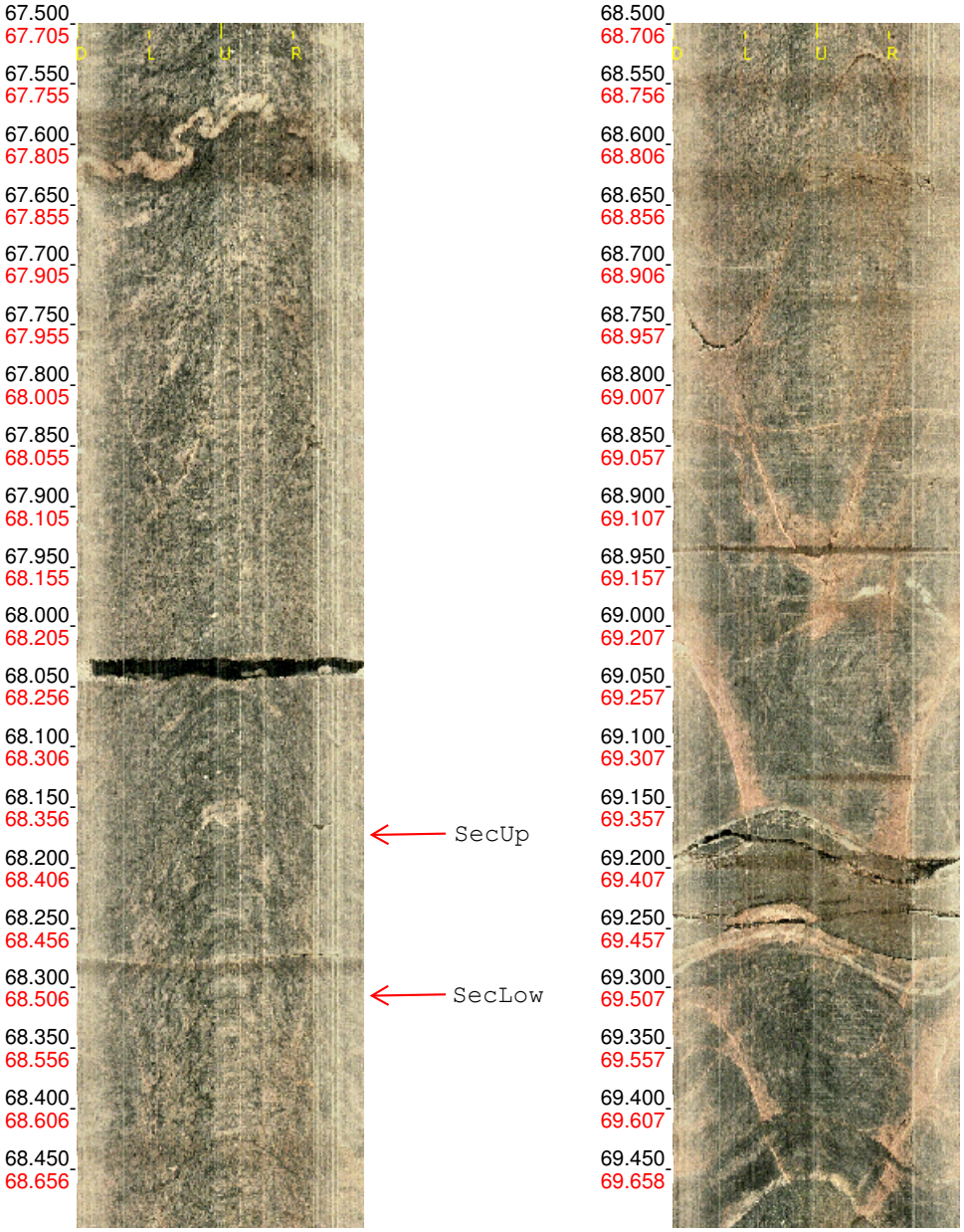

Borehole: KFR106
Mapping:

Depth range: 84.200 - 86.200 m
Azimuth: 196.0
Inclination: -69.0

KFR106 85.13-85.52 m

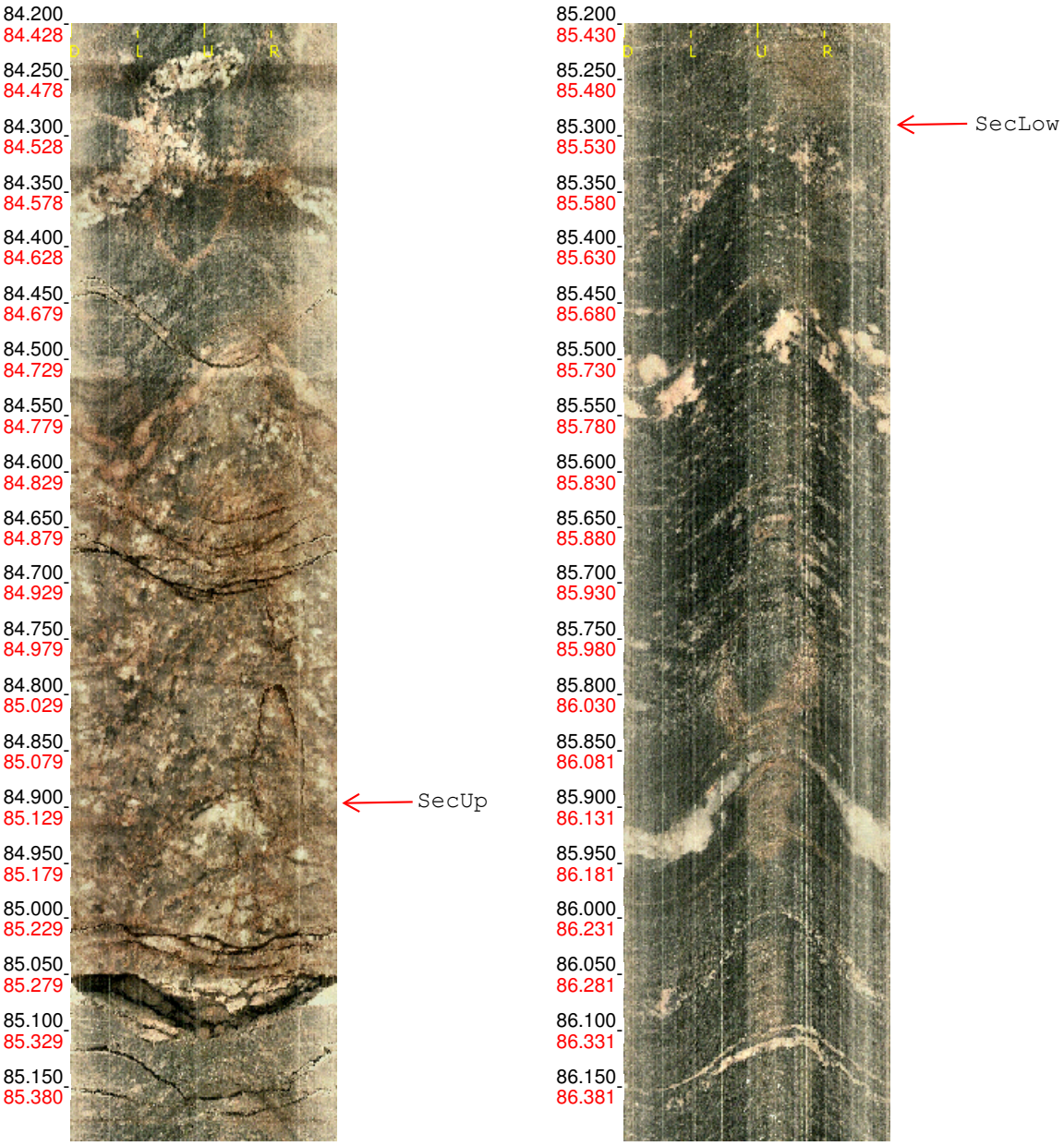

Borehole: KFR106
Mapping:

Depth range: 86.000 - 88.000 m
Azimuth: 196.0
Inclination: -69.0

KFR106 86.88-87.33 m

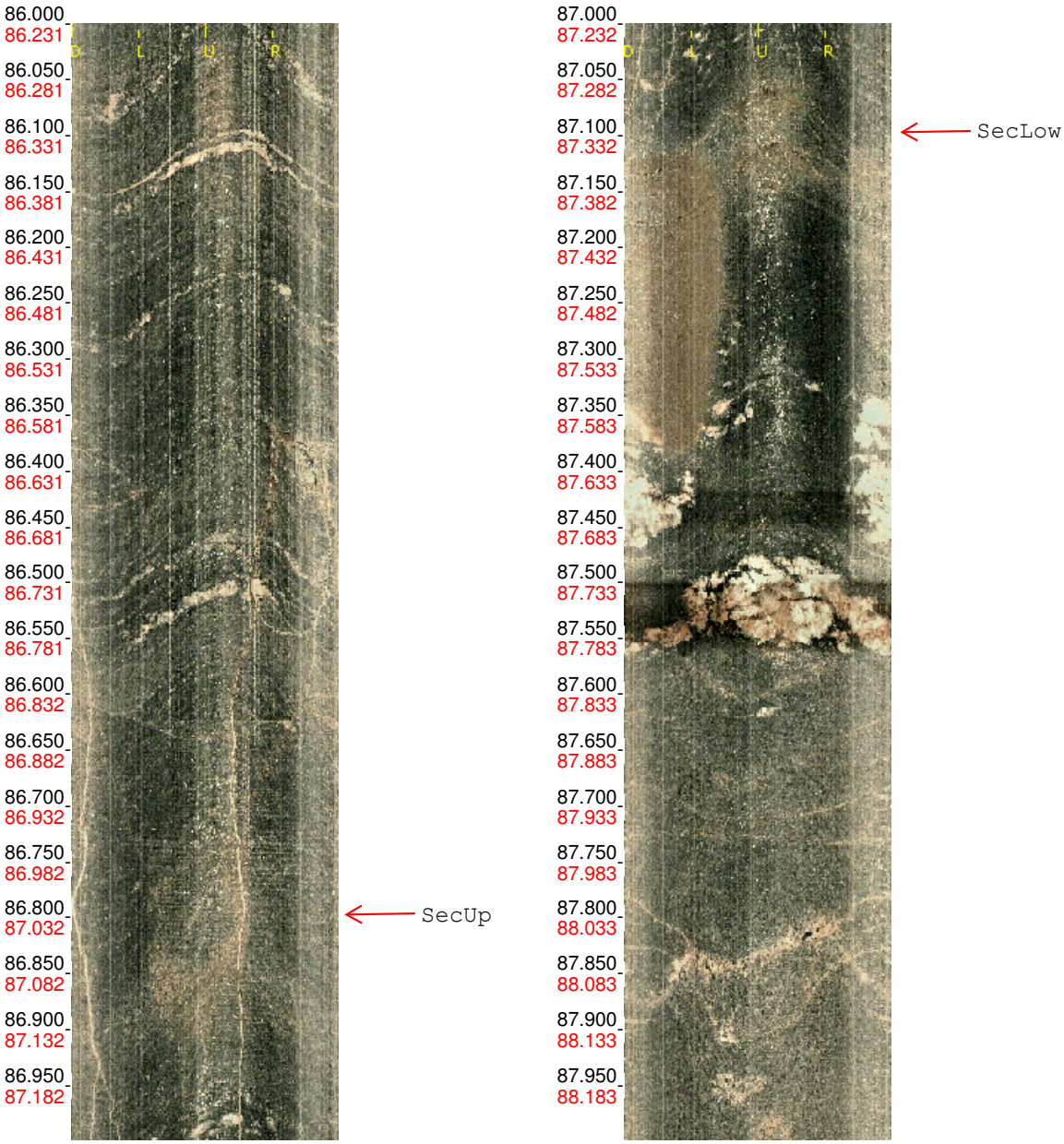

Borehole: KFR106
Mapping:

Depth range: 99.850 - 101.850 m
Azimuth: 196.0
Inclination: -69.0

KFR106 100.56-101.08 m

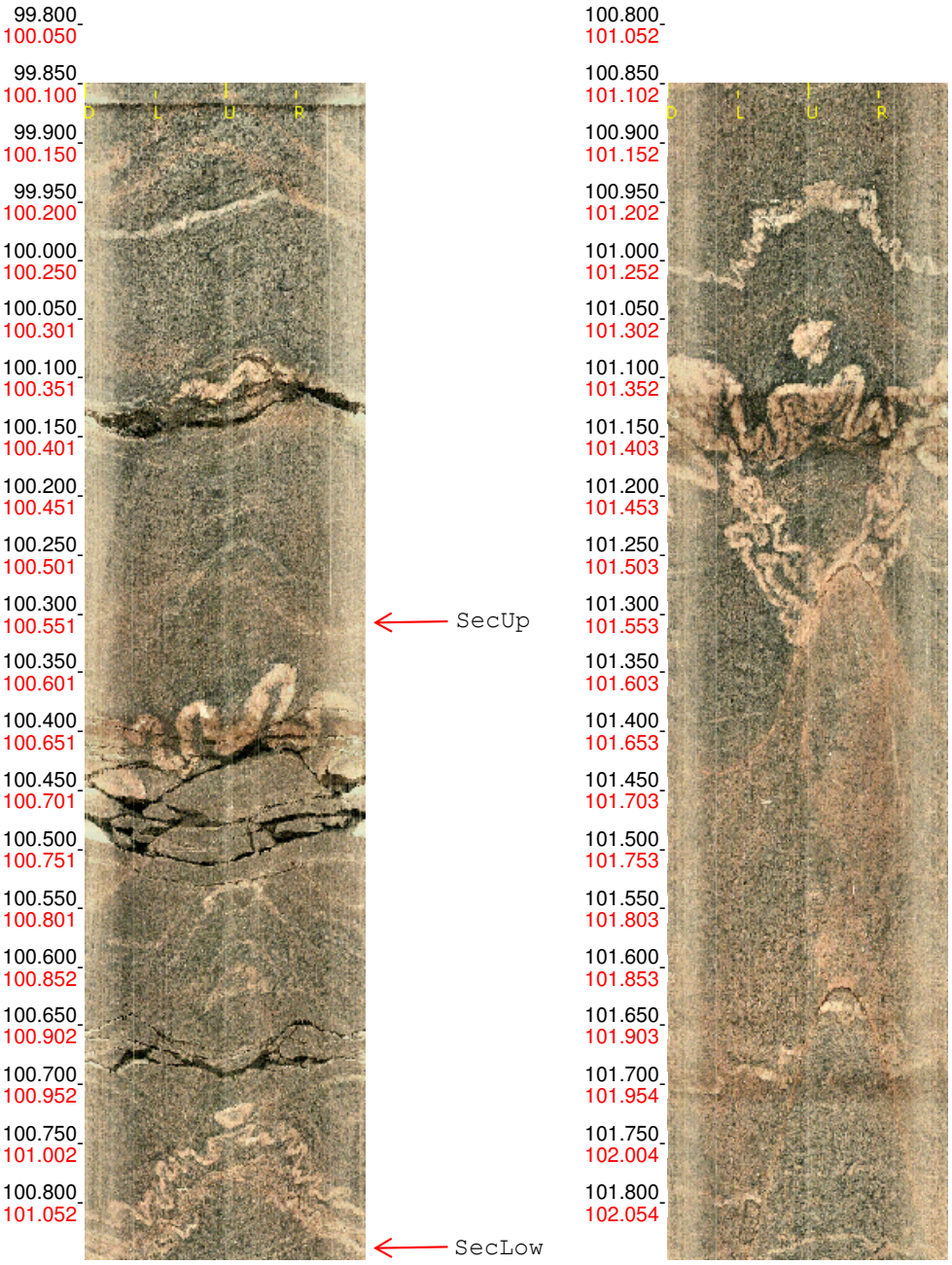

Borehole: KFR106
Mapping:

Depth range: 112.250 - 114.250 m
Azimuth: 196.0
Inclination: -69.0

KFR106 112.91-113.35 m

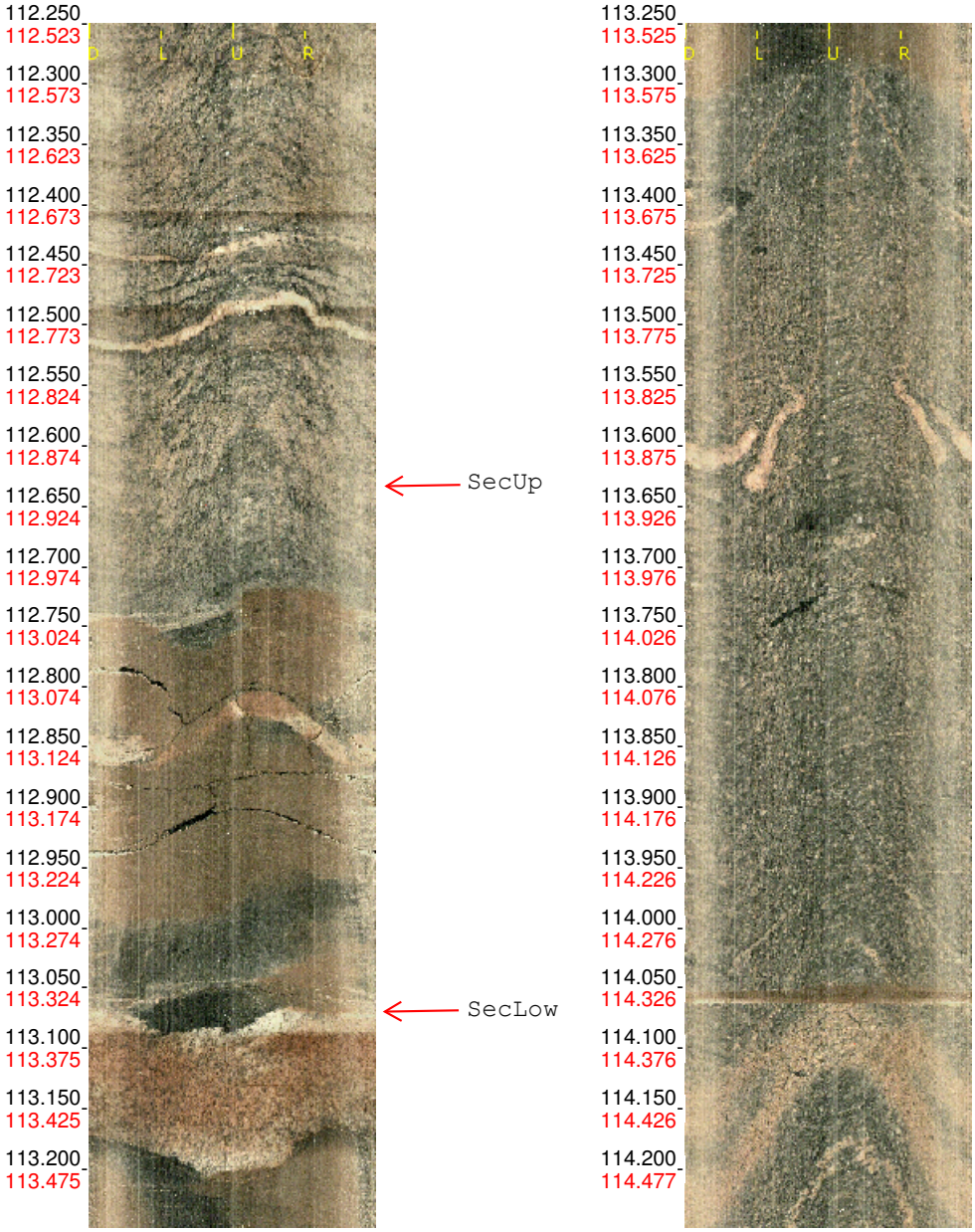

Borehole: KFR106
Mapping:

Depth range: 131.000 - 133.000 m
Azimuth: 196.0
Inclination: -69.0

KFR106 131.42-131.72 m

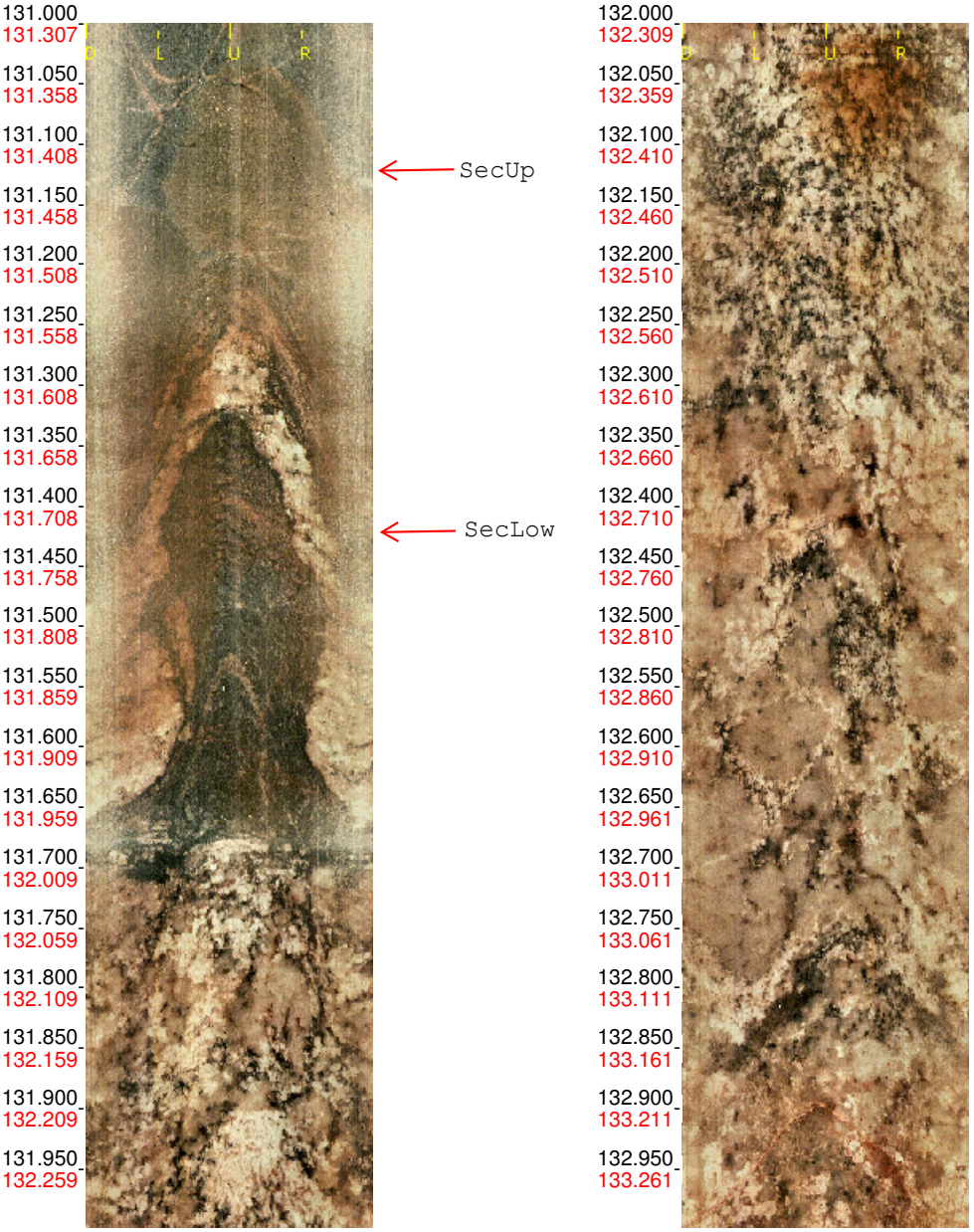

Borehole: KFR106
Mapping:

Depth range: 153.500 - 155.500 m
Azimuth: 196.0
Inclination: -69.0

KFR106 154.22-154.99 m

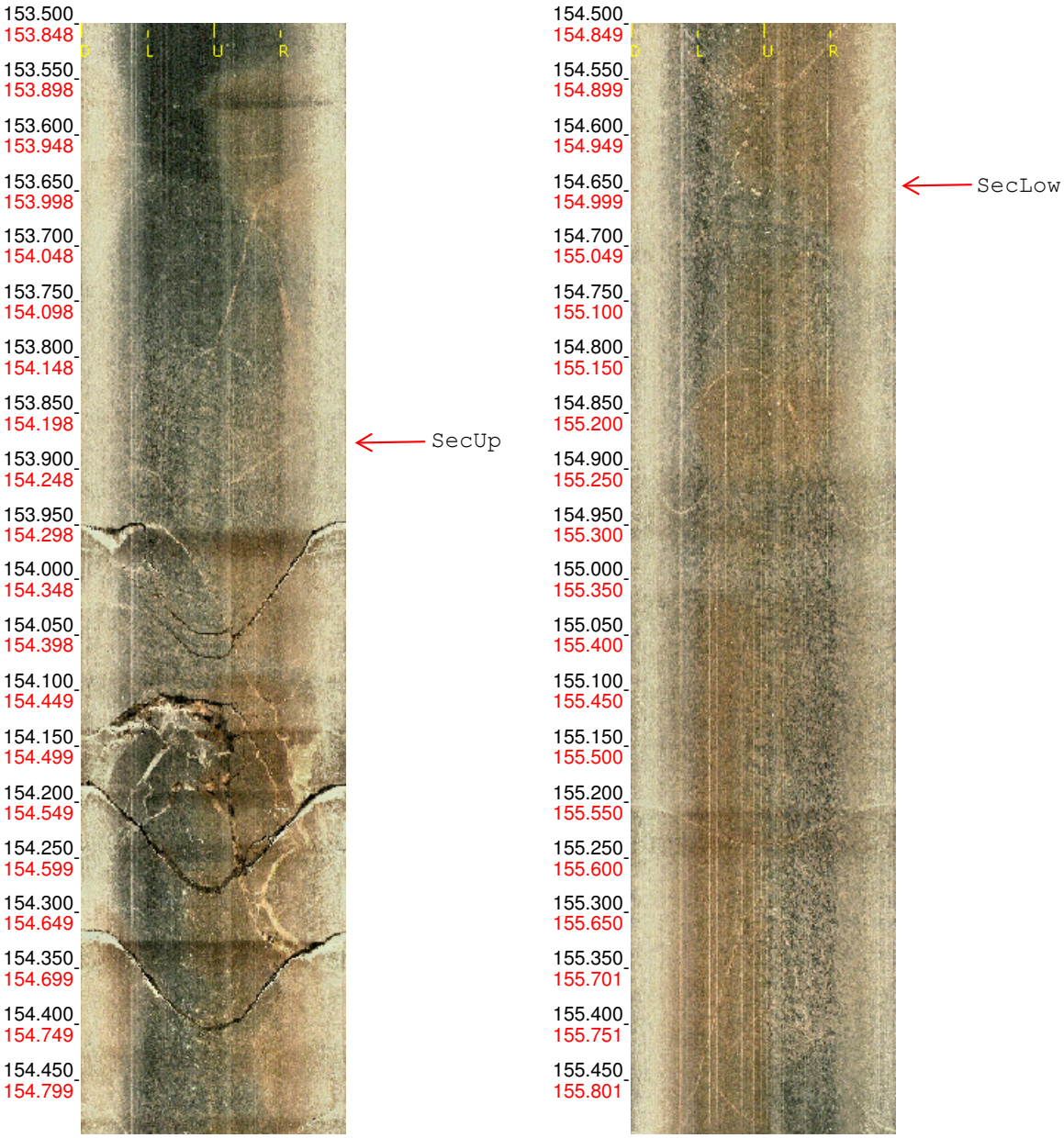

Borehole: KFR106
Mapping:

Depth range: 155.200 - 157.200 m
Azimuth: 196.0
Inclination: -69.0

KFR106 156.11-156.20 m

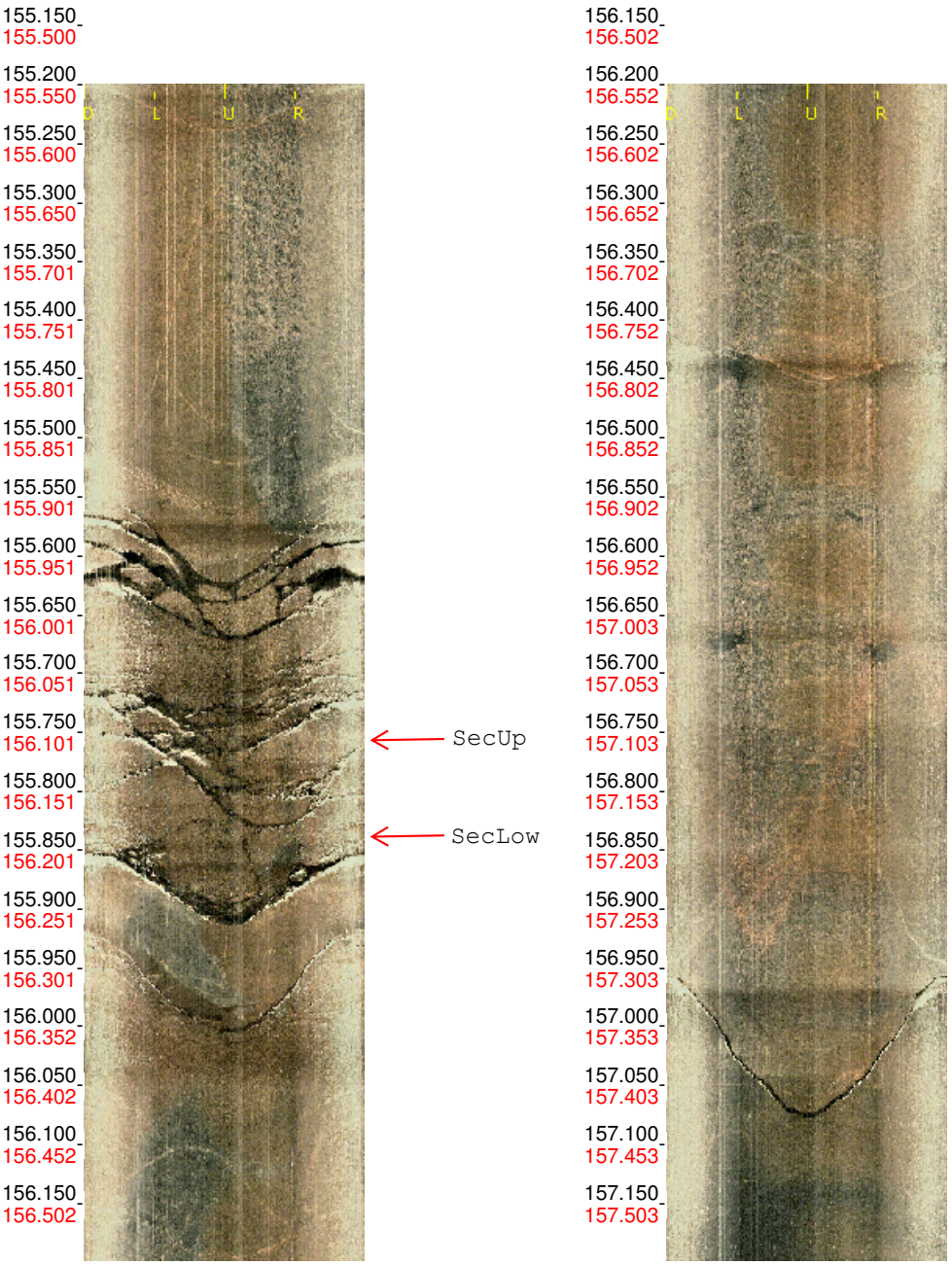

Borehole: KFR106
Mapping:

Depth range: 174.500 - 176.500 m
Azimuth: 196.0
Inclination: -69.0

KFR106 175.25-175.58 m

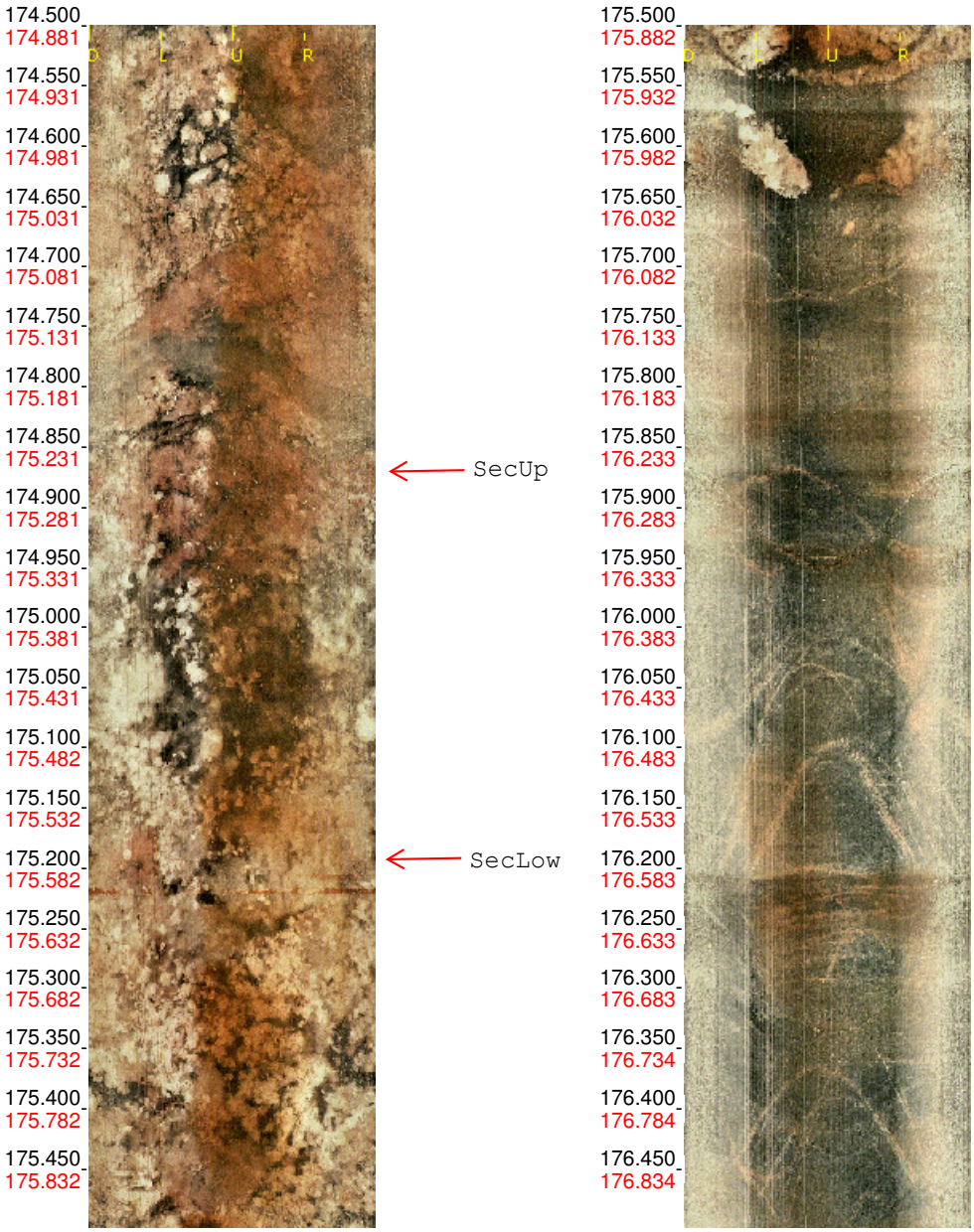

Borehole: KFR106
Mapping:

Depth range: 186.800 - 188.800 m
Azimuth: 196.0
Inclination: -69.0

KFR106 188.14-188.56 m

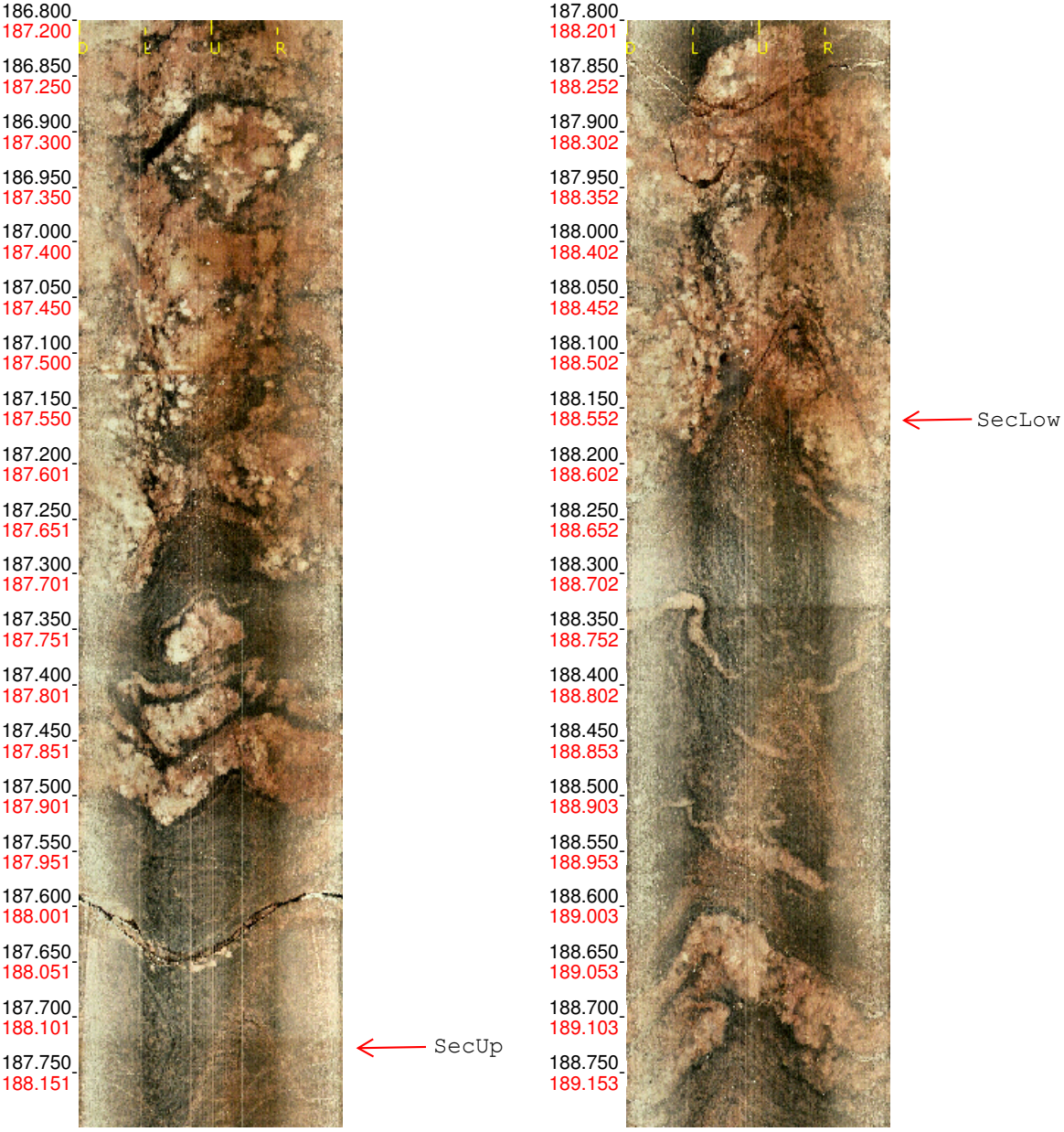

Borehole: KFR106
Mapping:

Depth range: 229.000 - 231.000 m
Azimuth: 196.0
Inclination: -69.0

KFR106 229.59-230.11 m

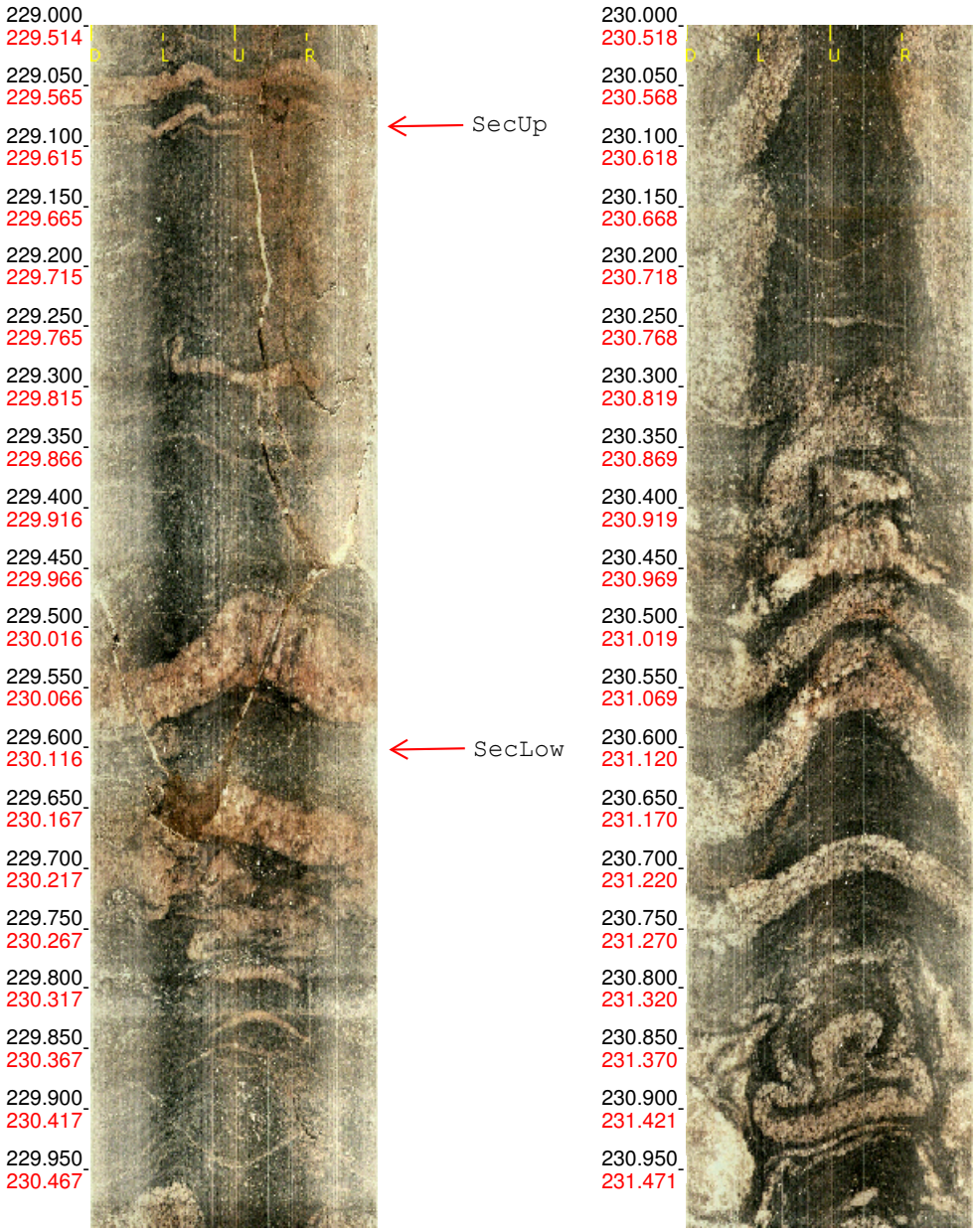

Borehole: KFR106
Mapping:

Depth range: 242.900 - 244.900 m
Azimuth: 196.0
Inclination: -69.0

KFR106 244.83-245.35 m

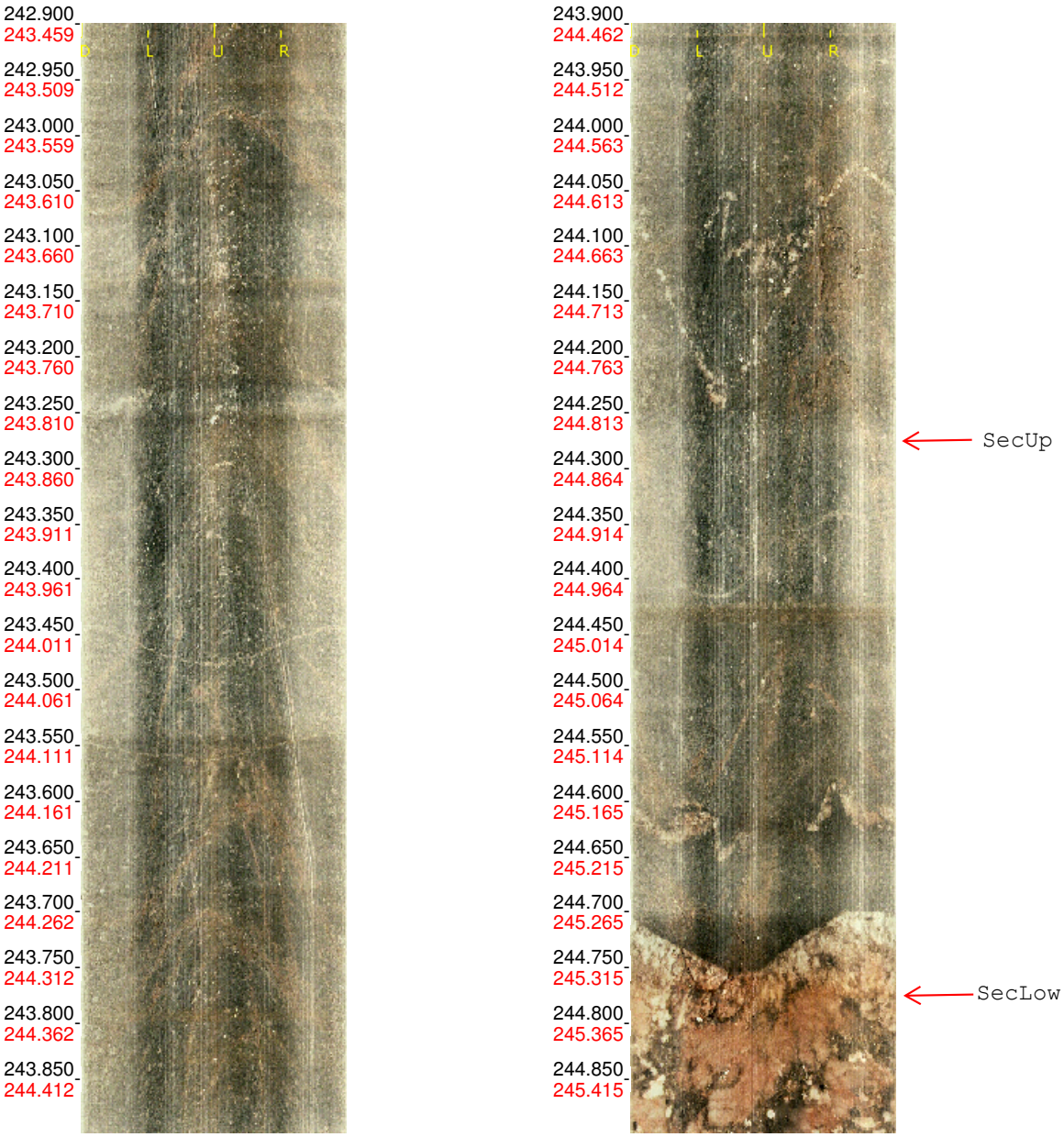

Borehole: KFR106
Mapping:

Depth range: 261.000 - 263.000 m
Azimuth: 196.0
Inclination: -69.0

KFR106 262.48-262.97 m

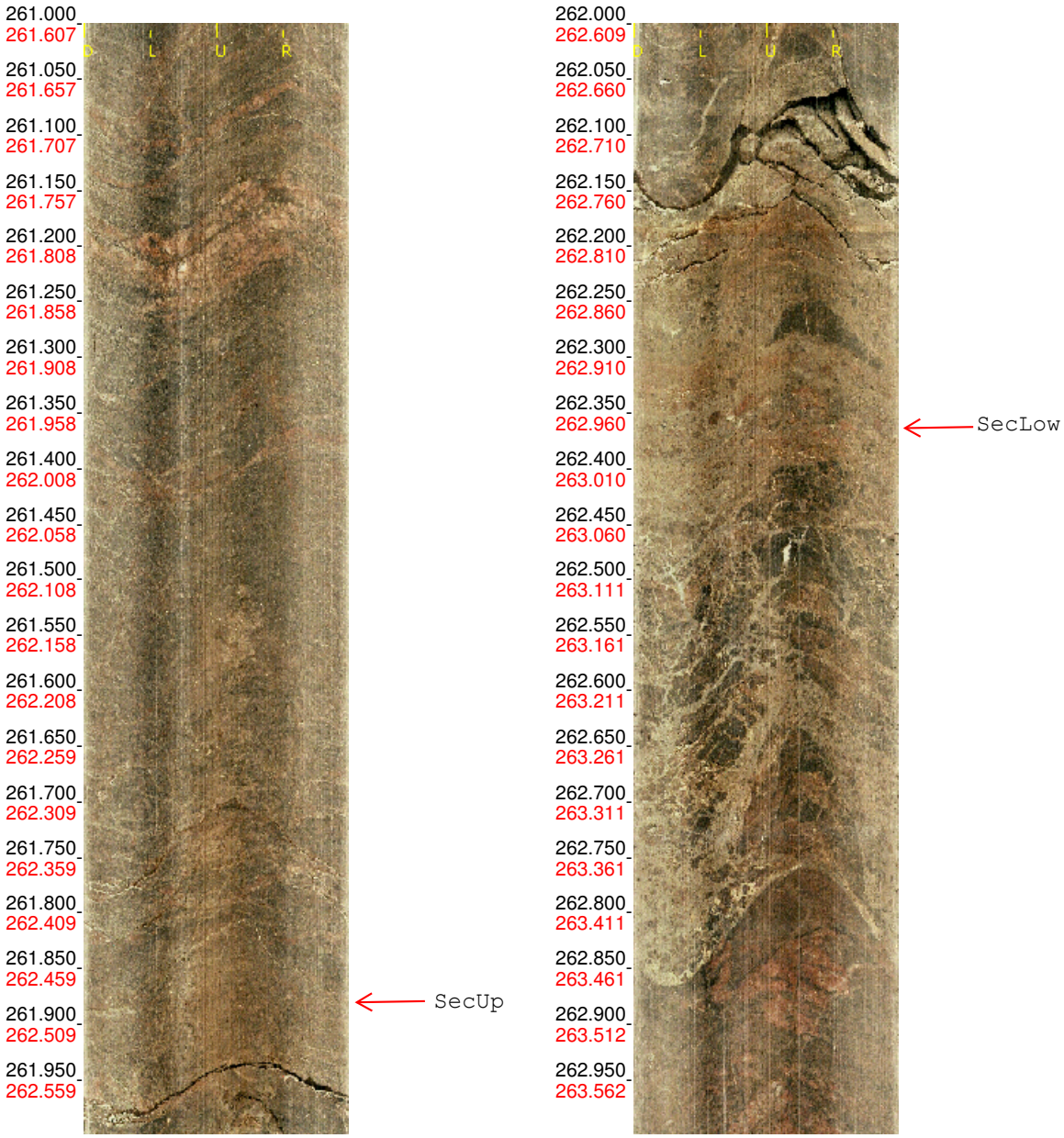

Borehole: KFR106
Mapping:

Depth range: 294.000 - 296.000 m
Azimuth: 196.0
Inclination: -69.0

KFR106 295.79-296.19 m

Borehole: KFR106
Mapping:

Depth range: 291.000 - 293.000 m
Azimuth: 196.0
Inclination: -69.0

KFR106 292.03-292.07 m